Nitric oxide synthase dysfunctionality in the umbilical cord vascular system during twin birth correlates with maturity and birth weight of the neonates

Ph.D. Thesis

Payal Chakraborty

Supervisor

Dr. habil. Edit Hermesz

Associate Professor

Doctoral School of Biology

Department of Biochemistry and Molecular Biology

University of Szeged, Faculty of Science and Informatics,

Szeged

2021

Preface

The maternal physiological state during pregnancy have an excess demand for oxygen supply which can easily disrupt the redox homeostasis balance. There is a change in the maternal haemodynamic profile with an increased cardiac output, reduced systemic vascular resistance and blood pressure (de Haas et al., 2017). In response to this high oxygen demand red blood cell (RBC) mass level steadily increases by 20-30% from 8 to 10 weeks of the gestational period till the end of pregnancy (Foley, 2018). In connection to that, there are increasing evidences of enhanced oxidative insults during intrauterine development leading to severe abnormalities or pathological states like spontaneous miscarriage, preterm delivery, preeclampsia, ectopic pregnancy, intrauterine growth restriction (IUGR), placental abruption, perinatal death etc. Moreover, in cases of multiple/twin pregnancy there is an additional stress with the greater risks of miscarriage, anaemia, preterm delivery, gestational hypertensive disorders, IUGR, diabetes operative delivery and related postnatal and neonatal illnesses. Modern usage of *in-vitro* fertilization (IVF) therapies led to higher incidence of multiple pregnancies. There have been relevant data on the increasing foetal, neonatal and perinatal mortality rate of 3-6 times in twin and 5-15 times in other multiple pregnancies with comparison to the singleton pregnancies.

During pregnancy, the connection between the mother and the foetus is provided by the placenta and the umbilical cord. The umbilical cord vascular system is the sole pathway of oxygen and nutrient transport to the foetus from the placenta. Therefore, the major obstetric complications are directly or indirectly connected to the placental or umbilical cord disorders causing intrauterine hypoxia and/or impaired blood flow to the developing foetus. The major part of umbilical cord lacks innervations and hence the vascular tone is mainly regulated by nitric oxide (NO), i.e. derived from the endothelial nitric oxide synthase (NOS3). The NO being a potent vasoactive agent causes vasodilation and

increases the rate of perfusion, nutrient and oxygen supply. Usually intensive prenatal care and surveillances are done in high risk cases like multiple/twin pregnancy by the advanced non-invasive biomedical devices. The usage of high performance equipment like Blood oxygen level-dependent–magnetic resonance imaging was utilized to study changes in the placental oxygenation status in human pregnancies. It can also assess the placental perfusion and oxygen transport. Similarly, ultrasound and Doppler flow measuring techniques, not only can visualize the umbilical cord but simultaneously can assess the foetal blood flow parameters through the umbilical cord vessels. These approaches can easily detect any abnormalities in the umbilical cord circulation, but lacks to highlight the underlying molecular mechanisms behind any kind of impaired functionality in the foetal vascular system that can highly influence the *in-utero* development. Further on this topic we elaborated in details.

Table of Contents

List of abbreviations

4-HNE	4-Hydroxynonenal
ACC	Advanced cell classifier
ACOG	American College of Obstetricians and Gynaecologists
ANOVA	One-way Analysis of Variance
APGAR	Appearance, Pulse, Grimace, Activity and Respiration.
BSA	Bovine Serum Albumin
DAPI	4', 6-diamidino-2-phenylindole
DZ	Dizygotic
ED	Endothelial Dysfunction
FACS	Fluorescence-activated cell sorting
H_2O_2	Hydrogen Peroxide
Hws	High birthweight singletons
IUGR	Intrauterine Growth Restriction
IVF	In-vitro Fertilization
Lws	Low birthweight singletons
MFI	Mean Fluorescence Intensity
M-Hwt	Mature Non-Discordant High birthweight Twin
M-Lwt	Mature Non-Discordant Low birth weight Twin
MZ	Monozygotic
NO	Nitric Oxide
NOS2	Inducible Nitric Oxide Synthase
NOS3	Endothelial Nitric Oxide Synthase
$O_2^{\bullet -}$	Superoxide Anion
$OH^{\bullet}$	Hydroxyl radical
$ONOO^-$	Peroxynitrite
PB	Phosphate Buffer
PrD-Hwt	Premature Discordant High birth weight twin
PrD-Lwt	Premature Discordant Low birth weight twin
Pr-Hws	Premature High birth weight singletons
Pr-Hwt	Premature High birth weight twins

Pr-Lwt	Premature Low birth weight twins
PUFAs	Polyunsaturated Fatty Acids
RBCs	Red Blood Cells
ROS	Reactive Oxygen Species
RSI	Reactive Species Interactome
SOD	Superoxide Dismutases
UC	Umbilical Cord

1. Introduction

1.1. Demography and Implications of Multiple/Twin Pregnancy

In the last 30 years, rates of twinning and multiple pregnancies have been increased to 3% of all births worldwide (Young and Wylie, 2012). In the United States**,** the rate of twin birth increased by more than 75% from 1980 to 2009 (Figure 1), with similar trends in Western Europe and other countries (Bortolus et al., 1999; Pison and D'Addato, 2006; Collins, 2007; Martin et al., 2012). A detailed survey dataset by WHO also indicated that 35.2% of multiple births were preterm delivery (< 37 weeks' gestation); with 6.1% of births taking place at < 32 weeks' gestation, 5.8% were during weeks 32 and 33 and the majority 23.2% were during weeks 34 through 37 (Stock and Norman, 2010; Vogel et al., 2013).

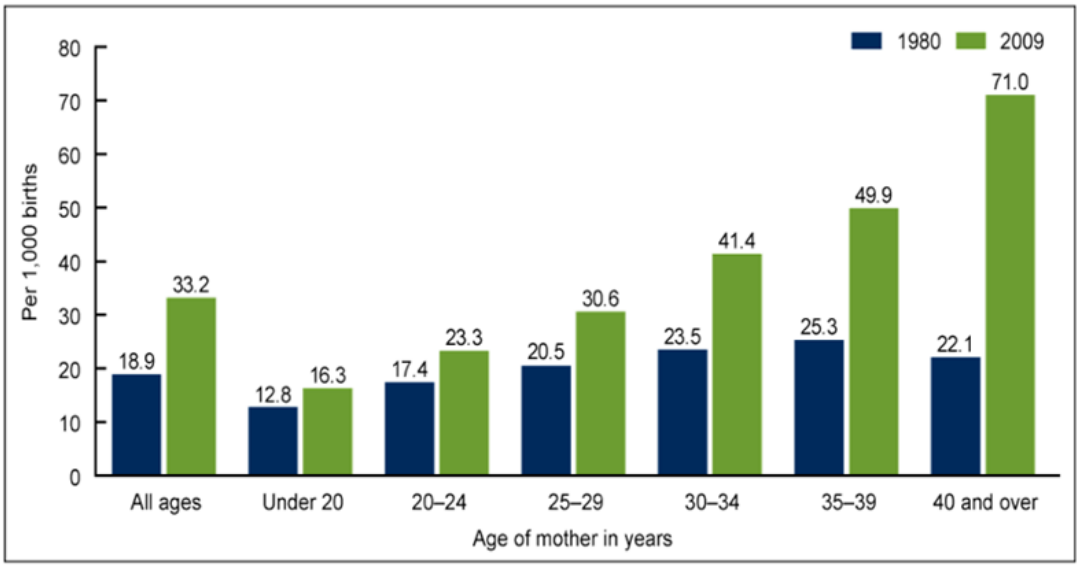

Figure 1: Twin Birth Rates, by Age of Mother: United States, 1980–2009 (Martin et al.; 2012)

The graphical representation demonstrates twin birth rates increased for women of all ages over the three decades, with the largest increases among women aged 30 and over. From 1980 to 2009, rates increased by 76% for women aged 30–34, nearly 100% for women aged 35–39, and more than 200% for women aged 40 and over.

A higher prevalence of multiple births has been observed in countries with high to middle socio-economic status. There is a diverse range of factors owing to the high risk of multiple pregnancies like (i) assisted reproductive technologies - IVF e.g. approximately

20% of twins in the UK Millennium Cohort study were conceived using IVF. (ii) Infertility therapy - usage of clomiphene citrate (selective oestrogen receptor modulator) prescribed to women with sub-fertility owing to an ovulation or oligo-ovulation. (iii) maternal age of women with more than ~35 years of age. (iv) genetic background (v) nutritional factors (Blondel and Kaminski, 2002; Jacobsson et al., 2004; Hayes, 2005; Jones et al., 2011; Gremeau et al., 2012). The background mechanism in the twinning depends on zygosity - one zygote (monozygotic, MZ) or two zygotes (dizygotic, DZ). MZ twins' makeup approximately 30% of twin pregnancies and occur when one single embryonic mass divides. Further classification of MZs twins is based on chorionicity and amnionicity. MZ twins result in 33% dichorionic-diamniotic, 66% monochorionic–diamniotic and 1% monochorionic-monoamniotic. MZ twins having identical genetic traits in comparison to DZ. Major discordances between the MZ twins are mostly owed to common intrinsic and extrinsic stressor factors**,** unlike DZ twins which can get influenced by both genetic and environmental factors (Machin, 2009; Weber and Sebire, 2010). In general, ~ 16% of twin gestations have discordance *i.e*. difference in the weights of the foetuses (Miller et al., 2012). As per the American College of Obstetricians and Gynaecologists (ACOG)**,** discordant growth is a common phenomenon in cases of multiple or twin gestation. Most likely it gets associated with anomalies like IUGR, preterm birth, infection of one of the foetuses, umbilical arterial pH <7.1**,** and respiratory distress. In our experimental study design**,** we followed the consensus laid down by ACOG where the threshold of discordance has been considered to be a 15-25% difference in actual weight among the siblings (American College of Obstetricians and Gynecologists, 2016). The threshold of discordance is calculated taking the larger twin as the standard of growth by the equation:

$$\frac{\text{(weight of the larger twin – weight of the smaller twin) x 100}}{\text{weight of the larger twin}}$$

The variable risk factors that influence this divergence of growth in the twins are mainly due to maternal age > 35, higher rate of IVF, maternal tobacco intake, fluctuating change in the maternal body mass index, lack of prenatal care, monochorionic twin foetus, opposite sex of the foetuses, small for gestational age in either foetus (*i.e*. below $<10^{th}$ percentile) or trans placental viral infections (Bortolus et al., 1999; Choi et al., 2010). There are several instances where multiple/twin pregnancy gets associated with detrimental outcomes (Krotz et al., 2002; Norwitz et al., 2005; Pharoah et al., 2009) such as women going through IVF therapies imposes a greater risk of miscarriage, anaemia, hypertensive disorders like pre-eclampsia, gestational diabetes, operative deliveries and related postnatal illnesses (Sibai et al., 2000). Though the mortality rate is low, the associated morbidities increase by 2-3 times in women with a twin pregnancy. The twin foetuses are always at a higher risk ~ at least 6 times of developing chromosomal anomalies, cerebral palsy, birth asphyxia, hyaline membrane disease, respiratory disorders and long term developmental morbidities (Buhling et al., 2003; Obiechina et al., 2011). Around 60% of the twin cases are recorded as preterm birth (*i.e.* delivery before 37 weeks) and contribute to nearly 10-20% of all low birth weight neonates. Mostly the major complications in the twins are due to increased preterm birth and having low birth weight (<2500 gr), very low birth weight (<1500 gr)**,** and extremely low birth weight (<1000 gr) ranges. In comparison to singleton births, foetal, neonatal**,** and perinatal mortality rates are 3–6 times higher in twins, where more than 60% of twin survivors suffer from significant health issues in their later life (Hollier et al., 1999; Cleary-Goldman and D'Alton, 2008; Breathnach et al., 2011).

1.2. Fetoplacental Circulation

During pregnancy, the normal circulatory dynamics in the foetus are unique. Understanding its changes both at the molecular and physiological level improves our knowledge regarding the pathophysiological mechanisms associated with impairment in the fetoplacental system. There had been several studies based on the morphological aspects of the placenta and umbilical cord that can assess the perinatal outcome and can be associated with pathological conditions like preeclampsia, foetal growth retardation, diabetes**,** and foetal demise (Di Naro et al., 2001).

As a part of the fetoplacental circulation, the placenta is the foremost temporary, vascular part that is closely connected to the maternal uterine wall and majorly responsible for sustaining life *in-utero*. Intact placental circulation with adequate perfusion rate ensures the requisite supply of oxygen and nutrient substrates for the developing foetus along with the effective elimination of the metabolic wastes. The placenta has two separate circulatory blood systems, the maternal-placental (uteroplacental) circulation that processes blood flow from the mother end and the foetal–placental (fetoplacental) blood circulation from the foetal system.

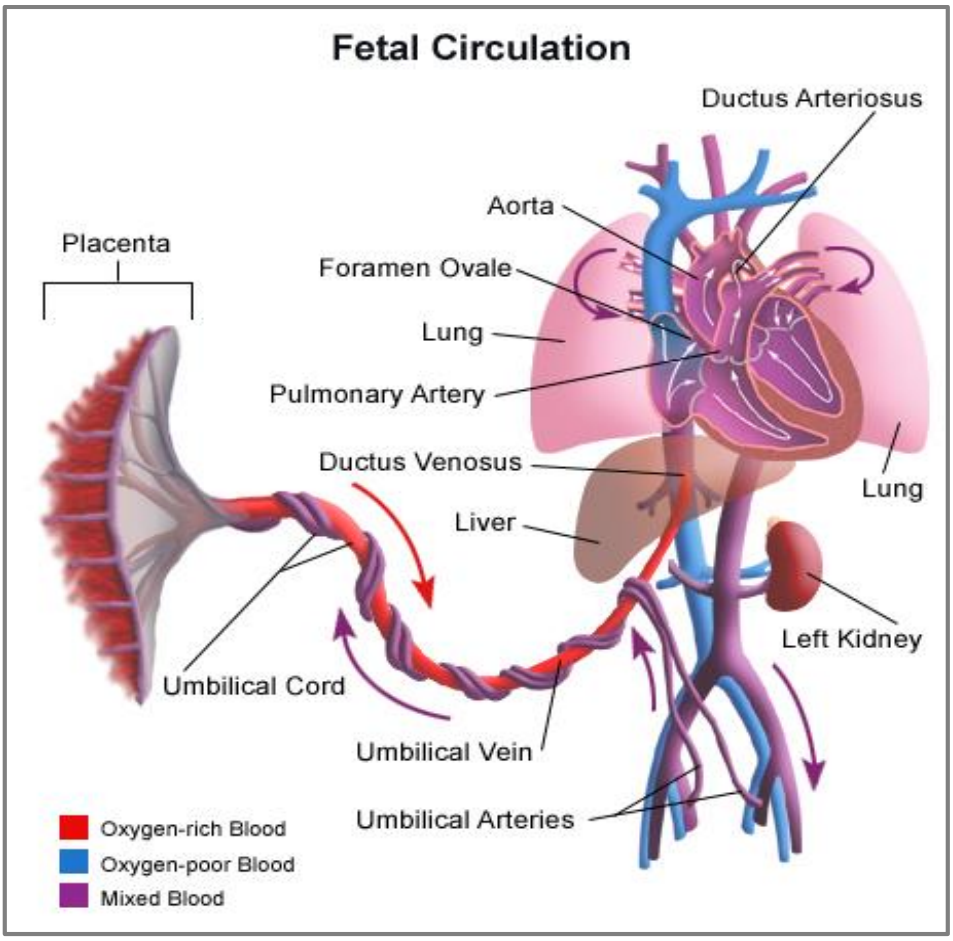

Figure 2: Illustration of Fetoplacental Circulation (www.stanfordchildrens.org)

The next pivotal anatomical structure of the fetoplacental circulation is the umbilical cord (Figure 2). It is a unique mammalian foetal attachment to the centre of the placental disk that bridged the connection between the foetus and placenta (Blanchette, 2011). The umbilical cord protects the embedded vessels that participate in the transfer of nutrients and oxygen supply to the foetus. It also carries the blueprints that determine the intrauterine conditions throughout the *in-utero* development (Fahmy, 2018), and can be subjected to both intrinsic and extrinsic stressors leading to various pathophysiological processes (Hackshaw et al., 2011). The umbilical cord is 50-60 cm long, originates from the embryonic stem**,** and is formed by the fifth week of gestational development (Bydlowski

et al., 2009). Umbilical cord containing two arteries and a single vein that branches into the amnion (Figure 3) (Njaa, 2011; Benirschke et al., 2012a).

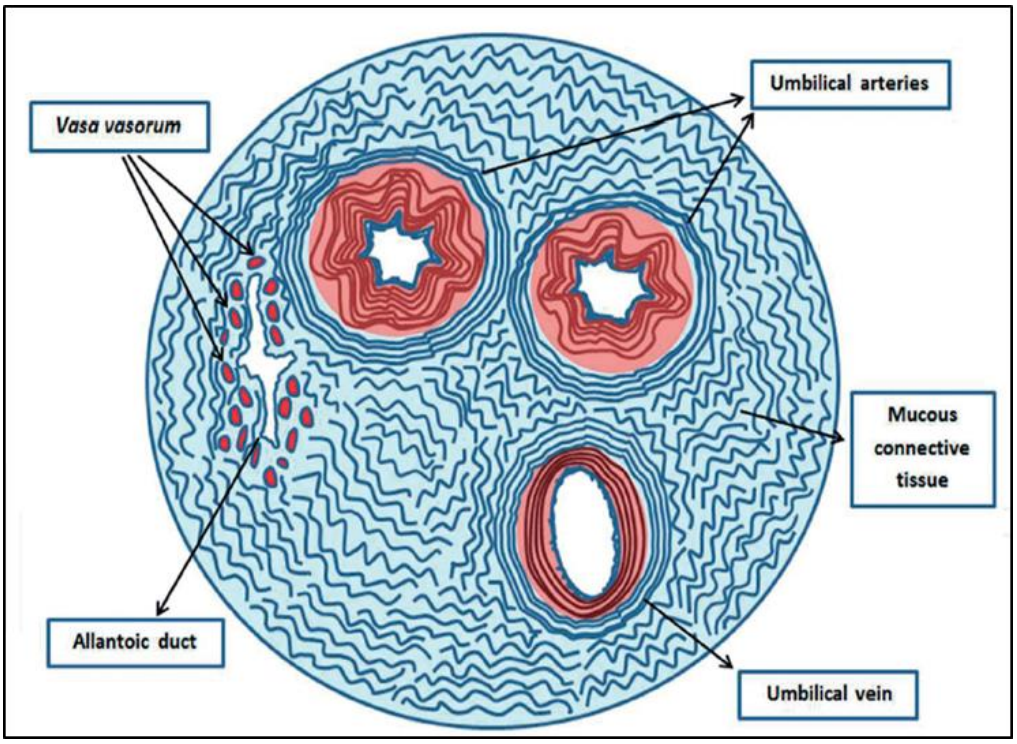

Figure 3: Schematic Diagram of the Umbilical Cord Structure (Manuel Barrios Arpi; 2019)

The umbilical arteries carry deoxygenated and nutrient-depleted foetal blood from the foetus to the intervillous space where the maternal-foetal exchange of blood rich in oxygen and nutrients takes place and further the oxygenated blood and nutrients are carried by the umbilical vein (Weissman et al., 1994; Meekins et al., 1997; Spurway et al., 2012). The histological studies showed the characteristic features of the umbilical cord arteries and veins that have large lumen with irregular shapes. The umbilical cord vessels are constituted mainly by three layers' tunica intima, media**,** and adventitia. The intima layer consists of elongated endothelium to the long axis of the blood vessel and lacks both internal and external elastic lamina. The endothelium of tunica intima corresponds to the thinnest layer comprised of simple squamous epithelium. The tunica media layer is located below the sub endothelial space and constitutes double-layered bundles of smooth muscles

containing collagen, elastic and reticular fibres with the presence of capillaries and absence of the elastic lamina. This layer distinctly consists of inner circular muscular layers and the outer longitudinal layer. The outermost tunica adventitia layer mainly forms the umbilical cord wall. This layer also consists of collagen, smooth muscle**,** and elastic fibres which partly invade the tunica media and muscle fibres. In contrast to "normal" arteries and veins**,** tunica adventitia varies in thickness and displays the number of transversal nerves in all thickness fibres which is completely absent in the umbilical vessels, thus both the umbilical arteries and vein lacks innervations (Manuel Barrios Arpi, 2019).

The fetoplacental circulation from a very early onset of pregnancy gets adapted with efficient mechanisms to meet the requirements of the rapidly growing foetus. The main characteristic features are (i) there is no intermixing of the maternal and foetal blood (ii) There co-exists homeostatic balance between both the utero-placental and fetoplacental circulatory pathways and (iii) maintains a low placental vascular resistance and normal umbilical blood flow. In simple terms, the foetus possessed complicated physiology and different circulatory pathway with proportionally higher mass of "internal organs". This fact suggests that the foetal system needs a greater amount of oxygen consumption compared to the adult which gets maintained by higher foetal cardiac output (Foley, 2018). The oxygen tension and saturation in the maternal part of the placental circulation is pivotal which gets continued through the foetal umbilical vein blood and thereby regulates and determines the foetal oxygenation status. However, the vascular endothelium of the umbilical cord vessels is highly vasoactive along their whole length (Mauro et al., 2011). Umbilical vessels liberate a wide range of vasoactive entities like serotonin, angiotensin II and oxytocin where the most potent and pivotal is NO, primarily derived from endothelial NOS. Mainly NO, regulates the vascular tone and normal functioning of the placenta and

umbilical cord throughout the gestation term for healthy foetal development (Karbowski et al., 1989; Giles et al., 1997; Benirschke et al., 2012b).

1.3. Reactive Oxygen Species – friend or foe?

A healthy state of pregnancy with normal *in-utero* foetal growth and subsequent survival of the perinatal period mainly depends on the vascular development and function of both the placenta and the umbilical cord. An orchestrated pattern of the uteroplacental and fetoplacental circulations is essential to meet the rising foetal demands for oxygen. To sustain this higher oxygen demand, the cellular metabolism rate increases with excessive production of reactive oxygen species (ROS). Chemical entities are containing an atom of oxygen with an unpaired electron termed as "free radicals" like as $^{\bullet}NO$, superoxide ($O_2^{\bullet-}$), hydroxyl radical ($OH^{\bullet}$), lipidperoxyradical ($LOO^{\bullet}$) that highly react with other radicals/non-radical in multiple ways which can be collectively termed as "oxidants" or ROS (Halliwell, 1991; Kalyanaraman, 2013; Phaniendra et al., 2015)

Currently, in a way to rationalize the complex chemical interactions of the reactive species within themselves or their targets, a novel integrative concept defined as the reactive species interactome (RSI) has been introduced (Kuhn et al., 2017). RSI constitutes reactive oxygen species, reactive nitrogen species, and reactive sulfur species as important mediators or signalling molecules. Under a wide range of human reproductive physiological processes likewise follicular development, ovulation, fertilization, embryogenesis, corpus luteum and uterine function, placental differentiation, fetoplacental development, and growth, etc. RSI maintains a multilevel redox regulatory system (Al-Gubory et al., 2010; Agarwal et al., 2012). It mainly targets the regulatory cysteine redox switches in proteins, affecting gene regulation, ion transport, intermediary metabolism, and mitochondrial function. This shows at physiological levels RSI has beneficiary roles in common (Nordberg and Arnér, 2001; Sharma et al., 2015; Kuhn et al., 2017). Under balanced redox homeostasis conditions, the physicochemical properties of the implied RSI

allow efficient sensing and rapid adaptation to environmental changes and various other stressors to elicit fitness and resilience response (Selye, 1955; Kültz, 2005; Mattson, 2008)

Redox biological reactions are mostly considered to bear the Janus faceted feature, which can promote both physiological signalling responses and pathophysiological cues. The endogenous antioxidant system becomes an active part of these scenarios and follows a basic understanding of antioxidant-based therapeutic interventions in redox-related diseases (Tan et al., 2018). Antioxidant molecules are nucleophilic and reductant molecules that can react with oxidants. Antioxidants scavenge biologically important ROS like $O_2^{\bullet-}$, peroxynitrite ($ONOO^-$), hydrogen peroxide (H_2O_2), $OH^{\bullet}$, hypochlorous acid, ferryl, peroxyl, and alkoxyl, thus actively takes part in the biological repair mechanisms by limiting the ROS formation. There lies an intricate balance between ROS and the endogenous antioxidant system to carry out vital cell function, regulation, and adaptation to diverse growth conditions. Antioxidants also ensure a defense mechanism against ROS-induced damage to lipids, proteins, and DNA (Young and Woodside, 2001; Espinosa-Diez et al., 2015).

The cellular antioxidant systems are divided into two major groups, enzymatic detoxifiers like superoxide dismutases SOD1 (Cu, Zn-SOD) and SOD2 (Mn-SOD or SOD2), catalases, glutathione peroxidases which are the major defence pathways. The primary enzymatic antioxidant pathway *i.e.* followed is dismutation, where mainly SOD1 and SOD2 catalyse $O_2^{\bullet-}$ to H_2O_2 formation. The alterations in the expression and activity of the SODs signifies ROS level with subsequent oxidative stress (Hileman et al., 2001; Gongora et al., 2006; Mccord and Fridovich, 2014). Dysfunction or failure in the dismutation process abruptly increases the level of $O_2^{\bullet-}$ that gets involved in the formation of deleterious pro-oxidants like $ONOO^-$ and $^{\bullet}OH$. Peroxynitrite is formed by a spontaneous reaction of $O_2^{\bullet-}$ and $^{\bullet}NO$, (Koppenol et al., 1992; Packer et al., 1996; Kirkinezos and

Moraes, 2001) whereas highly reactive $^{\bullet}OH$ gets generated with the interaction between $O_2^{\bullet-}$ and H_2O_2 in the presence of free unbound iron ions, known as the Haber–Weiss reaction. Anyhow, the secondary antioxidative step limits the H_2O_2 production and its elimination before their subsequent transformation to $^{\bullet}OH$ (Kehrer, 2000; Ježek and Hlavatá, 2005).

Extensive studies were conducted within a wide array of defensive antioxidant mechanisms in the neonates or preterm infants during theirs *in-utero* foetal development. The overall antioxidant efficiency was found significantly low during the early stages of the first trimester that fails to counteract with harmful effects of the generated ROS species. This fact might lead to foetal or neonatal diseases and obstetric complications associated with prolonged oxidative stress conditions (Georgeson et al., 2002; Perrone et al., 2012, 2019). The increased amount of radical/oxidants like $^{\bullet}OH$ and $ONOO^{-}$ in the system enhances the rate of lipid peroxidation by subsequent ß cleavage of n-6 polyunsaturated fatty acids (PUFAs) (Marla et al., 1997). The most abundant and bioactive yield of lipid hydroperoxide product i.e. alkenal 4-hydroxy-2-trans-nonenal (4-HNE) (Benedetti et al., 1980; Esterbauer et al., 1991) is estimated to determine the extent of macromolecular damages. The 4-HNE is highly reactive and can form adducts with DNA (Chung et al., 2000; Nair et al., 2007), with phospholipids (containing PUFAs such as linoleic and arachidonic acid) and nucleophilic amino acids, such as cysteine, histidine, and lysine residues. Thus, even 4-HNE cross-linked conjugates propagated lipid peroxidation with subsequent damages and loss in redox homeostasis that lead to pathological disorders (Uchida and Stadtman, 1993; Doorn and Petersen, 2003).

1.4. Oxidative Stress and Intrauterine Hypoxic Conditions

The aetiological factors that are prone to cause an imbalance between the oxidants and antioxidants in favour of oxidants state the "oxidative stress" condition. Oxidative stress causes extensive oxidative macromolecular damages likewise in lipid, protein, and DNA with subsequent complications and severe pregnancy outcomes (Bak & Roszkowski, 2013; Burton & Jauniaux, 2011; Messner & Bernhard, 2014; Hubinont et al., 2015). Under additional stressor conditions like multiple/twin pregnancy, continuous adaptations were invoked within the maternal-placental-foetal interface by the process of “foetal programming” with epigenetic control. These further regulate and influence the development of non-communicable diseases such as diabetes, obesity, metabolic syndrome, and cardiovascular diseases in adulthood (Barker et al., 1993; Godfrey and Barker, 2001). Thus during multiple/twin pregnancy, the intrauterine environment remained as a key factor where both the mother and foetuses are exposed to the persistent hypoxic environment in the uteroplacental and fetoplacental circulation, respectively. The equilibrium conditions are particularly disturbed with an alteration in the intra-placental oxygen content.

Since adequate perfusion and transfer of oxygen to the foetus is dependent on both uteroplacental and fetoplacental circulations, intrauterine hypoxia or foetal hypoxia can be classified into (i) pre-placental hypoxia – this occurs due to reduced oxygen content in the maternal blood. Here both the mother and the foetus is hypoxic which mainly occurs due to multiple pregnancies, maternal smoking, maternal anaemia and other chronic infections (ii) uteroplacental hypoxia – here the oxygen tension in the maternal blood are normal but due to any occlusion the oxygenated blood entry is restricted to the uteroplacental arterioles such as in the cases of pre-eclampsia and IUGR (iii) post placental hypoxia – the oxygenated maternal blood cannot perfuse in the fetoplacental circulation mainly due to

any congenital fetoplacental obstruction or disease (Kingdom and Kaufmann, 1997; Stanek, 2013).

Therefore, an adverse *in-utero* environment arises due to continuous intrauterine pre-placental, utero-placental**,** and post-placental hypoxic conditions. Here we mainly like to highlight the intrauterine pre-placental hypoxic state in cases of multiple/twin pregnancy that have a different spectrum of outcomes in both maternal and foetal conditions. Due to multiple pregnancies, the uterus gets highly distended with decreased oxygen pressure in the environment. This condition ultimately lowers the intra-placental oxygen content which hinders the maturation process of the utero-placental intervillous exchange surface causing low materno-foetal oxygen transfer. Thus there exists a chronic state of maternal hypoxemia (Kingdom and Kaufmann, 1997, 1999; Hutter et al., 2010; Stanek, 2013). The maternal blood with reduced oxygen content then passes through the placenta and flows into the foetus via the umbilical cord vein. This phenomenon causes acute foetal hypoxia with excessive activation of cellular stress signalling and inflammatory pathways in response to energy intake which might strongly exceed the energy expenditure. The fetoplacental circulation showed an abrupt reduction in the blood flow via arterial cord vessels leading to deprivation of oxygen and nutrients in the developing foetus, with consequent intrauterine hypoxia and malnutrition (Yoshida et al., 2018).

Similar conditions of intrauterine pre-placental hypoxia also arise due to maternal smoking conditions during pregnancy where it increases the rate of lower birthweight in the new-borns and predisposes deleterious effects with chronic diseases in theirs later life (Hackshaw et al., 2011; Courtney et al., 2018). In cases of maternal cardiovascular complications and haematological disorders like sickle cell anaemia, directly affect the oxygen transfer to the foetus and are at higher risk for maternal (i.e., preterm labour, preterm rupture of membranes, and postpartum infections) and foetal complications (i.e.,

abortion, prematurity, IUGR, low birth weight, and stillbirth) (Singla et al., 1997; Williams et al., 1997; Siu et al., 2002). Anyhow**,** cellular metabolism gets enhanced during normal pregnancy terms, which directs the antioxidant mechanisms reacting by way of enzyme activity and non-enzyme free radical deactivators to maintain the redox homeostasis balance. However, the aetiologies behind the development of such pathological conditions affecting female reproductive processes cannot be fully guarded by the selective endogenous antioxidant mechanisms as anticipated (Casas et al., 2015; Sies, 2015). This indicates our current understanding of the redox diseases underlying such pathophysiological processes, and needed to be further explored.

1.5. Nitric Oxide Synthase Pathway – NO synthesis

Foetal homeostatic conditions and the intrauterine environment critically depend on the efficiency of the placental and umbilical cord circulation. The prevalence of intrauterine hypoxic state causes vasoconstriction with the definite shortage in the bioavailable NO, elevation in the local oxidizing environment by triggering free radical generation, and chronic inflammatory reactions leading to severe oxidative stress conditions (Hutter et al., 2010; Zhou et al., 2020). As the umbilical cord lack innervations, in the fetoplacental system to maintain the vascular tone, cord vascular endothelium releases potent vasoactive substances like NO derived from endothelial NOS that acts as a central regulator for the maintenance of vascular homeostasis (Mauro et al., 2011; Benirschke et al., 2012b; Vanhoutte et al., 2017). Any kind of impaired response and loss in the bioactivity of endothelium-derived NO within the umbilical cord vascular system causes intrauterine hypoxia, increased fetoplacental vascular resistance, and retardation in the foetal growth (Tomasian et al., 2000; Prieto et al., 2011).

The NOS isoforms are distinct from one another based on their gene origin, localization, regulation, catalytic properties, and inhibitor sensitivity. The common characteristic of all NOS isoforms is "dimeric" in their active form. These isoforms are referred to as nNOS/NOS1 predominantly found in neuronal tissue, iNOS/NOS2 being the isoform that is inducible in a wide range of cells and eNOS/NOS3 abundant in vascular endothelial cells. These NOS isoforms have been differentiated based on their constitutive NOS1 and NOS3 versus inducible NOS2 expression, and their calcium (Ca^{2+}) dependence in the case of NOS3 and NOS1 or independence as like NOS2 (Alderton et al., 2001). The NOS1 in addition to perivascular nerve fibres also gets expressed in the vascular wall (Schwarz et al., 1999; Tsutsui, 2004) and atherosclerotic plaques (Schödel et al., 2009) and contributes to vasodilation (Capettini et al., 2011). Contrastingly, NOS2 under normal

physiological conditions is present in the vasculature but its expression mainly gets induced due to pathological states like inflammation, sepsis, or oxidative stress (Pautz et al., 2010; Yu et al., 2018). NOS2 serves as a widely diffusible and long-lasting source of NO that might adequately compensate for a fall in the NO level but due to its high catalytic activity compared to NOS3, it produces cytotoxic levels of NO and triggers cytokines and inflammatory reactions (Ratovitski et al., 1999; Colton et al., 2006). It had been also noted that endothelial and inducible nitric oxide synthases derived NO respectively regulated the vascular tone and even showed a wide range of pivotal roles in the placental vascular development, *in-utero* embryo implantation, and trophoblast invasion (Krause et al., 2011).

In the endothelial cell, NOS3 is constitutively expressed and tightly gets regulated by its substrate L-arginine concentration, availability of cofactors, rate of electron transfers, subcellular localization, post-translational modifications, and diverse interacting proteins (Michel and Feron, 1997; Shu et al., 2015a). The process of NOS3 coupling/dimerization is the most crucial step towards its activation that can produce functional vasoprotective factor NO. Mechanistically deficiency of cofactors like tetrahydrobiopterin (BH4) and low concentration of L-arginine substrate is likely to be the major causes for NOS3 uncoupling and dysfunctionality (Förstermann & Münzel, 2006; Li & Förstermann, 2013; Li, Horke,& Förstermann, 2013). As mentioned in (Figure 4), initially the NOS3 resides in the Golgi apparatus, where it gets anchored to the membrane via one myristoyl and two palmitoyl groups (Liu et al., 1996; Özüyaman et al., 2008). Through the vesicular transport system, NOS3 localizes to the plasma membrane where it gets associated with caveolae. In the caveolae, NOS3 binds to caveolin-1 via its scaffolding domain and remains catalytically inactive (Feron et al., 1998). Due to receptor dependant agonists or by physical stimuli including shear stress the intracellular Ca^{2+} concentration increases, calmodulin binds to NOS3, disrupts the NOS3-caveolin-1 interaction and NOS3 gets catalytically activated.

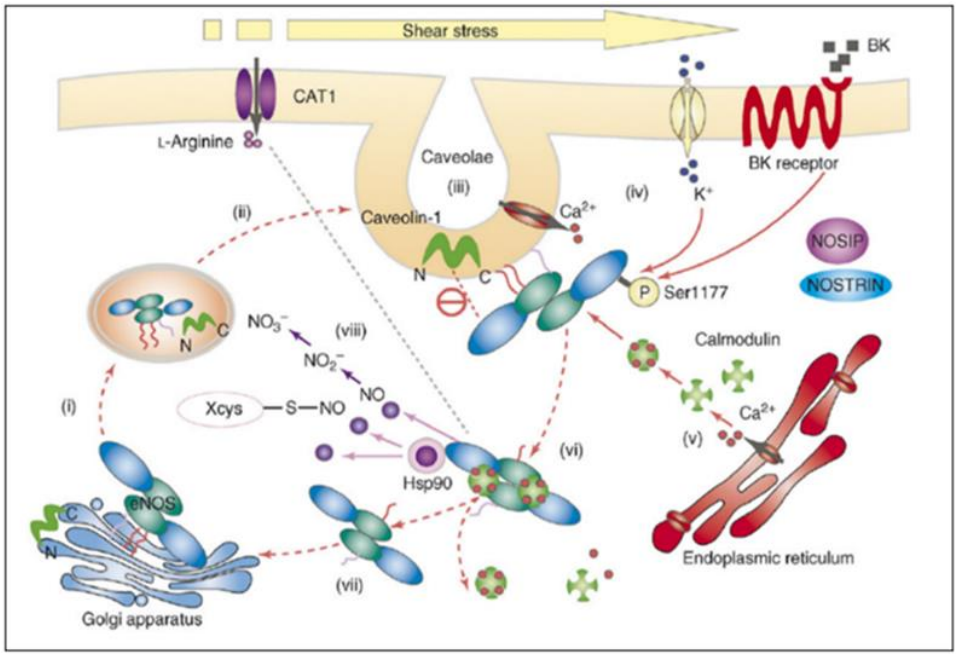

Figure 4: Regulation of NOS3 in the Endothelial Cells (Özüyaman et al., 2008)

The representative figure describes in detail the regulatory pathway of NOS3 in the endothelial cells. NOS3 via vesicular transport gets transported to the plasma membrane from the Golgi apparatus and gets bound to caveolin-1 in the caveolae and remains inactive. Under increased shear stress conditions, the potassium channel activates with an increase in the intracellular Ca^{2+}, leading to consecutive phosphorylation of NOS3 at Ser1177residue.

The activated NOS3 enzyme translocated in the cytosol and via the PI3-Akt pathway gets phosphorylated at Ser1177 residue. In resting endothelial cells, Ser1177 is usually not phosphorylated. Post-translational modification of NOS3 by phosphorylation is induced when the cells are exposed to a kind of shear stress or other factors like vascular endothelial growth factor (VEGF). Human endothelial NOS have two important functional phosphorylation sites at Ser1177 and Thr495. The process of phosphorylation increases the influx of electrons through the reductase domain from NADPH to the haem in the oxygenase domain and enhances the enzyme activity of the kinases such as AMP-activated protein kinase, protein kinase A, serine/threonine kinase Akt and Ca^{2+}/calmodulin dependent protein kinase II. In the presence of serine/threonine kinase Akt as shown in (Figure 5) NOS3 gets catalytically active by the phosphorylation at Ser1177 whereas

Thr495 residue of NOS3 acts as the negative regulatory site, and its phosphorylation is associated with a decreased electron influx and enzyme activity.

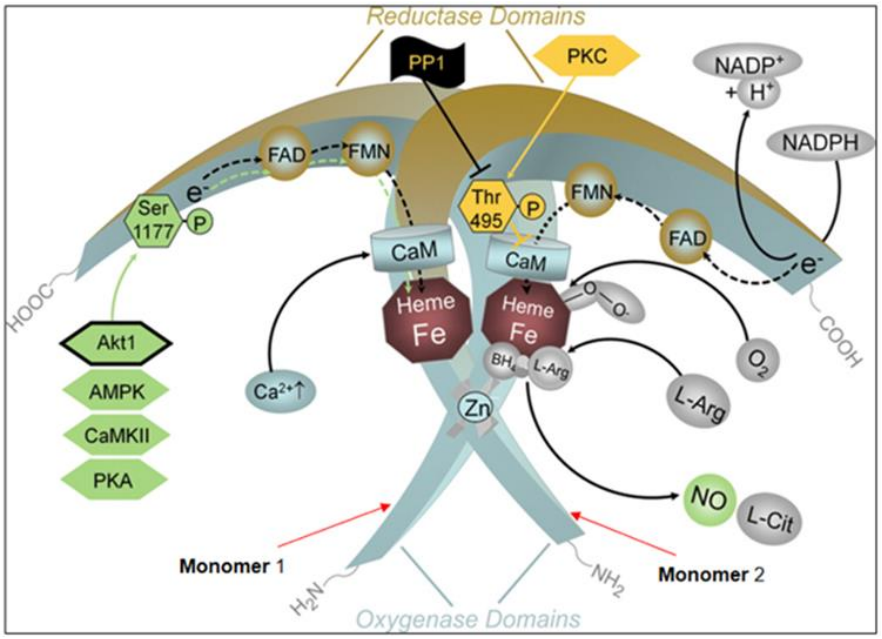

Figure 5: Dimerization and Activation of NOS3 (Förstermann and Münzel, 2006)

The above figure demonstrates the process of dimerization and regulation of NOS3 activity by intracellular Ca^{2+} and phosphorylation. NOS3 gets functionally active by important phosphorylation sites at Ser1177 and Thr495 residue. The intracellular Ca^{2+} facilitates the flow of electrons from NADPH in the reductase domain to the haem in the oxygenase domain. Through the PI3/Akt pathway, the NOS3 gets activated by phosphorylation at Ser1177 and deactivated by phosphorylation at Thr495 in the presence of protein kinase C.

The post-translational modification leads to further activation of NOS3 which acts on its substrate L-arginine in the presence of cofactors like BH4, flavin-adenine-dinucleotide, flavin-mononucleotide, and nicotinamide-adenine-dinucleotide-phosphate that catalyses the reaction to form L-citrulline and produce bioavailable vasoactive NO (Dimmeler et al., 1999; Fulton et al., 1999). The available L-arginine substrate concentration is pivotal for NOS3 activation, where NOS3 competes with Arginase that indirectly influences the NOS3 activation process (Durante et al., 2007; Pernow and Jung, 2013; Yang et al., 2013). Under severe oxidative stress conditions influenced by any intrinsic or extrinsic pathophysiological factors, there is obvious production of ROS like $O_2^{\bullet-}$, H_2O_2, and $^{\bullet}OH$. Alteration in the redox homeostasis induces elevated expression and activation of

Arginases (Silva et al., 2012; Lucas et al., 2014). The increased activation of Arginase "steals away" the common substrate L-arginine, i.e. required to generate NO and L-citrulline. Due to depletion in the common L-arginine substrate concentration, the NOS3 protein remained uncoupled in their inactive monomer state and produces an excess of $O_2^{\bullet-}$ instead of vascular bioactive NO. The elevated level of $O_2^{\bullet-}$ undergoes a spontaneous reaction and scavenges the limited bioavailable NO in the vascular system by forming a deleterious pro-oxidant $ONOO^-$ an entity (Cau et al., 2012; Yang and Ming, 2013; Lucas et al., 2014). Thus, any disruption in the redox homeostasis balance signifies endothelial dysfunction (ED) with impaired endothelial growth and vasodilation due to low bioavailable NO production in the vessels.

ED stands as a hallmark for any kind of vascular comorbidities (Berk et al., 2000; Granger et al., 2001; Nedeljkovic et al., 2003). Chronic conditions e.g. oxidative stress, smoking, environmental pollutants, and oxidation of low-density lipoproteins cause drastic downregulation of bioavailable NO in the endothelium that leads to the consequences of ED (Ding and Triggle, 2005; Barthelmes et al., 2017). It contributes to the complications and diseases like diabetes, atherosclerosis, hypertension, obesity, asthma, neurodegenerative diseases, etc. These kinds of comorbidities collectively signify "redox diseases" (Schächinger et al., 2000; Heitzer et al., 2001; Watson, 2014; Casas et al., 2015).

There has been strong evidence showed, NO released by the vascular endothelium has crucial roles and serves as an important endothelial-derived relaxation factor (Vanhoutte et al., 2017). Thus the development of ED mainly involves three major harmful NO associated events like (i) scavenging of NO due to overproduction of $O_2^{\bullet-}$, (ii) reduced vascular antioxidant capacity and (iii) altered NOS3 expression and its functional activity (Nedeljkovic et al., 2003; Montorfano et al., 2014; Krüger-Genge et al., 2019).

Endothelium being the innermost framework of all vascular systems acts as a major interface between blood circulation and diverse organ systems in regulating vascular homeostasis conditions, blood pressure, blood fluidity, or permeability (Krüger-Genge et al., 2019; Minami et al., 2019). It directly comes in contact with all the blood components and especially shares an intimate crosstalk with the predominant circulating RBCs. Red blood cells are unique in their both structural and functional features. In general, RBCs were mainly ascribed as carriers transmitting oxygen and NO into the vascular bed. The ground-breaking fact vividly described and demonstrated NO synthase (NOS) transcript and/or protein within RBCs (RBC NOS), showing an “erythrocrine function” that can synthesize and significantly contribute to the intravascular NO pool to regulate physiologically relevant mechanisms (Kleinbongard et al., 2006; Cortese-krott and Kelm, 2014). Thus currently RBCs have been known to regulate vascular function through the modulation of oxygen delivery along with scavenging and generation of NO, so now RBCs are not only being considered as the "sink" but also the "source" for NO production. Though RBCs unlike endothelial cells lack cellular organelles like the nucleus, endoplasmic reticulum, and Golgi complex, we supposed that the RBC-derived NOS has common but distinct regulatory mechanisms (Figure 6) when compared with endothelial NOS3 (Özüyaman et al., 2008).

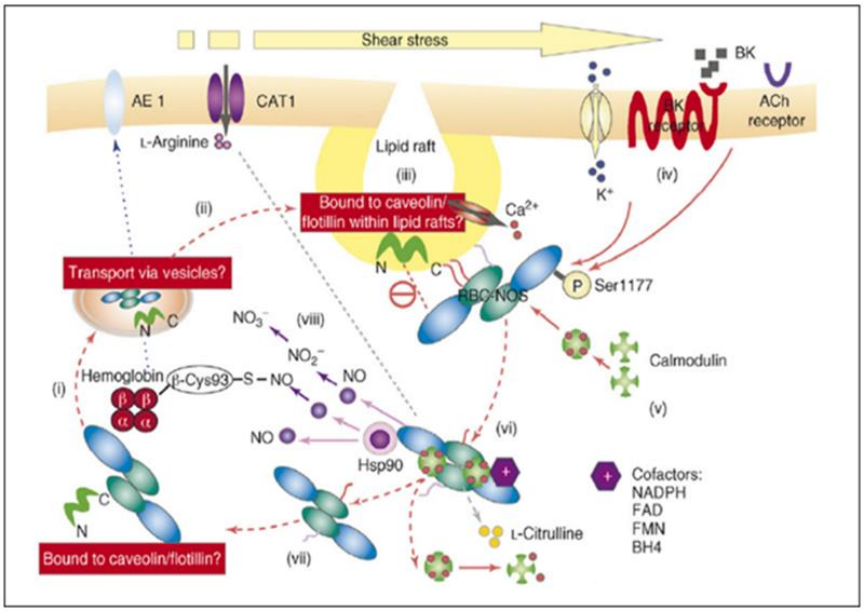

Figure 6: Possible Regulatory Pathway for RBC NOS (Özüyaman et al., 2008)

The above figure illustrates the hypothetic cycle involving RBC NOS regulatory pathway. RBC NOS gets bound to caveolin-1 in the cytoplasm and is located near the lipid rafts in its inactive form. An influx of intracellular Ca^{2+} causes stimulation and further activation of NOS by phosphorylation at Ser1177 residue.

Even though the redox regulation in RBCs, intervenes with numerous sources of oxidants including high levels of molecular oxygen that gets bound to haemoglobin, endogenously it has a well-equipped redox buffering system. Therefore, RBCs can maintain the redox balance and get actively involved in the regulation of vascular tone, especially during hypoxic and ischaemic conditions by the release of bioactive NO and adenosine triphosphate (Cortese-krott and Kelm, 2014; Kuhn et al., 2017). Under pathological states, the RBC redox status gets altered and fails to counteract the pro-oxidant status of the microenvironment. Instead, RBCs themselves become a source of reactive species and consequently, its typical structural and functional features are lost (Minetti et al., 2007; Zhou et al., 2018a; Dugmonits et al., 2019). Based on an intimate crosstalk mechanism between the RBCs and vascular endothelium, Pernow and colleagues demonstrated that under disease states like Type 2 diabetes mellitus RBCs showed excess levels of ROS, marked alteration in their protein profile and enzymatic activities with

increased adhesion capabilities. This further induced and synergized the process of vascular impairment, termed as ‘erythropathy’ (Zhou et al., 2018a; Pernow et al., 2019b). Long-term intrauterine hypoxic conditions prevail during multiple/twin pregnancy, this intrinsic factor can regulate the short and long-term NO synthesis and its vasoactive effects in the umbilical cord vessels. Due to persistent hypoxia, via the intimate cross-talk mechanism, the redox homeostatic conditions both in the vascular endothelium and RBCs get perturbed which might augment the rate of vascular endothelial dysfunction.

2. Aims

The presence of intrauterine hypoxia causes excessive production of ROS and leads to foetal oxidative stress, which variedly contributes to the occurrence of pathological conditions in post-natal or adult life. From the clinical purview, comparison of singleton versus twin neonates always experience enhanced intrauterine hypoxia with advanced cellular stress conditions, that might directly or indirectly get associated with several RBC and umbilical cord disorders. The establishment of an efficient cross-talk between the vascular endothelium and circulating RBCs is necessary to improve the rate of blood flow in the cord vessels by vasodilation. The developmental status of neonates is mainly determined by several multifactorial and complex processes, where the involvement of the NOS3 signalling pathway and its subsequent activation steps becomes pivotal. The NOS3 pathway significantly controls the level of bioavailable NO and in this way can modulate the supply of oxygen and nutrition to the developing foetus.

In our work, taking into account the highly hypoxic intrauterine circumstances due to twin pregnancy, we have pursued the molecular and functional consequences and its harmful effects on the vascular cord endothelial layer and the circulating RBCs of the developing foetuses. We searched for major alterations in the regulatory parameters which play crucial roles in the NOS3 signalling pathway to maintain the bioavailable NO level. Further, we tried to shed light on the activation of any rescue/or compensatory mechanisms to combat the higher demand of bioavailable NO in both the umbilical cord vessels and foetal circulating RBCs. In detail following the NOS pathway, our study targeted to identify an early marker for cardiovascular disorders and/or other relevant comorbidities.

In connection to this, we studied in detail to find answers for the following questions: -

- How do alterations in the NOS3 expression and its post-translational modifications along with the ROS-inducible NOS3 competitor of Arginase1 expression affects the functionality of the UC endothelial layer and circulating foetal RBCs?
- Is there any evidence of the circulating foetal RBCs that can show a compensatory or alternative mechanism to increase the bioavailable NO level in the vessels?
- What is the level of free radicals'/oxidants formation in the RBCs derived from the twins and the singletons?
- What are the significant changes in the distribution pattern of different phenotypic variants in the RBC populations derived from singletons and twin populations?
- What are the consequences/extent of damages occurred due to a higher level of pro-oxidants both in the UC vessels and circulating RBCs?
- Is there any connection between the birth weight of the foetus and the expression/activation of the NOS3 system in the UC vessels and the circulating RBC population?

3. Materials and Methods

3.1. Human samples

In accordance with the Declaration of Helsinki, informed consent was collected from the pregnant women in order to procure a small portion of the umbilical cord along with foetal cord blood samples. The study protocol (16/2014; Investigation of oxidative stress markers in maternal and neonatal blood samples) was approved by the Ethics Committee from the Department of Obstetrics and Gynaecology at the University of Szeged, Hungary. The study protocol strictly followed several exclusions criteria for collection of the clinical samples such as (i) maternal age below 18 years, (ii) gestational diabetes, infection and inflammatory conditions or disorders such as cardiovascular diseases, (iii) complications or difficulty during delivery, (iv) dizygotic twin birth (v) foetal distress, (vi) malformations or evidence of genetic disorders and (vii) neonates born from mothers addicted to alcohol and /or smoking habit. The nutritional status of the mothers during pregnancy was satisfactory; no case of malnutrition occurred.

The collected clinical samples were grouped under different inclusions criteria as mentioned:-In the first group, a total of 21 pairs of mature non-discordant twin neonates and 32 age- and weight-matched singletons were taken as controls in comparison. Twin neonates were categorized based on their birth weight; 3000 – 3200 gr (High birthweight twin-Hwt) and 2400–2600 gr (Low birthweight twin-Lwt) in comparison to age- and weight-matched singletons as High birthweight singleton (Hws) and Low birthweight singleton (Lws). Here, the clinical parameters of the study group and the maternal age are presented in the following Table 1.

Clinical Parameters	Full-term single neonates	Full-term twin neonates
Numbers of Samples (N)	Hws: N = 22 Lws: N = 10	Hwt: N = 24 Lwt: N = 18
Gestational age at delivery (weeks)	37.52 ± 0.50	37.35 ± 0.47
Birth weight (kg)	Hws: 3.30 ± 0.172 Lws: 2.59 ± 0.171	Hwt: 3.19 ± 0.073 Lwt: 2.6 ± 0.174
APGAR score at 10 min	9.92 ± 0.27	9.69 ± 0.53
Ratio of vaginal delivery /caesarean section	28:4	34:8
Maternal age (years)	29.5 ± 6.11	31.9 ± 7.12
Blood sample pH	7.26 ± 0.13	7.29 ± 0.12

Table 1. The clinical parameters of the study groups and the maternal age

The second group consisted of clinical samples obtained from 16 pairs of premature non-discordant twin neonates. Similarly, the twin neonates were categorized based on their birthweight 2430-2570 gr (Premature High birthweight twin – Pr-Hwt) and 1940-1990 gr (Premature Low birthweight twin – Pr-Lwt). In this group as per the inclusion criteria 15 age (33-35 weeks) and weight (2200-2500 gr) matched singleton samples were collected taken as control (Pr-Hws) for the Pr-Hwt group. The clinical parameters of the study group and the maternal age are presented

in the following Table 2.

Clinical Parameters	Preterm single neonates	Preterm twin neonates
Numbers of Samples (N)	Pr-Hws: N= 15	Pr-Hwt: N = 20 Pr-Lwt: N = 12
Gestational age at delivery (weeks)	33.72 ± 0.53	34.27 ± 0.67

Birth weight (kg)	Pr-Hws: 2.41 ± 0.11	Pr-Hwt: 2.47 ± 0.04 Pr-Lwt: 1.97 ± 0.02
APGAR score at 10 min	9.88 ± 0.32	9.56 ± 0.66
Ratio of vaginal delivery /caesarean section	12:3	22:10
Maternal age (years)	30.52 ± 3.34	32.7 ± 4.73
Blood sample pH	7.27 ± 0.07	7.25 ± 0.12

Table 2. The clinical parameters of the study groups and the maternal age

The third group in total considered 10 pairs of premature monozygotic discordant twin pair neonates with both monochorionic-diamniotic and dichorionic-diamniotic origin. The criteria for discordance was followed as per the guidelines laid down by ACOG USA, with a minimum of 25% discordance in their birthweight between the twin pairs. The twin pairs were compared and grouped according to their discordance in birthweight as 2600-2890 gr/35-35+4 weeks (Premature Discordant High birthweight twin – PrD-Hwt) and 1860-2040 gr/35-35+4 weeks (Premature Discordant Low birthweight twin – PrD-Lwt). The clinical parameters of the study group and the maternal age are presented in the following Table 3.

Clinical Parameters	**Preterm Discordant twin neonates**
Numbers of Samples (N)	PrD-Hwt: N= 20 PrD-Lwt: N= 20
Gestational age at delivery (weeks)	35.21 ± 0.23
Birth weight (kg)	PrD-Hwt: 2.63 ± 0.15 PrD-Lwt: 1.87 ± 0.12
APGAR score at 10 min	9.52 ± 0.65

Ratio of vaginal delivery /caesarean section	4:6
Maternal age (years)	33.42 ± 4.08
Blood sample pH	7.22 ± 0.06

Table 3. The clinical parameters of the study groups and the maternal age

3.2. Red blood cell smear image processing and data analysis

Using the validated calculation software MatLab tool CIDRE (Smith et al., 2015) we processed and analysed eosin-stained blood smear images, that gets originated from each of the collected sample groups. Identification of different phenotypic variations in the RBC population was conducted in an automated bioimage analysis tool CellProfiler™, (available on http://cellprofiler.org) (Carpenter et al., 2006), The CellProfiler™ offered methods to extract features of the cells, that uses intensity statistics likewise minimum-, maximum, mean-, median intensities and their standard deviation and could also extract different characteristic cell shape and features such as area. Applying an intelligent analysis software platform like the Advanced Cell Classifier (Horvath et al., 2011) (ACC, available on http://cellclassifier.org), we could identify and populate distinct phenotypes present in the populations. The automated analysis software ACC is completely based on the model trained techniques that could predict any given cellular phenotypic variations with the usage of advanced machine learning methods like active learning and neural networks, having minimal user interaction. The dataset analysis by ACC provided a detailed insight into the distribution pattern of each phenotype of interest with their frequency count in comparison to the control within the different study populations.

3.3. Preparing umbilical cord and arterial cord blood samples for immunostaining

Small portions of the dissected umbilical cord (UC) were fixed with 4% (w/v) paraformaldehyde in 0.05M phosphate buffer pH 7.4 (PB) and cryopreserved with 30% (w/v) sucrose in PB with addition of 0.1% (w/v) Na-azide. Specimen samples were embedded in Tissue-Tek® O.C.T.™ (Sakura Europe, 4583) and cryosectioned with a slice thickness of 16 µm. Further, it gets mounted on Superfrost™ ultra plus® (Thermo scientific, J3800AMNZ) microscope slides and kept on -80ºC till further processing (Nishikawa et al., 2016). The whole blood derived from the cord arteries of the neonates was subjected to centrifuge at 200 x g for 10 min at 4°C. The lower two-thirds of the RBC phase was collected, washed with physiological salt solution (0.9 % NaCl, w/v), and fixed with 4% (w/v) paraformaldehyde in 0.05M PB at 4°C for 1hr and further processed for immunostaining (Cortese-Krott et al., 2012). To test the homogeneity and purity of the isolated RBCs, the cells were immunostained with RBC-specific marker anti-Glycophorin A, where the purity of the samples was > 95% for RBCs. (Chakraborty et al., 2019).

3.4. Immunolabelling and image processing of the umbilical cord sections

The umbilical cord sections were fixed and stained as per the standard protocols (Chakraborty et al., 2020). Slides with UC sections were withdrawn from - 80°C, thawed, and dried at room temperature. After consecutive washing with 0.05M PB, the sections were permeabilized by 0.1% Triton X-100 at room temperature for 20 min. This was followed by blocking the non-specific antibody binding with 4% (w/v) bovine serum albumin (BSA) and 5% (v/v) normal goat serum in PB. UC sections of the samples were immunolabelled with primary antibodies overnight at 4°C, then washed and further incubated with goat anti-mouse/anti-rabbit Alexa®647- or goat anti-rabbit/anti-mouse Alexa®488-conjugated secondary antibodies in 1:2000 dilution, for 2 h in dark at room temperature. Following the secondary antibody incubation step, the slides were

consecutively washed and counterstained with 4', 6-diamidino-2-phenylindole (DAPI) (D9542) from Sigma-Aldrich (St. Louis, MO, USA) in a final concentration of 1µg/ml, for 5 min in dark. The slides were completely dried and mounted using Antifading, BrightMount/Plus aqueous mounting medium (Abcam, ab103748). The slides were visualised and images were captured under an epifluorescence microscope (Nikon Eclipse 80i, 100x and 50x immersion objective; Nikon Zeiss Microscopy GmbH, Jena, Germany) with a QImaging RETIGA 4000R camera, using Capture Pro 6.0 software (QImaging, Surrey, BC, Canada).

During imaging, the arteries and veins of each sample were captured at 5-10 independent fields, resulting in at least 50 individual images of each vessel circumferences. Images were processed and analysed using ImageJ® software (http://imagej.nih.gov/ij/). In brief, the composite pictures were split into channels, corresponding to one specific antibody labelling. The endothelial layer was marked out by using the software-derived indicator tool and analysed the relevant signal particles by running a pre-recorded macro, which was optimized to our study protocol. The parameters were kept constant throughout the evaluation protocol. As a result, we saved the relevant regions of interest and projected it to the parent images. The mean grey values were measured, which are proportional to the mean fluorescent intensities (MFI) of the original images. These values were further corrected by subtracting the background fluorescence and quantifying five independent non-antibody specific fluorescent areas in each image.

3.5. Immunohistochemistry on the isolated RBCs and analysis by florescence activated cell sorting (FACS)

The isolated and fixed RBCs were washed thoroughly and permeabilized by 0.1% Triton X-100 at room temperature for 20 min. After permeabilization, cells were centrifuged at 3000 x g for 5min to discard the supernatant and consecutively washed using

0.05 PB. Further, RBCs were blocked for the non-specific antibody binding with 4% (w/v) bovine serum albumin (BSA) and 5% (v/v) normal goat serum in PB and incubated with primary antibodies for overnight at 4°C. This was followed by incubation with goat anti-mouse Alexa®647 and goat anti-rabbit Alexa®488-conjugated secondary antibodies in 1:2000 dilutions, for 2 h in dark at room temperature. Finally, RBCs were washed and processed for quantitative analysis (FACS, BD FACSCalibur™, BD Biosciences) (Mizrahi et al., 2018; Chakraborty et al., 2019). The FACS data were analysed using FlowJo™ (FlowJo™ Software for Windows Version 10). The antibody list used for immunostaining **is** mentioned below in Table 4.

Antibody	**Host**	**Dilution**	**Code**	**Distributor**
anti-Glycophorin A	mouse	1:50	MA5-12484	Thermo Fisher Scientific, Madison, WI, USA
anti-NOS3	mouse	1:100	sc-376751	Santa Cruz Biotechnology Inc., Dallas, TX, USA
anti-pSer1177 NOS3 (pNOS3)	rabbit	1:100	SAB-4300128	Sigma Aldrich, Saint Louis, Missouri, USA
anti-Arginase1	mouse	1:100	sc-166920	Santa Cruz Biotechnology Inc., Dallas, TX, USA
anti-NOS2	rabbit	1:100	ab3523	Abcam, Cambridge, UK
anti 4-hydroxy-2-nonenal (4-HNE)	mouse	1:100	ab48506	Abcam, Cambridge, UK
goat anti-mouse Alexa®647	mouse	1:2000	ab150115	Abcam, Cambridge, UK
goat anti-rabbit Alexa®488	rabbit	1:2000	ab150077	Abcam, Cambridge, UK
goat anti-mouse Alexa®488	mouse	1:2000	ab150113	Abcam, Cambridge, UK

goat anti-rabbit Alexa®647	rabbit	1:2000	ab150079	Abcam, Cambridge, UK

Table 4. List of the sources and dilutions of primary and secondary antibodies

3.6. Assay for the viability of RBCs

Arterial cord blood was collected and centrifuged at 200x g for 5 min. From the lower two-thirds of the RBC phase, 10 µl was diluted by 10x in 0.9% (w/v) physiological salt solution having pH 7.4. The diluted 1µl of the RBCs were mixed with 250µl of Annexin binding buffer and 2.5µl Annexin V using the Annexin V-FITC Apoptosis/Staining Detection kit (Abcam ab14085). The quantitative measurement was done by FACS (FACS, BD FACSCalibur™, BD Biosciences) (Fan et al., 2018) and all data were analysed using FlowJo™ (FlowJo™ Software for Windows Version 10).

3.7. Measurement of Hydrogen Peroxide Production in the RBCs populations

The assay was performed according to standard protocol (Villegas and Gilliland, 1998), RBC fraction was haemolysed by the addition of distilled water at a ratio of 1 : 9. Spectrophotometric measurements were performed using GENESYS 10S UV–Vis spectrophotometer (Thermo Fischer Scientific, Madison, WI, USA). In determining the level of H_2O_2, 10x haemolysate of the samples was diluted in 50 mM PB at pH 6.0 in a ratio of 1:250. Serial dilutions of H_2O_2 between 27.5 and 440 µM were prepared and used as standard. Samples were incubated with 0.1% (w/v) horseradish peroxidase and 1% (w/v) o-dianisidine in methanol for colour development, at 37^{o}C for 10 minutes. Reaction mixture without blood sample was used as blank. To stop the reaction 4N HCl is added. The H_2O_2 concentration of each sample was determined by the absorbance reading at 400 nm and the results were calculated to a standard curve normalized with protein concentration (µmol/mg protein) (Gilliland and Speck, 1969).

3.8. Determination of the $ONOO^-$ level in the RBCs populations

Following the $ONOO^-$ levels, the haemolysate of each sample was diluted in 1M NaOH solution in a ratio of 1: 250. The spectrophotometric measurements were performed at 302 nm, where the increase in absorbance was considered until it reached a stable equilibrium. Then the samples were added into 100mM PB at neutral pH of 7.4 in the same ratio as the reference. At neutral pH, the $ONOO^-$ decomposes and its decrease in absorbance is recorded till it reaches the equilibrium point (Huie and Padmaja, 1993). According to Lambert-Beer's law, the $ONOO^-$ concentration was calculated as the difference in the absorbance at the two distinct pH values. The final results were normalized with protein concentration (μmol/mg protein) (Lowry et al., 1951).

3.9. Statistical Analysis

All statistical analysis was considered with one-way analysis of variance (ANOVA) and Newman-Keuls multiple comparison test using GraphPad Statistical Software version 6.0. The level of statistical significance was accepted at $*p \leq 0.05$, $**p \leq 0.01$, $***p \leq 0.001$, and $****p \leq 0.0001$.

4. Results

4.1. Expression of endothelial and inducible NOS and Arginase1 in the Umbilical Cord Vessels and the Isolated RBCs

The pre-placental hypoxia leads to a severe intrauterine oxidative stress condition, and thus the NO producing NOS pathways both at the translational and phosphorylation levels are important for the maintenance of vasodilation. Here we followed in detail the NOS pathway -within the vascular cord endothelium and isolated arterial cord RBC populations taken from different categories of mature and premature twins in comparison to their age- and weight-matched singletons.

4.1.1. Mature Non-Discordant Study Population

UC sections originated from mature non-discordant high (Hwt) and low (Lwt) birth weight twins along with their age- and weight-matched singletons were immunolabelled in parallel with anti-NOS3/anti- phosphorylation at Ser1177 residue (pNOS3) and subjected to Image J© evaluation. In the endothelium of both the arteries and veins, originated from Hwt, as compared to their age and weight-matched controls (Hws) showed a significantly lowered intensity level of NOS3 and pNOS3. The NOS3 gets lowered by ~ 25% and 50%, while the pNOS3 by ~35% and 69%, in the artery and vein, respectively (Figure 7).

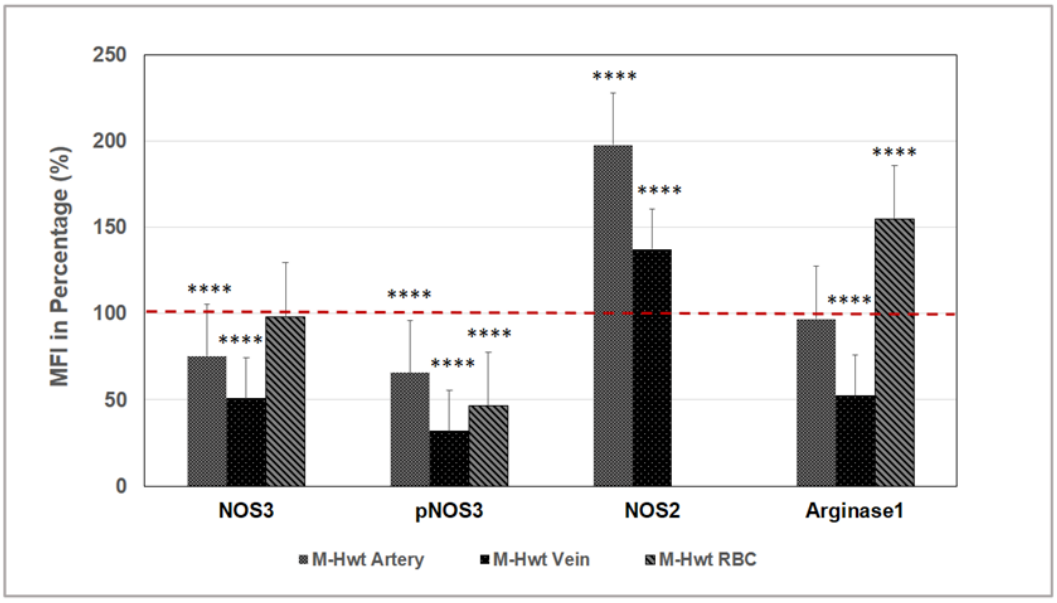

Figure 7: Quantification of the expression of NOS3 and its phosphorylation level at Ser1177 residue, NOS2, and Arginase1 in the vascular endothelium and arterial cord RBCs of the high weight mature non-discordant twin neonates

Mean fluorescence intensity (MFI) was expressed in percentage of NOS3 and its activated level pNOS3, NOS2, and Arginase1 of the mature non-discordant high birth weight (M-Hwt) N=24 twin neonates in comparison to their age and weight-matched singletons N=22 taken as control. The red dotted line represents the control intensity level at 100% within the cord vessel endothelial cells and isolated arterial cord RBCs. The significant differences were accepted at **** $p < 0.0001$ based on one-way ANOVA using the Newman-Keuls multiple comparison test.

In the Lwt group, only the vein endothelium demonstrated a significant low level of NOS3 (~37%) and pNOS3 (52%) in comparison to their matching low weight singleton (Lws), while the artery showed no significant changes in either of the value (Figures 8). Based on the ratio of NOS3/pNOS3 values, the NOS3 phosphorylation status was somewhat increased in the vein, while remained more or less unchanged in the arteries. The detailed representative epifluorescent images are in the Appendix section (Figure S1 and S2).

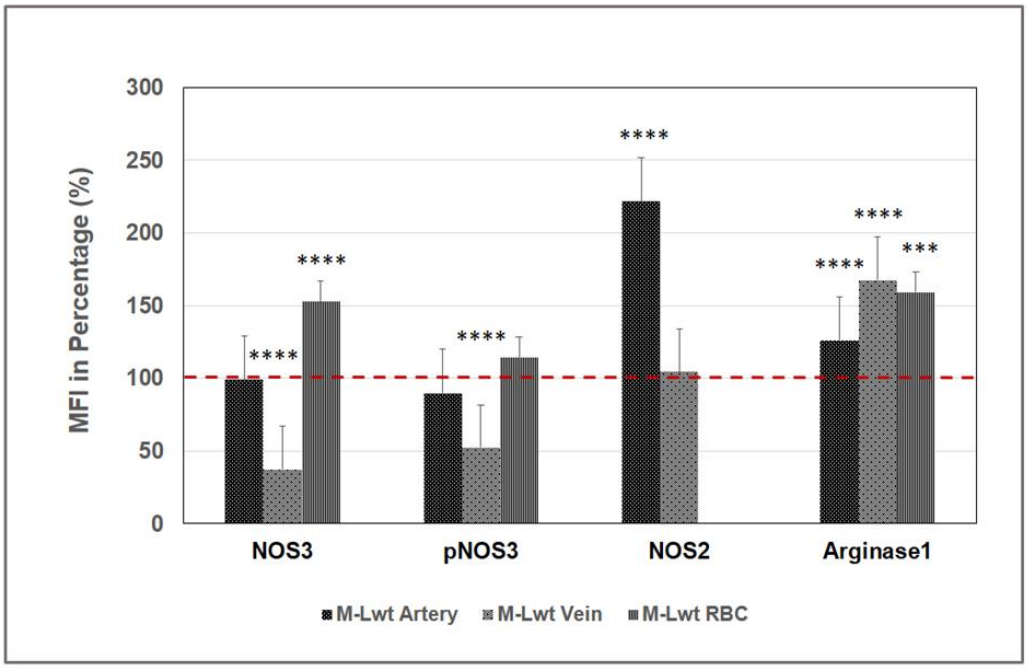

Figure 8: Estimation of the expression of NOS3 and its phosphorylation level at Ser1177 residue, NOS2, and Arginase1 in the vascular endothelium and arterial cord RBCs of the low weight mature non-discordant twin neonates

Quantifying the MFI were expressed in percentage of NOS3 and its activated level pNOS3, NOS2, and Arginase1 of the mature non-discordant low birth weight (M-Lwt) N=18 twin neonates in comparison to their age and weight-matched singletons N=10 taken as control. The red dotted line represents the control intensity level at 100% within the cord vessel endothelial cells and isolated arterial cord RBCs. The significant differences were accepted at ***$p < 0.001$ and ****$p < 0.0001$ based on one-way ANOVA using the Newman-Keuls multiple comparison test.

The NOS3 activation pathway gets highly influenced by the Arginase1 competing for the common substrate L-arginine. Following the UC sections immunolabelled with Arginase1, showed a significant difference between the vein and arterial endothelium in Hwt and Lwt groups. In the Hwt artery, the Arginase1 intensity level was almost similar to their age -and a weight-matched singleton, whereas it is decreased by 48% in the vein (Figure 7). Contrastingly, the Lwt group indicated an increase of 26% in the artery and 68% in the vein (Figure 8). The detailed representative epifluorescent images are in the Appendix (Figure S3 and S4).

Under shear stress conditions, the inducible NOS2 expression might serve as an alternative NO-producing pathway that increases the bioavailable NO level in the vascular endothelial layer. The arterial endothelium showed a significant rise in the NOS2 level with 98% in Hwt (Figure 7) and 122% in Lwt groups (Figure 8) in comparison to their matched singletons. In the Hwt vein endothelium, the NOS2 level indicated a moderate increase of 37% (Figure 7), while it remained unchanged in the Lwt category (Figure 8). The detailed representative epifluorescent images are shown in the Appendix part (Figure S3 and S4).

The isolated arterial RBC populations underwent quantitative FACS analysis, following the NOS3 level and its phosphorylation status at Ser1177 residue. In the Hwt category, NOS3 was in a close match with the respective Hws (Figure 7), while there was a significant increase of ~53% in the Lw twins (Figure 8). The pNOS3 level highly lagged by ~54% in the Hwt in comparison to their matched control (Figure 7), while in the Lwt group a moderate increase by ~14% was measured (Figure 8). There had been an increased distribution of high NOS3 expressing cell population in the Hw and Lw twin neonates by 60% and 48%, respectively but it does not state an upregulation in the NOS3 activation level since its phosphorylation status remained low in comparison to their age and weight-matched singletons (Figure 9).

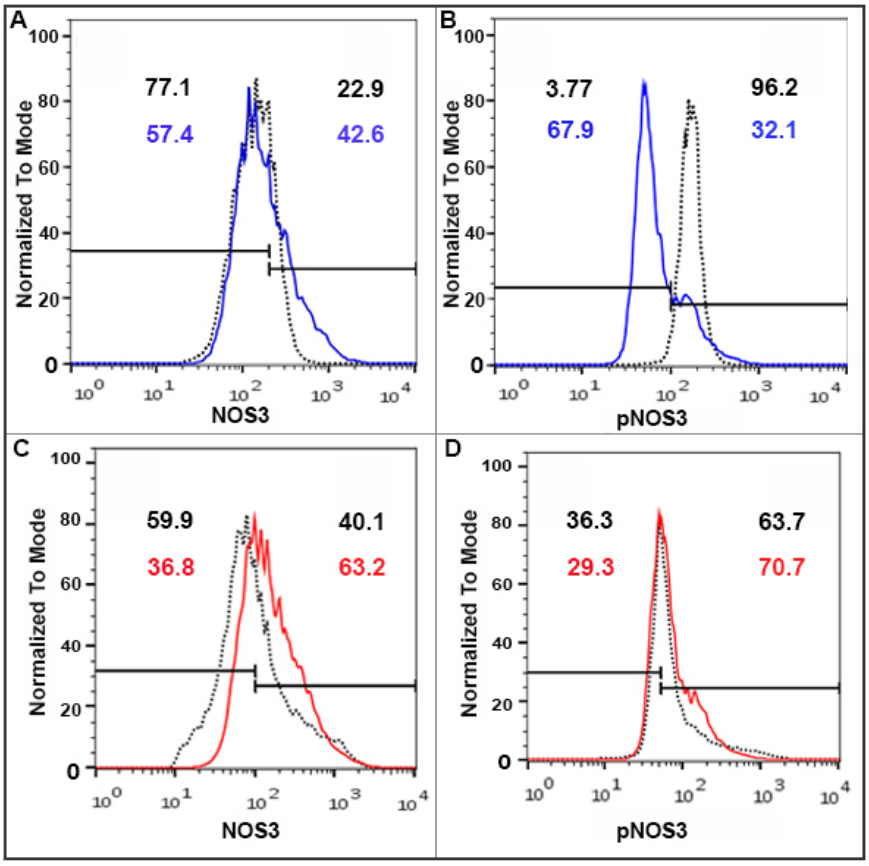

Figure 9: FACS (Fluorescence-activated cell sorting) analysis on arterial cord RBCs immunolabelled with NOS3 and pNOS3 from the mature twin neonates and their matched singletons

Representative histograms using FACS analysis show the NOS3 (A, C) and pNOS3 (B, D) intensities, respectively in the M-Hwt (blue line) and M-Lwt (red line) with their matched singletons (black dots). In each case, an arbitrary borderline was considered which divides the total RBC population into basal and high-intensity levels.

Furthermore, Arginase1 expression gets upregulated in both the Hw and Lw twins by 54.60% and 59.23%, respectively (Figure 7 and 8) along with a significant increase in the frequency of high Arginase1 expressing cells population i.e. 86% in Hwt and 67% in the Lwt group irrespective of their differences in birthweight (Figure 10).

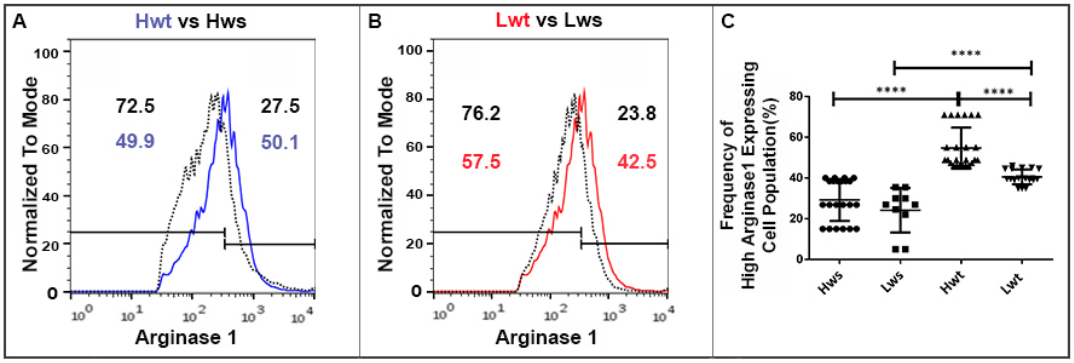

Figure 10: Evaluation of FACS analysis on the Arginase1 immunolabelled arterial cord RBCs

Panels (A, B) show representative histogram plots as measured by the FACS analysis using anti-Arginase1 primary antibodies on the foetal arterial cord RBCs derived from the mature twin neonates and their matched singletons respectively. In the control and twin samples, an arbitrary borderline was considered along the x-axis dividing the total RBC population into basal and high Arginase1 expressing cells. The graphical representation in the (C) panel indicates the frequency of high Arginase1 expressing RBC population from M-Hwt (N=24) vs M-Hws (N=22) and M-Lwt (N=18) vs M-Lws (N=10). The statistical significance was accepted at ****p<0.0001 based on one-way ANOVA using the Newman-Keuls multiple comparison test.

4.1.2. Premature Non-Discordant Study Population

Here the preterm non-discordant high birth weight twin neonates were compared to their age- and weight-matched singletons and age-matched twin pairs born with low birth weight. The UC sections were immunolabelled with anti-NOS3/anti-pNOS3. The cord arterial endothelium of the Hwt showed a significant increase in the NOS3 expression and its phosphorylation intensity level by ~13% and ~17% respectively in comparison to their age – and weight-matched singletons (Hws). In this vein, both the values of NOS3 and pNOS3 intensity levels remained unaltered (Figure 11).

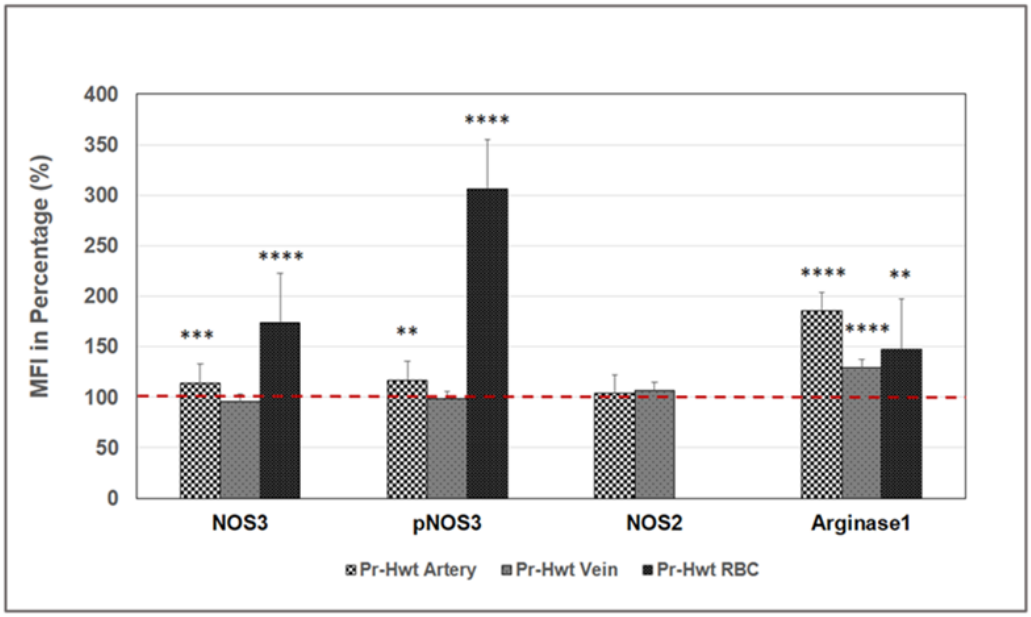

Figure 11: Estimation of the expression of NOS3 and phosphorylated NOS3, NOS2, and Arginase1 in the vascular endothelium and arterial cord RBCs of the high weight preterm twin neonates

Mean fluorescence intensity was expressed in percentage of NOS3 and its activated level i.e. phosphorylated NOS3 (pNOS3), NOS2, and Arginase1 of the preterm non-discordant high birth weight twin neonates (Pr-Hwt) N=20 in comparison to their age and weight-matched singletons (Pr-Hws) N=15 taken as control. The red dotted line represents the control intensity level at 100% within the cord vessel endothelial cells and isolated arterial cord RBCs. The significant differences were accepted at $^{**}p < 0.01$, $^{***}p < 0.001$ and $^{****}p < 0.0001$ based on one-way ANOVA using the Newman-Keuls multiple comparison test.

The comparison between the Hw versus Lw twin populations indicated that the NOS3 expression in the Lwt arteries to some extent remained behind the Hwt values (~28%) with about the same phosphorylation intensity level. The NOS3 expression in the Lw vein stayed unaltered with a significant increase by ~26% in the pNOS3 intensity level (Figure 12). The detailed representative epifluorescent images are in Appendix (Figure S5 and S6).

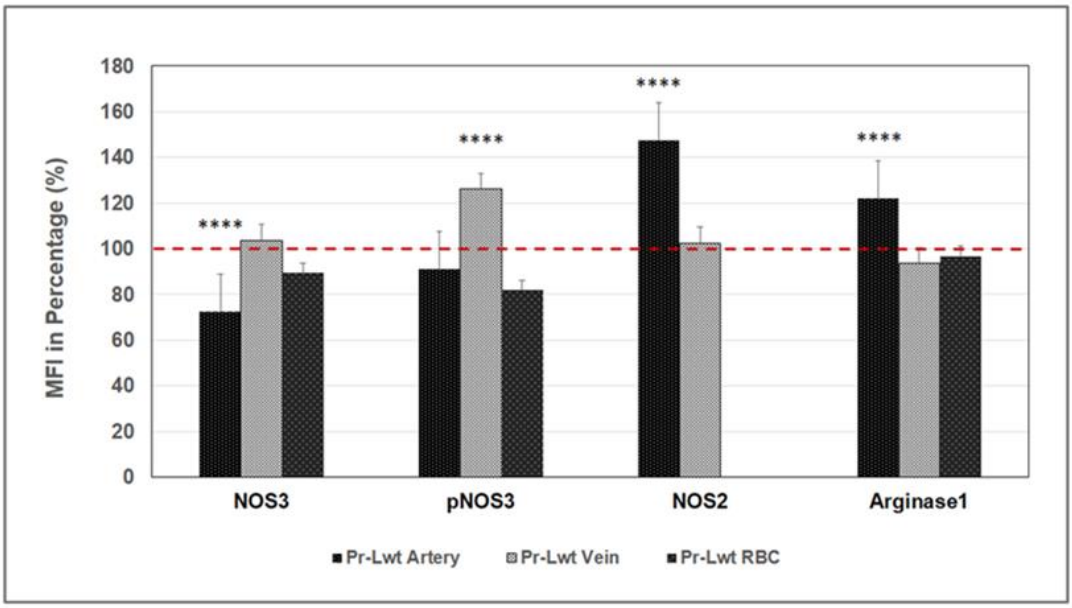

Figure 12: Quantification of the expression of NOS3 and phosphorylated NOS3, NOS2, and Arginase1 in the vascular endothelium and arterial cord RBCs of the low weight preterm twin neonates

Estimation of the MFI was expressed in percentage of NOS3, phosphorylated NOS3, NOS2, and Arginase1 of the preterm non-discordant low birth weight (Pr-Lwt) N=12 twin neonates in comparison to their high weight twin group (Pr-Hwt) N=20 taken as control. The red dotted line represents the control intensity level at 100% within the cord vascular endothelial cells and isolated arterial cord RBCs. The significant differences were accepted at ****$p < 0.0001$ based on one-way ANOVA using the Newman-Keuls multiple comparison test.

As a consequence, the phosphorylation status of NOS3 gets upregulated in both the vessels of Lwt in comparison to the Hwt group. Considering the role of Arginase1, being a critical modulator of NOS3 we find that the Arginase1 expression is elevated significantly in both the arteries and veins of the Hw twins by ~85% and ~30%, respectively in comparison to the Hws (Figure 11). In correlation, with the Lwt and Hwt populations, there was a ~22% increase in the Arginase1 expression within the Lw arteries while no significant difference was detectable in the veins (Figure 12).

Upregulation of NOS2 might be an important biomarker that can maintain the bioavailable NO level in the vascular endothelial layer under shear stress conditions. The age -and weight-matched singleton versus Hwt indicated no significant difference in the

NOS2 expression for any of the cord vessels (Figure 11). In the case of Lwt in comparison to Hwt samples, the NOS2 expression was significantly higher in the Lwt arteries ~ 47%, while there were no detectable changes in the vein (Figure 12). The detailed representative epifluorescent images are in the Appendix part (Figure S7 and S8).

Following the NOS3 and pNOS3 intensity level by FACS analysis in the isolated arterial RBC population, the Hwt in comparison to Hws showed an elevated expression of NOS3 by ~ 73.64% and almost ~ 206.35% higher NOS3 phosphorylation intensity level (Figure 11 and 13). While in between the Hw and Lw twin neonates there lies no significant variation in the NOS3 and phosphorylated NOS3 intensity values (Figure 12 and 13).

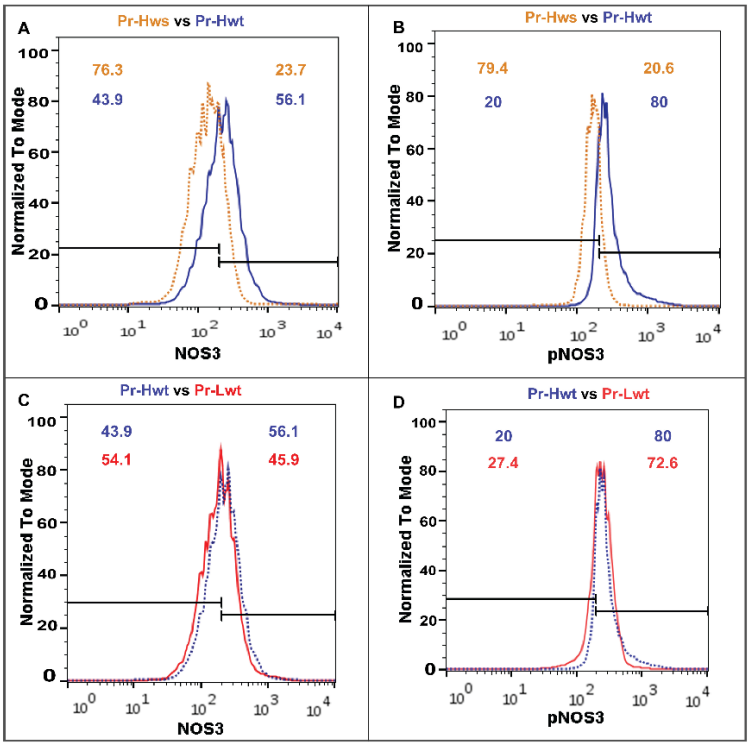

Figure 13: FACS analysis on NOS3 and pNOS3 immunolabelled foetal RBC populations originated from preterm, non-discordant twin and matched singleton neonates

Representative histograms (A, B) showing NOS3 and pNOS3 intensity levels in preterm, high weight twin (Pr-Hwt, blue line) in comparison with their age and weight-matched singleton (Pr-Hws, orange dots). Similarly, histograms (C, D) represent the comparison between Pr-Hwt (blue dots) with low weight (Pr-Lwt, red line) twin samples. In each case, an arbitrary borderline was considered dividing the total RBC population into basal and high-intensity levels.

The expression of Arginase1 in the isolated RBCs via FACS analysis clearly indicated an elevation by 48% in the Hwt to their age and weight-matched singletons (Figure 11 and 14), while in the Hwt versus Lwt group there was no significant difference in Arginase1 expression level (Figure 12 and 14).

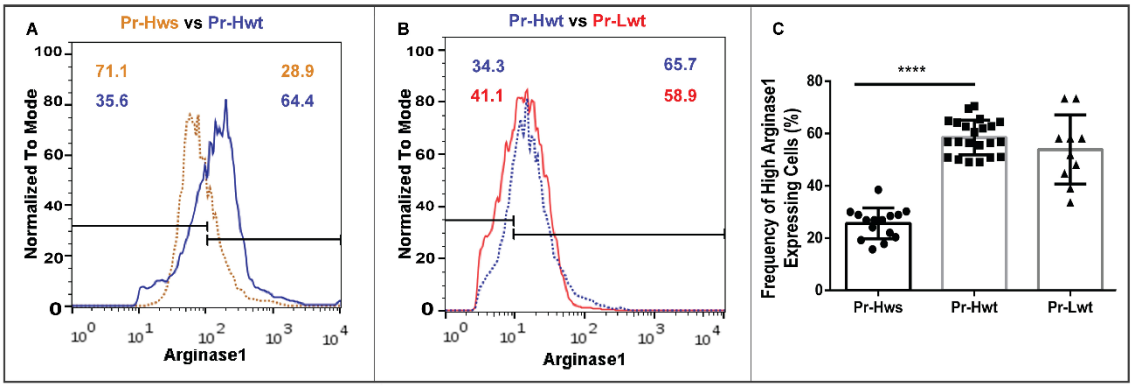

Figure 14: FACS analysis on RBC populations, immunolabelled with Arginase1

Representative histograms as measured by the FACS analysis using anti-Arginase1 primary antibodies showed in panel (A) the comparison between foetal RBCs derived from preterm, non - discordant high weight twin (Pr-Hwt, blue line) with their age-matched high weight singleton (Pr-Hws, orange line) and (B) presents the comparison between Pr-Hwt and low weight (Pr-Lwt, red line) twin sample. For each control and twin sample, an arbitrary borderline was considered along the x-axis dividing the total RBC population into basal and high expressing cells. The graphical plot (C) indicates the frequency of high Arginase1 expressing RBC populations in the preterm, non-discordant twin neonates (Pr-Hwt-N=20; Pr-Lwt-N=12) and age -weight-matched singletons (Pr-Hws-N=15). The statistical significance was accepted at ****$p<0.0001$ based on one-way ANOVA using the Newman-Keuls multiple comparison test.

4.1.3. Premature Discordant Study Population

The NOS3 activation pathway was followed in twin siblings, born with high birth weight differences i.e. more than 25%.

The UC sections derived from the discordant preterm twin pairs were immunostained and subjected to Image J© evaluation. The NOS3 expression and its phosphorylated level of the Lw neonates significantly lag behind in comparison to their high weight siblings; in the artery by 37% and 45%, while in the vein ~19% and ~26%, respectively (Figure 15). The detailed representative epifluorescent images of the vascular endothelium are

described in Appendix (Figure S9 and S10). As a result, the phosphorylation status of NOS3 was low in both the vessels of the Lw-siblings originated from the discordant twin pair.

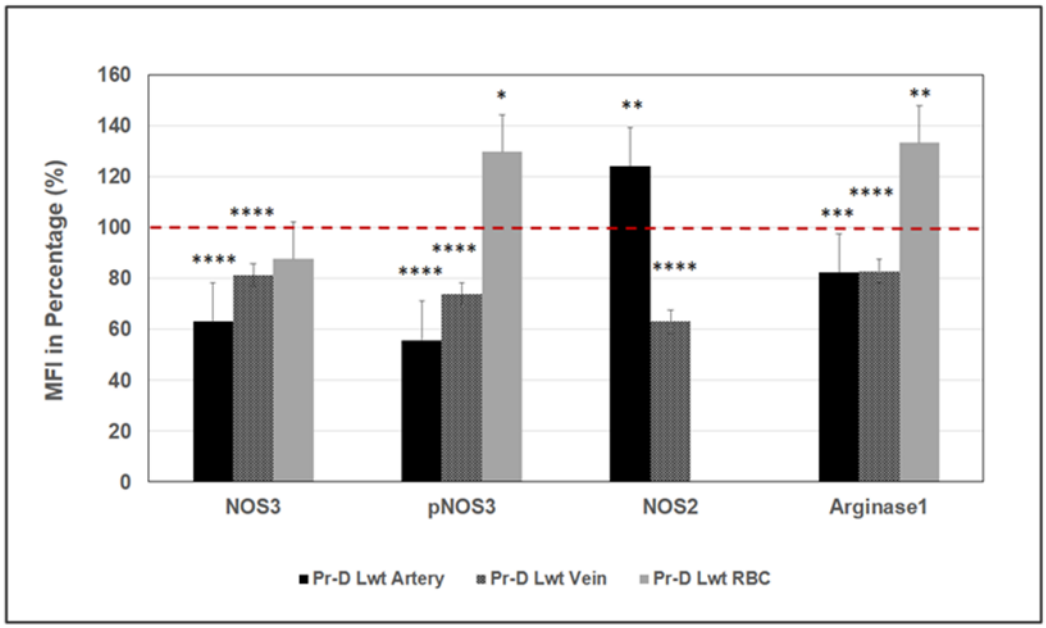

Figure 15: Estimation of the expression of NOS3 and activated pNOS3, NOS2, and Arginase1 in the vascular endothelium and arterial cord RBCs between the premature discordant twin pair

Quantification of the MFI was expressed in percentage of NOS3, phosphorylated NOS3, NOS2, and Arginase1 of the preterm discordant low birth weight twin neonates (N=20) in comparison to their high weight twin pair (N=20), considered as control. The red dotted line represents the control intensity level at 100% within the cord vascular endothelial cells and isolated arterial cord RBCs. Statistical significances were accepted at *p < 0.05, **p < 0.01, ***p < 0.001 and ****p < 0.0001 based on one-way ANOVA using the Newman-Keuls multiple comparison test.

We know in the NOS3 regulation pathway the expression of Arginase1 plays a very vital role. Here we find that the Arginase1 expression in the Lw-neonates is significantly lower in both the arteries and vein by ~17-18% compared to their siblings (Figure 15). Whereas, the NOS2 being an alternative source for bioavailable NO, was present at a much higher level in the cord arterial endothelium of the low weight siblings to almost ~24%, while in the vein it was significantly lowered by ~37% (Figure 15). The detailed representative epifluorescent images are in the Appendix section (Figure S11 and S12).

In parallel, isolated cord arterial RBCs were immunostained for FACS analysis. No significant difference was detected in the NOS3 expression and frequency of the high NOS3 expressing cells between the discordant twin pairs (Figure 15 and 16).

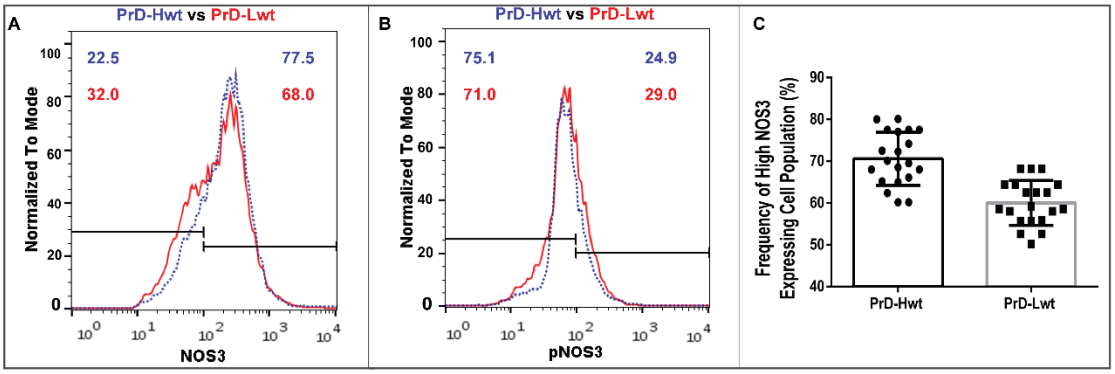

Figure 16: FACS analysis on foetal RBC populations originated from preterm, discordant twin neonates, immunolabelled with NOS3 and pNOS3

FACS analysis on foetal RBCs from preterm, discordant twin siblings, immunolabelled with anti-NOS3 and anti-pNOS3. The representative histograms (A, B) using FACS analysis show the NOS3 and pNOS3 intensity levels in preterm, high weight (PrD-Hw twin, blue line) and low weight twin samples (PrD-Lwt, red line) respectively. The graphical representation (C) exhibits the frequency of high NOS3 expressing cell population derived from preterm discordant twins where N=20 pairs.

However, we find that the pNOS3 intensity level was significantly higher in the low weight neonates by ~29% (Figure 15), as a result, the phosphorylated status of NOS3 significantly increases (Figure 17).

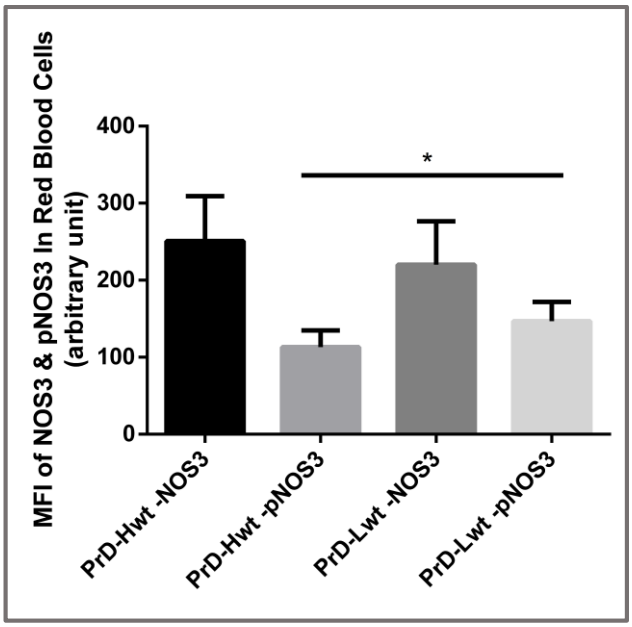

Figure 17: Illustration of MFI on the NOS3 expression and its phosphorylated level (pNOS3) in the foetal RBC populations

The graphical plot illustrates the MFI of NOS3 expression and its activation/phosphorylated level at Ser1177 residue in the foetal RBCs, derived from preterm, discordant twin neonates. The significant differences were accepted at *p< 0.05 based on one-way ANOVA using the Newman-Keuls multiple comparison test.

The Lw siblings show a significantly higher level of Arginase1 expression to almost ~33% (Figure 15 and 18) due to increased distribution of high Arginase1 expressing cell populations by ~ 8-10%.

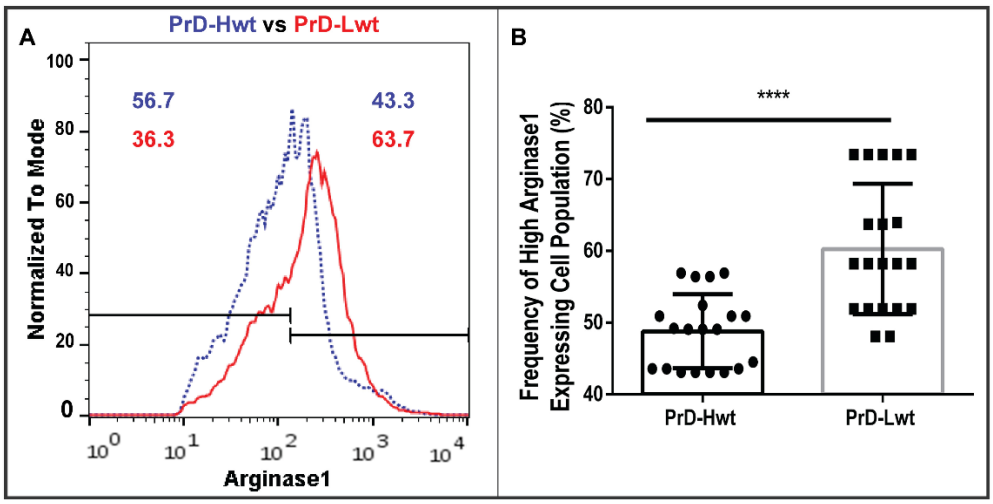

Figure 18: FACS analysis on foetal RBC populations from preterm, discordant twin neonates, immunolabelled with Arginase1

Representative histogram plot (A) and the graphical representation (B) presents the intensity level and the frequency of high expressing Arginase1cell population respectively by the FACS analysis using anti-Arginase1 primary antibodies on foetal RBCs originated from the arterial cord of preterm, discordant high weight (PrD-Hwt, blue dot) and low weight (PrD-Lwt, red line) twin siblings where N=20 pairs. For each control and twin sample, an arbitrary borderline was considered along the x-axis dividing the total RBC population into basal and high expressing cells. The statistical significance was accepted at ****$p<0.0001$ based on one-way ANOVA using the Newman-Keuls multiple comparison test.

4.2. Quantitative estimation of lipid peroxidation, determined by the 4-Hydroxynonenal level and Annexin V positive population in the UC vessels and the isolated RBCs

Due to the overproduction of ROS, the rate of lipid peroxidation gets enhanced. The most common products formed are the oxygenated α, β-unsaturated aldehydes such as 4-hydroxynonenal (4-HNE). The formation of this aldehyde was followed by immunolabelling the aldehyde-protein adduct with an anti-4-HNE antibody. Furthermore, due to the excess rate of lipid peroxidation, the level of phosphatidylserine gets altered in the outer leaflet of RBC plasma membranes which is easily detected by Annexin V and quantified using FACS analysis.

4.2.1. Mature Non-Discordant Study Population

Measurement of the 4-HNE intensity level in the cord vessels' endothelium, indicated a significant increase in the arteries of Hwt (~65%) and Lwt (~214%) neonates. The vein endothelium showed a moderate increase of 20% in Hw and 33% in Lw twin population in comparison to their age and weight-matched singletons (Figure 19 A-B). The detailed representative epifluorescent images are mentioned in the Appendix (Figure S3 and S4).

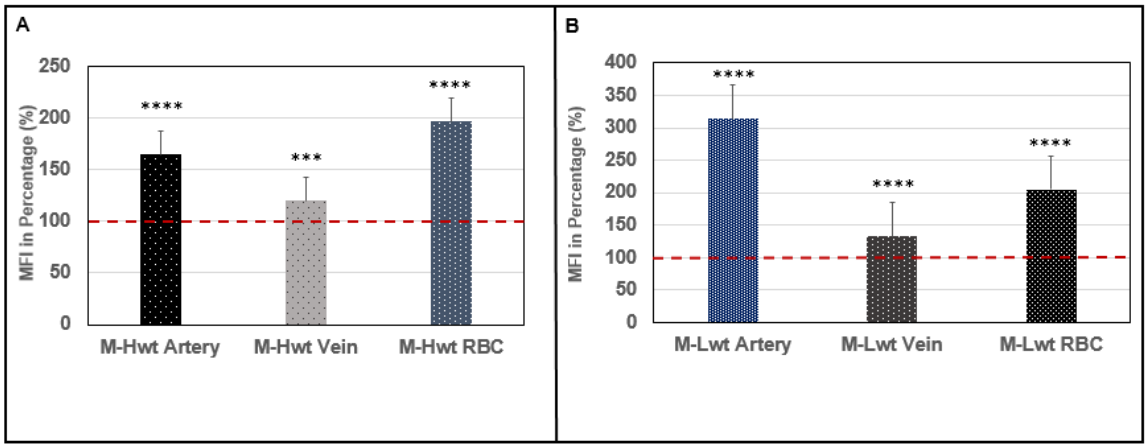

Figure 19: Quantification of the 4-HNE level in the vascular endothelium and arterial cord RBCs of the mature non-discordant twin neonates

Panels (A-B) indicate the MFI value in percentage of the 4-HNE level in M-Hwt (N=24) vs M-Hws (N=22) and M-Lwt (N=18) vs M-Lws (N=10) respectively. The red dotted line represents the control (i.e. age and weight-matched singletons) intensity level at 100% within the cord vessel endothelial cells and isolated arterial cord RBCs. The significant differences were accepted at ***p < 0.001 and ****p < 0.0001 based on one-way ANOVA using the Newman-Keuls multiple comparison test.

The arterial cord isolated RBCs were considered for FACS analysis to estimate the 4-HNE intensity level and Annexin V positive population. The 4-HNE intensity level gets prominently increased in both the twin groups irrespective of their birth weight (Figure 19 A-B and 20), which highly correlates with the increased frequency of high 4-HNE expressing cells by ~ 422% and ~ 153% in the Hwt and Lwt group respectively (Figure 20).

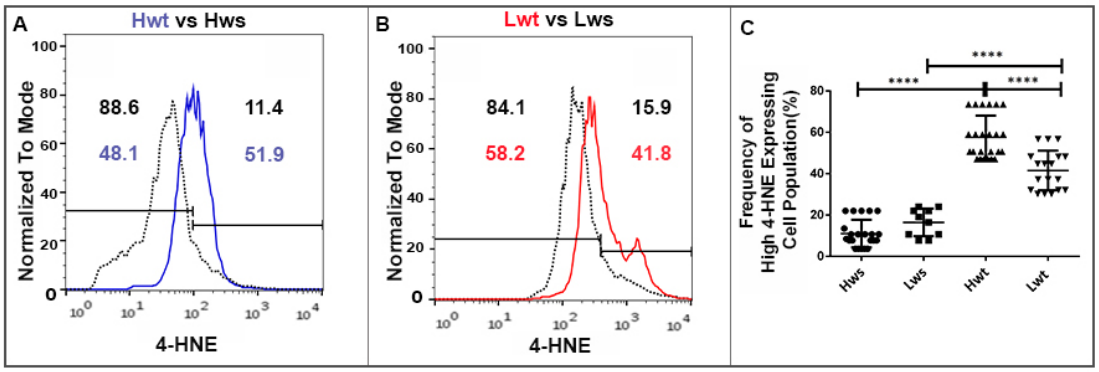

Figure 20: Evaluation of the immunolabelled 4-HNE level on the arterial cord RBCs by FACS analysis

Panels (A-B) show the representative histogram plots as measured by the FACS analysis using anti-4-HNE primary antibody on the foetal arterial cord RBCs derived from M-Hwt (blue line) and M-Lwt (red line) with their matched singletons (black dots) respectively. For each control and twin sample, an arbitrary borderline was considered along the x-axis dividing the total RBC population into basal and high 4-HNE expressing cells. The graphical representation in the (C) panel indicates the frequency of high expressing 4-HNE levels in the RBC population of the mature Hw (N=24) and Lw (N=18) twin neonates compared to their age-matched Hw (N=22) and Lw (N=10) singletons. The statistical significance was accepted at ****$p<0.0001$ based on one-way ANOVA using the Newman-Keuls multiple comparison test.

Again, the isolated RBCs, derived from the age –and weight-matched singletons and twin groups were commonly stained by Annexin V, which indicates the level of phosphatidylserine in the outer leaflet of RBC plasma membranes. The distribution of Annexin V positive population is significantly higher by ~19% and ~27% in the Hw and Lw twin groups respectively, when compared to their matched singletons (Figure 21).

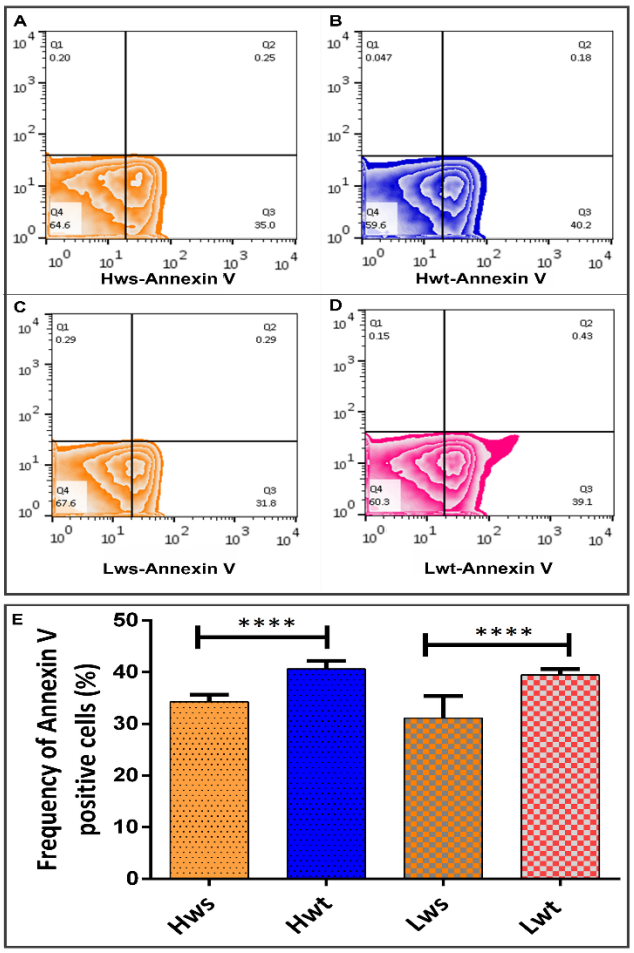

Figure 21: Viability assay on isolated RBCs by the FITC-conjugated Annexin V

Viability assay on isolated RBCs by the FITC (Fluorescein IsoThioCyanate) –conjugated Annexin V. Panel (A–D) are representative zebra plots derived from isolated RBCs of the age and weight-matched M-Hws (N=12), M-Hwt (N=15), M-Lws (N=8) and M-Lwt (N=11), respectively. For control and twin samples, an arbitrary borderline was considered along the x-axis, where the Q3 quadrant represents the AnnexinV positive cells. The graphical summary (E) shows the percentage distribution of AnnexinV positive RBCs localized in Q3 quadrant. Statistical significance was accepted at ****p<0.0001 using the Newman-Keuls multiple comparison test.

4.2.2. Premature Non-Discordant Study Population

Here the intensity levels of 4-HNE as evaluated by Image J©, in the cord arteries of the Hw twin neonates, showed a significant increase of ~31% with no alterations in the vein as compared to their age -and weight-matched singletons. In the Hwt versus Lwt group, the values significantly increased to ~17% in the arterial endothelium while the

intensity level remained unchanged. in the veins (Figure 22 A-B). The detailed representative epifluorescent images are mentioned in the Appendix (Figure S7 and S8).

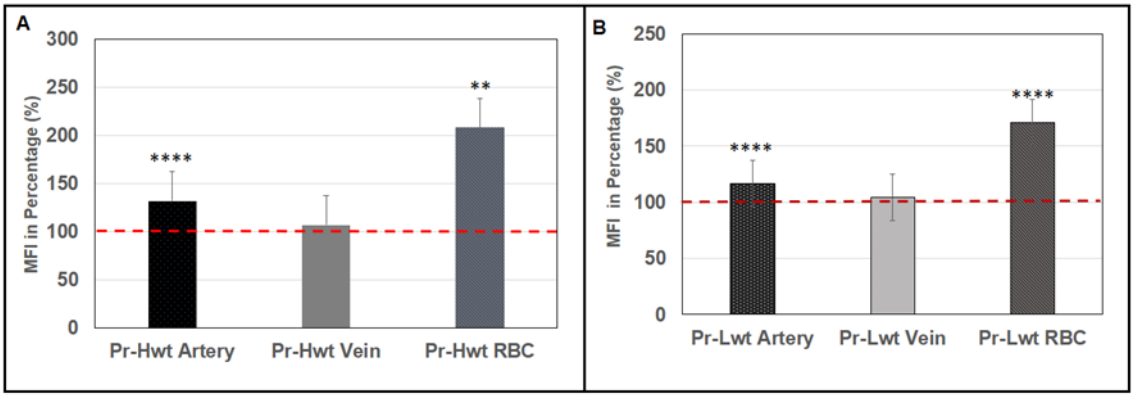

Figure 22: Quantification of the 4-HNE level in the vascular endothelium and arterial cord RBCs of the premature non-discordant twin neonates

Graphical illustration in panels (A-B) indicates the MFI values in percentage of the 4-HNE level in the preterm non-discordant Hw (A; N=20) and Lw (B; N=12), twin neonates, in comparison to age and weight-matched singletons (A; N=15) and Pr-Hwt (B; N=20) respectively, taken as control. The red dotted line represents the control intensity level at 100% within the cord vessel endothelial cells and isolated arterial cord RBCs. The significant differences were accepted at **$p < 0.01$ and ****$p < 0.0001$ based on one-way ANOVA using the Newman-Keuls multiple comparison test.

The isolated RBCs by FACS analysis exhibited an up rise to ~108% in the Hwt when compared to the age-matched singleton group. The Lwt neonates in comparison to Hwt also showed a significant increase of 71% (Figure 22 A –B and 23).

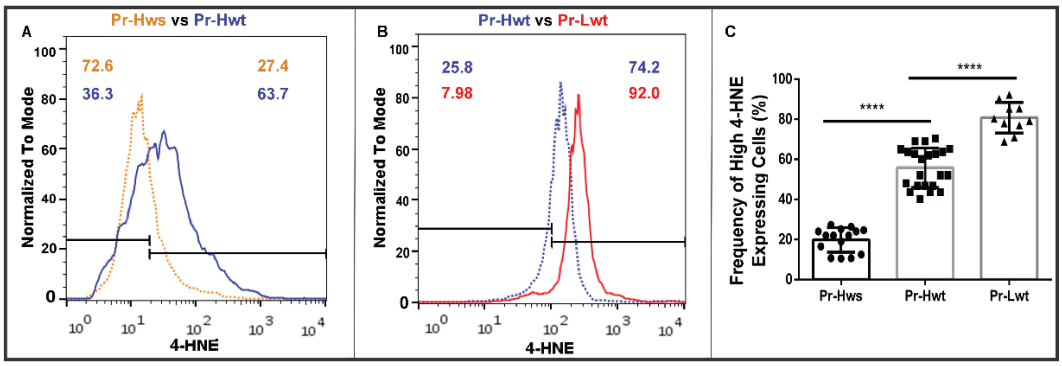

Figure 23: FACS analysis on RBC populations, immunolabelled with 4-HNE

Representative histograms as measured by the FACS analysis using anti-4 HNE primary antibodies showed in panel (A) the comparison between foetal RBCs derived from preterm non-discordant high weight twin (Pr-Hwt, blue line) and age-matched high weight singleton (Pr-Hws, orange line) and (B) present the comparison between Pr-Hwt and low weight (Pr-Lwt, red line) twin sample. For each, control and twin sample, an arbitrary borderline was considered along the x-axis dividing the total RBC population into basal and high expressing cells. The graphical plot (C) indicates the frequency of high 4-HNE expressing RBC populations in the preterm, non-discordant Hw (N= 20) and Lw (N=12) twin neonates and age-weight matched singletons (Pr-Hws; N=15). The statistical significance was accepted at ****$p<0.0001$ based on one-way ANOVA using the Newman-Keuls multiple comparison test.

In parallel, RBC populations were stained with Annexin V and revealed an elevated frequency of ~ 12.5% in the Annexin V positive RBCs originated from Hwt in comparison to the Hws populations. However, no significant difference existed between the Hwt and Lwt categories (Figure 24).

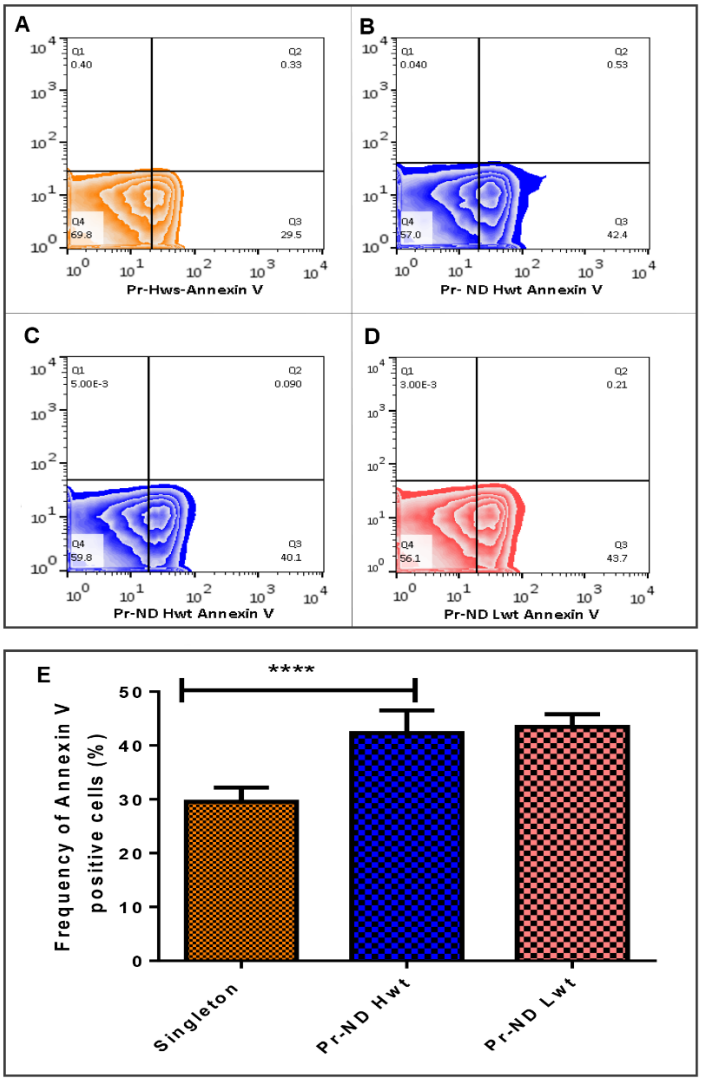

Figure 24: Viability Assay on the isolated arterial cord RBCs derived from preterm non-discordant twin siblings

Representative panels (A, B) and (C, D) of zebra plots showed the isolated RBCs of the premature Hwt (N=15) with their age and weight-matched singletons Hws (N=10), and Pr- Hwt (N=15) in comparison to their non-discordant Lwt (N=12) group respectively that are treated with FITC (Fluorescein IsoThioCyanate) - conjugated Annexin V. For control and twin samples, an arbitrary borderline was considered along the x-axis, where the Q3 quadrant represents the Annexin V positive cells. The graphical summary (E) shows the percentage distribution of Annexin V positive RBCs localized in the Q3 quadrant. **** Marks the significant differences based on the Newman-Keuls multiple comparison test at $p < 0.0001$.

4.2.3. Premature Discordant Study Population

In the discordant twin population, the low birthweight siblings exhibited a significant increase of the 4 HNE level in the cord arteries and vein by ~42% and ~25%, respectively

(Figure 25) and detailed representative epifluorescent images are in the Appendix section (Figure S11 and S12).

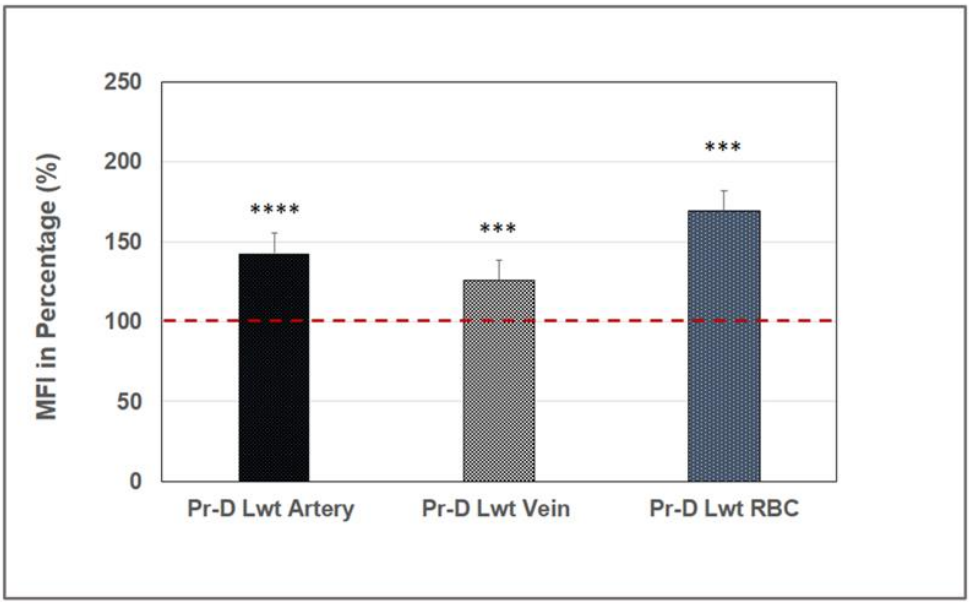

Figure 25: Measurement of the 4-HNE level in the vascular endothelium and arterial cord RBCs of the premature discordant twin neonates

The MFI of the 4-HNE level in the preterm discordant low birthweight siblings was expressed as a percentage in comparison to their high weight twin pair, considered as control. The red dotted line represents the control intensity level at 100% within the cord vascular endothelial cells and isolated arterial cord RBCs. Statistical significances were accepted at ***$p < 0.001$ and ****$p < 0.0001$ based on one-way ANOVA using the Newman-Keuls multiple comparison test.

The FACS analysis on the isolated cord arterial RBCs also indicated an upsurge by 69% in the HNE intensity level of the Lwt category in comparison to their Hw siblings (Figure 25 and 26).

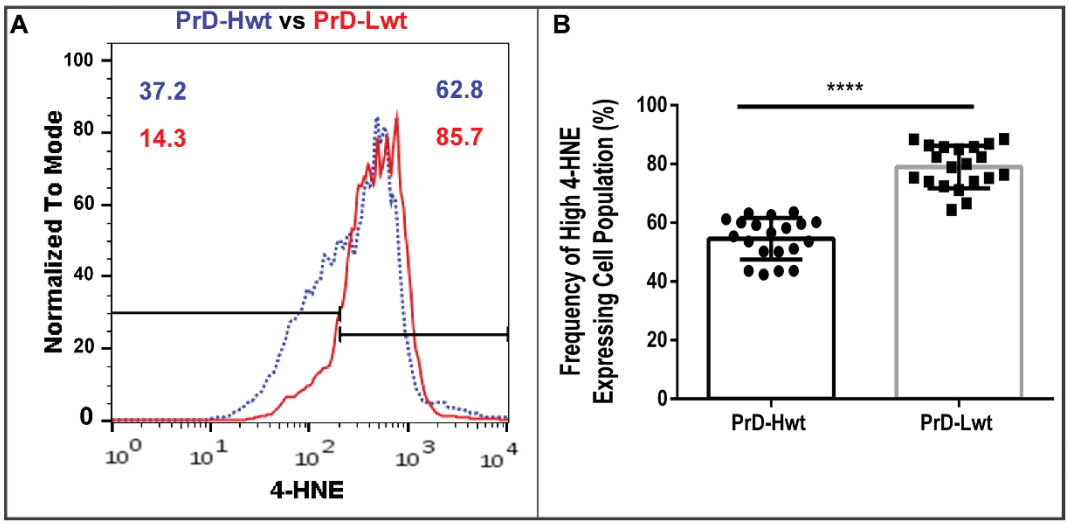

Figure 26: FACS analysis on foetal RBC populations from preterm, discordant twin neonates, immunolabelled with 4-HNE

Representative histogram plot (A) and the graphical representation (B) measures the intensity level and the frequency of high expressing 4-HNE cell population respectively by the FACS analysis using anti-HNE primary antibodies on foetal RBCs originated from the arterial cord of preterm, discordant high weight (PrD-Hwt; N=20, blue dot) and low weight (PrD-Lwt; N=20, red line) siblings. For each control and twin sample, an arbitrary borderline was considered along the x-axis dividing the total RBC population into basal and high expressing cells. The statistical significance was accepted at ****p<0.0001 based on one-way ANOVA using the Newman-Keuls multiple comparison test.

Further to test the Annexin V positivity, RBCs from the discordant twin pairs were subjected to FACS, where a significant increase in the frequency of Annexin V positive cells (~10%) was detected in the Lwt group in comparison to the Hwt origin (Figure 27).

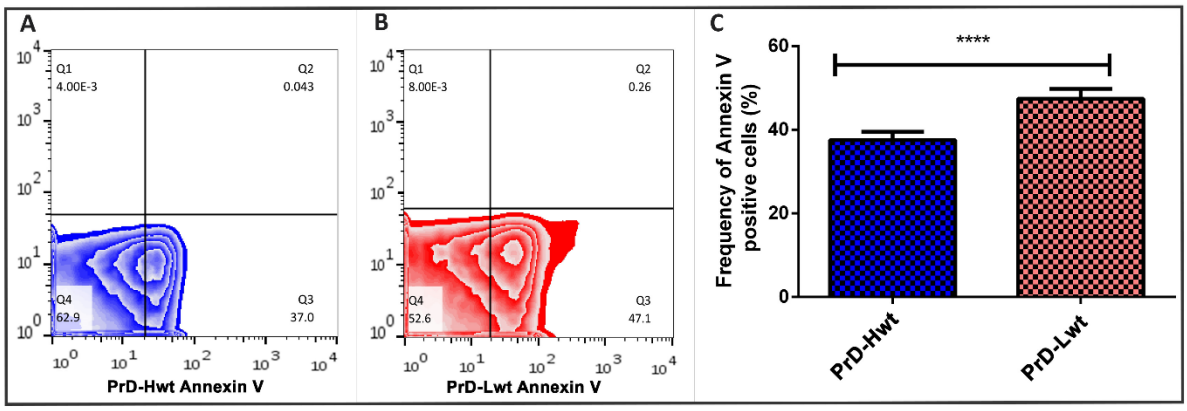

Figure 27: Viability Assay on the isolated arterial cord RBCs derived from the preterm discordant twin pairs

Panel (A and B) represents the zebra plots of the isolated arterial cord RBCs derived from preterm discordant twin N=20 pairs that are treated with FITC (Fluorescein IsoThioCyanate) - conjugated Annexin V. In the control and twin sample, an arbitrary borderline was considered along the x-axis, where the Q3 quadrant represents the AnnexinV positive cells. The graphical summary (C) shows the percentage distribution of Annexin V positive RBCs localized in the Q3 quadrant. Statistical significance was accepted at **** $p < 0.0001$ using the Newman-Keuls multiple comparison test.

4.3. Analysis of phenotypical variants in RBCs

In a preliminary platform increased frequency of different phenotypical variants in the RBC population can be an indication of various kinds of clinical disorders. Altogether, we screened over ~ 3000 RBCs from the singletons, ~ 2000 from the mature, and 4000 from the premature twin origins. We specifically looked for Burr cells, Elliptocytes, and Rouleaux phenotypes beside the regular healthy biconcave-shaped RBCs. There was no major significant alteration in the frequency of morphological variants between the mature and premature singleton groups. However, a significant difference was found between the singletons and twin neonates from mature and premature origins. In the mature twins, 3-fold and premature twin group 2-fold increase had occurred in the Burr cells type of the RBC population. It was almost negligible to identify Elliptocytes and Rouleaux variants in the singletons. The premature in comparison to the mature twin populations, demonstrated

~ 2 to 2.5-fold increase in the Elliptocytes and a ~5-fold increase in the Rouleaux phenotypes, irrespective of their birth weight (Figure 28).

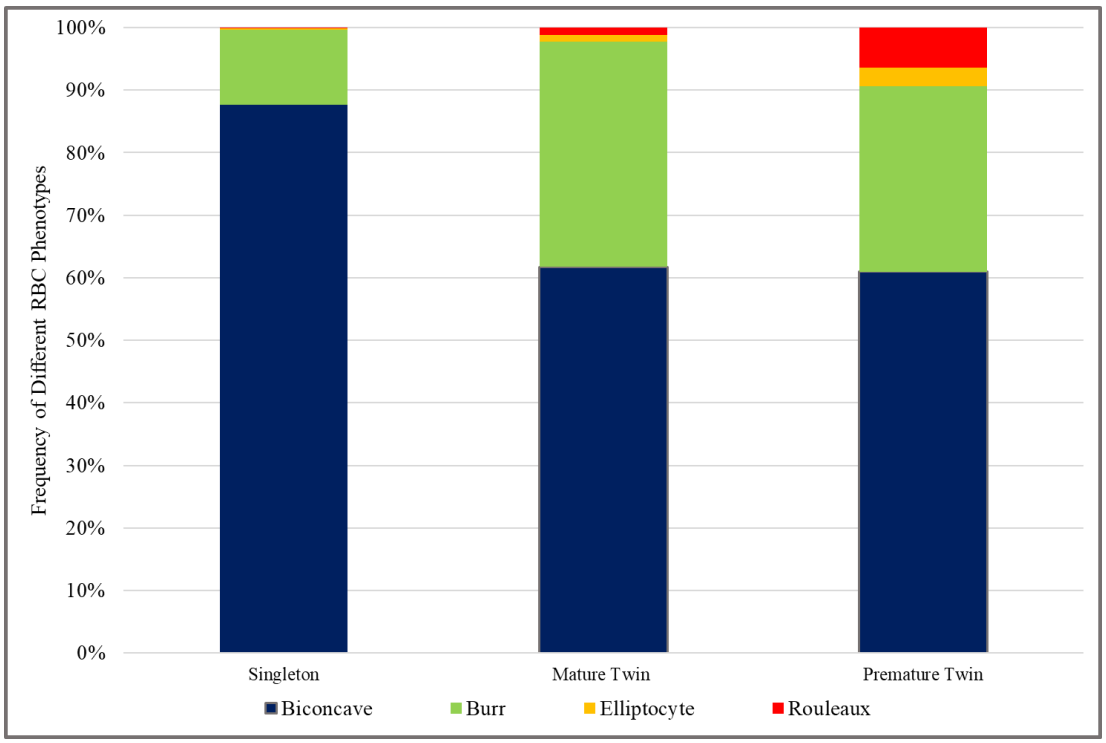

Figure 28: Distribution of morphological variants of RBCs derived from mature and premature twin siblings

The distribution of morphological variants in the isolated RBCs derived from singletons in comparison to mature and premature twin populations were analysed by the Advanced Cell Classifier software. Screening of RBCs (N=600 cells/sample) were counted from both singleton and twin origin. Statistical significance in the frequencies of the regular Biconcave at (*** $p < 0.001$), Burr at (*** $p < 0.001$ and **** $p < 0.0001$), Elliptocytes at (**** $p < 0.0001$ and ** $p < 0.01$) and Rouleaux at (**** $p < 0.0001$) were accepted by one-way ANOVA using the Newman-Keuls multiple comparison test.

4.4. Spectrophotometric measurement of H_2O_2 and $ONOO^-$ levels in the RBCs

RBCs originated from different mature and premature origins, mostly undergo a higher level of cellular oxidative stress condition. Here we see that irrespective of their birthweight differences the deleterious oxidant level of $ONOO^-$ was significantly increased by ~ 2.- 2.5 fold in the mature and ~1.5- 2 fold in the premature twin neonates

in comparison to the singletons. This was in good correlation with the significant rise of another strong oxidant, the H_2O_2 level by ~1.3-fold in the mature and ~1.7-fold in the premature twins, which further indicated an imbalance between the endogenous oxidant and antioxidant system (Figure 29).

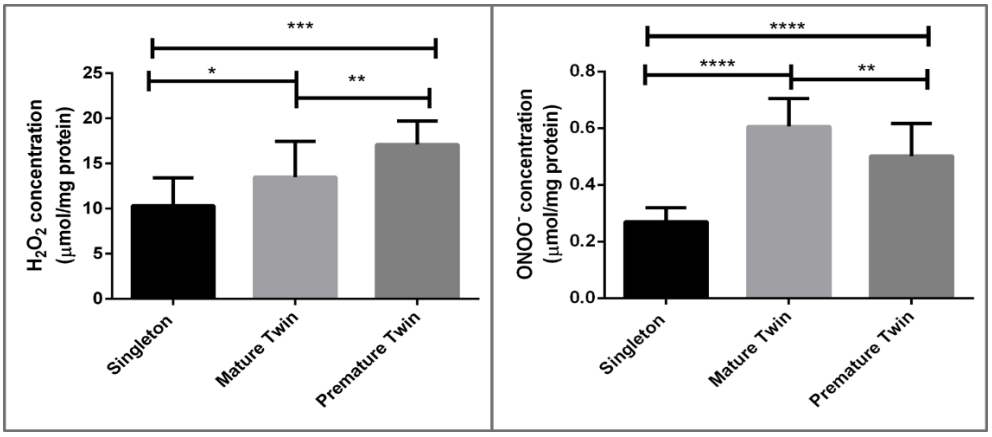

Figure 29: Spectrophotometric measurements of the strong oxidants in the isolated RBCs derived from twin origin

Estimation of the hydrogen peroxide (H_2O_2) and peroxynitrite ($ONOO^-$) levels were measured by spectrophotometric methods in the isolated arterial cord RBCs from singleton (N=14), mature (N=12 pairs) and premature (N=15 pairs) twin origin. Statistical significance was accepted at * $p < 0.05$, ** $p < 0.01$, *** $p < 0.001$ and **** $p < 0.0001$ by one-way ANOVA using the Newman-Keuls multiple comparison test.

5. Discussion

There had been increasing evidence that indicates towards enhanced rate of oxidative insults during intrauterine development and variedly contributes to the occurrence of pathological conditions in post-natal or adult life. An adverse intrauterine environment develops in all clinical cases of multiple/twin pregnancy, pre-eclampsia, ectopic pregnancy, and intrauterine growth restriction that gets directly or indirectly associated with placental or umbilical cord disorders (Ávila et al., 2015; Argyraki et al., 2019). In comparison between singleton and twin or multiple pregnancies, there always exists an additional oxidative stress condition due to long-term intrauterine hypoxia and causes impaired blood flow to the feto vascular system (Al-Gubory et al., 2010; Acharya et al., 2016; Rodríguez-Rodríguez et al., 2018).

At early stages of an *in-utero* development until late in the third trimester, along with the presence of low immunocompetence prevails a partially developed endogenous or passively acquired exogenous antioxidant system (Georgeson et al., 2002; Davis and Auten, 2010; Perrone et al., 2010, 2019). Specifically, in cases of preterm birth, the antioxidant system is not fully developed and gets associated with an increased oxidant burden which places these neonates at a much higher risk of injury. Thereby, any altered physiological and metabolic functions in the developing foetus can easily disrupt the delicate balance between ROS and their intrinsic antioxidant defense system. This shifting in the redox homeostasis increases oxidative stress and eventually predisposes to severe obstetric complications like birth asphyxia, respiratory disorders, prematurity, structural abnormalities, delayed development, and most commonly low birthweight (Thaete et al., 2004; Hayes, 2005; Buonocore and Perrone, 2009; Su et al., 2015).

During long-term oxidative stress conditions like twin pregnancy, mapping the efficacy of the NOS pathway becomes pivotal in the regulation of bioavailable NO for vasorelaxation and free flow of blood supply within the cord vascular system. Previously, our working group pioneered in demonstrating an increased ROS production and compromised antioxidant system in parallel with the increased level of NOS3, leading to elevated macromolecular damage in the foetal RBCs of the twin neonates (Dugmonits et al., 2016). Therefore, now in a detailed comparative study, we attempted to elucidate the significance of intimate crosstalk in between the foetal RBCs and the cord vascular endothelium that involves the signalling pathway of NOS3 activation. Our results clearly highlighted the morphological alterations, functional and physico-chemical changes parallelly in both the cord-derived RBCs and vascular cord endothelium of twin neonates.

Here we selected both mature and premature twin populations with a wide range of differences in the birth weights, along with their respective age and weight-matched singletons. The NOS3 expression and its activation in the cord vessels and circulating RBCs of the selected study populations show different statuses, with a high correlation to the neonatal birthweights.

In the mature high-weight twin category, the NOS3 expression and its activation gets somewhat impaired both in the cord vessels and the circulating foetal RBCs compared to weight and age-matched singletons. In the mature low weight non-discordant category, the NOS3 expression dropped drastically only in the cord vein, however, its phosphorylation at Ser1177 position increased, as a compensatory attempt to increase NO production. Similarly, as part of the rescue mechanisms elevated NOS3 expression was observed in red blood cells.

In the preterm twin population, the NOS3 regulation in the cord vessels remains almost undisturbed in both the Hwt and Lwt neonates. Moreover, their RBC population shows responsiveness to the intrinsic oxidative stress status and works as a rescue mechanism by the upregulation of the RBC-NOS3-NO pathway. Their elevated expression and phosphorylation levels signify an effort to improve blood flow in UC vessels, however, this capacity of the foetal RBCs decreases, as pregnancy progresses. Based on our data set, in most of the selected categories (with an exception for the Pr-Hwt) the UC vessels along with the RBCs, could not suffice to maintain the desired NO level, and thus another alternative NO producing pathway gets induced, the NOS2, in the arterial endothelium. Particularly, the lower-weight siblings from the discordant twin population showed an upregulated arterial NOS2 system along with the functional RBC-NOS3-NO pathway as a part of the rescue mechanisms. Initially, even a moderate increase in the NOS2 expression could sufficiently increase the NO level, regarding the higher rate of NOS2 catalytic activity i.e. (100-1000 fold that of the NOS3 (Ratovitski et al., 1999). Though at first, NOS2 upregulation seems to be beneficial by providing an alternative source for the bioavailable NO, the higher rate of its catalytic activity adds to ROS elevation and induced cell apoptosis through caspase-3 activation (Geng et al., 1996; Liu et al., 2002). Thus an elevated NOS2 level exhibits a pro-inflammatory profile and gets associated with pathological conditions like inflammation, sepsis, or oxidative stress (Kleinert et al., 2010) causing macromolecular damages in the vascular endothelium.

One of the major key steps in the NOS3 pathway is the coupling of NOS3 and dimer formation, which gets activated by phosphorylation at serine 1177 residue to liberate the bioavailable NO (Shu et al., 2015b). Arginase1 being a competitive inhibitor of NOS3 for common substrate L-arginine steals away the common substrate which inhibits the coupling and activation of NOS3. Imbalance in redox homeostasis generates excessive

ROS which further catalyses the upregulation of Arginase1 expression and activity by tightly regulating the NOS3 pathway, producing reactive species like $O_2^{\bullet-}$ instead of the bioavailable NO and L-citrulline. The limited amount of bioavailable NO in the system readily reacts with $O_2^{\bullet-}$ and instantaneously form deleterious pro-oxidant entities like $ONOO^-$ showing the "Janus faced" role of NO (Förstermann, 2006; Yu et al., 2018).

In general, Arginase1 influences the vascular function with the production of L-ornithine as its active metabolite but an excessive synthesis of polyamine and proline from L-ornithine also plays a pivotal role in pathological vascular remodelling, endothelial and smooth muscle cell proliferation, and collagen deposition (Yang and Ming, 2013; Lucas et al., 2014). In the mature non-discordant Hwt and Lwt groups, there was a major rise in the Arginase1 expression in the vascular endothelium and further even gets doubled in the RBC populations to their age and weight-matched singletons. As a sequel of this harmful consequence, it shows a strong impact on the functionality of the RBC-NOS NO pathway. In connection to the preterm birth, here the Arginase1 expression is also highly upregulated in the vascular endothelium of the non-discordant twins but gets significantly reduced in the Lw siblings from the discordant origin. Though in the case of premature twinning, we find a significant increase of Arginase1 expression in the foetal cord RBCs, still then the RBC-NOS3-NO pathway was activated, both at the translational and phosphorylation levels. The foetal RBCs retained their competency to show the compensatory mechanism under acute oxidative stress conditions. An elevated Arginase1 expression signifies the excessive generation of ROS and simultaneously has an impact on the NOS3 –NO pathway not only in the circulating RBCs but also in the vascular endothelium. In the mature twin population as well as in the case of neonates born to smoking mothers the high Arginase level always implies a drastic reduction in the bioavailable NO, exclusively due to an impaired NOS3-NO pathway both in the UC vessels and the circulating foetal RBCs. This

consequently causes indiscriminate macromolecular damages and aggravates ED (Dugmonits et al., 2019; Chakraborty et al., 2020; Zahorán et al., 2021). Moreover taking into account the intimate communication between the circulating RBCs and the endothelium, the enhanced Arginase1 level or its activity in the circulating RBCs are well implicated in various cardiovascular disorders and other pathological states like the Type 2 diabetes mellitus (Yang et al., 2013; Zhou et al., 2018b; Pernow et al., 2019a). However, the direct correlation between Arginase1 expression and NOS3 activation for their competition to the common substrate L-arginine becomes complicated with the emerging paradox that states L-arginine concentrations in endothelial cells remain sufficiently high to support NO synthesis on the approach of compartmentalization of intracellular L-arginine into distinct, poorly interchangeable pools (Elms et al., 2013). However, apart from other cell types, RBCs hold a unique cytoskeletal structure and are devoid of major intracellular organelles where the chances of intracellular L-arginine compartmentalization into distinct interchangeable pools becomes negligible.

Finally, with an alteration in the NOS3 functionality, following the extent of macromolecular damages in the vascular endothelium and the foetal circulating RBCs, we find a significant rise in the 4-HNE level. The 4-HNE level as an indicator of the rate of lipid peroxidation was highly marked irrespective of maturity and birth weight differences in the twin population. Moreover, it is also shown that due to the greater extent of lipid peroxidation in the predominant circulating foetal RBCs, the RBC lipid bilayer membrane characteristics gets altered with an increased loss in their membrane integrity and properties as similar to neonates derived from sustained maternal smoking (Balogh et al., 2020a). Therefore, the molecular alterations affecting the membrane cytoskeletal system in the RBCs as supported by the significant increase in the Annexin V positive RBCs

implies the altered RBC membrane asymmetry, membrane damage, and loss of functional properties in the twin neonates.

It is noteworthy to mention that the neonatal RBCs get functionally impaired far ahead of any detectable morphological aberrations as implied in the case of neonates derived from the smoking origin (Dugmonits et al., 2019). Further, a detailed survey on the phenotypic variants of RBCs always served as a preliminary platform for many clinical diagnoses (Mohandas and Gallagher, 2009). Studying the morphological variants in the mature and premature twin RBC populations we exhibited a significant rise of burr cell phenotype in the RBC morphology similar to the neonates derived from smoking origin which mainly occurs due to disproportionate distribution of fatty acids, lysophospholipids in the lipid bilayer of the RBC membrane (Gallagher, 2005; Dugmonits et al., 2019; Balogh et al., 2020b). In addition, specifically in the preterm twin category, we cited a significant distribution of elliptocytes and rouleaux phenotype. Literature reviews clinically suggest morphological differentiation of elliptocytes indicate iron deficiency and megaloblastic anaemia whereas RBC aggregates like rouleaux formation result due to high fibrinogen level causing lower blood flow rates that might lead to pathogenesis of circulatory and thromboembolic complications in clinical cases like septicaemia, pregnancy, diabetes, etc. (Linderkamp et al., 1984; Ford, 2013; Bosman, 2018).

Thus citing the detectable phenotypical variants of RBCs due to possible changes in their cytoskeletal network of the mature and premature twin pairs as compared to singletons would definitely recognize and intervene into the possible complications at earlier stages of theirs post-natal or adult life (Pretorius et al., 2013; Soma and Pretorius, 2015; Masilamani et al., 2016; Diederich et al., 2018). Here we have no supporting data that states any direct correlation between these phenotypical changes with their altered

functionality, which can be marked as a limitation to our conclusion. However, the functional alteration of NOS3/pNOS3 status in the circulating RBCs within twin origin at different maturity levels could be a real-time sensor for the possible adverse outcomes in theirs later development.

6. Conclusion

Overall, understanding the basic pathophysiological mechanisms in neonatal diseases necessitates a detailed knowledge about the wide range of complications that includes all three major constituents of the feto-vascular system (RBCs, arteries, and veins). Both the endothelial cells of UC vessels and the RBCs separately contribute to the NO metabolism, vascular function, systemic hemodynamics, and blood pressure homeostasis via NOS3.

Based on our data set we see a different pattern of cellular stress regulation in between the different maturity levels of the twin population. Comparing our data sets on premature twins it is completely vivid now that the NOS3-activation capacity of the cord vessels and foetal RBCs are far more efficient than in the case of the mature twin population or in neonates, born to smoking mothers. Irrespective of a common, highly hypoxic environment that characterizes the premature or mature twin pregnancies and maternal smoking-induced conditions in the neonates, the mediated oxidative stress response is based on the distinguishable level of Arginase1. There shows clear evidence of intimate crosstalk in between the RBCs and the vascular endothelium where the Arginase-dependent alterations in the RBC-NOS pathway seem to be a determining factor for the further development of ED in the vascular system. As during the progressive pregnancy period there occur rapid physiological and metabolic changes, thus it becomes an essential factor to map the NOS3 signalling pathway at different time points of gestation. Furthermore, from the clinical point of view under adverse intrauterine conditions monitoring the Arginase level might well serve as a prognostic marker to track the overall changes in the foetal circulating RBCs and the cord vascular microenvironment.

7. Acknowledgements

I would like to first express my extended gratitude and thanks to my supervisor Dr. Edit Hermesz, for giving me the opportunity to work on this very exciting project, and sharing with me all the necessary knowledge, laboratory space and equipment to conduct my PhD work.

I am greatly thankful to Prof. Csaba Vágvölgyi, as Head of the Doctoral School of Biology for giving me scope to work in the Department of Biochemistry and Molecular Biology at the Institute of Biology, University of Szeged. I was always inspired by his personality and be grateful for his extensive support over the years of my PhD work. Similarly, I am also grateful to Prof. Boros Imre for his encouraging words and motivational interactions with me about my research. I also like to thank Dr. László Bodai, the Head of the Department of Biochemistry and Molecular Biology to be supportive and give me the scope to work and utilize all the necessary instruments of the department during my research work.

I am especially thankful to our collaborator, Dr. Hajnalka Orvos, for arranging the clinical samples to conduct the experiments from Department of Gynecology and Obstetrics at the University of Szeged. My journey of PhD also remains incomplete without the kind help and co-operation from all my lab members, I heartedly thank and acknowledge Dr Ágnes Ferencz, Dr Krisztina Dugmonits, Ali Khamit and Dr Szabolcs Zahorán. I am also thankful to our administrative and academic staff members of the department who remained as an excellent support system to carry out my PhD work in Szeged.

I owe a lot to the funding sources supported by the European Union and the Hungarian Government in the framework of the GINOP-2.3.2-15-2016-00040 project and the Tempus Public Foundation that awarded me with the Stipendium Hungaricum Scholarship in 2015.

During my long stay in Szeged, it became my second home and I developed precious relationships which I would definitely cherish throughout my life, for their unconditional love care and support for me, here I would like to thank László and Edit, Ilona Szőllősi Varga, Mousumidi and Subhenduda, my uncle Atanu and aunt Jayashree for always being there beside me in my both good and tough times. My friends like Tanmoy, Dhirend, Rakesh, Phani, Rishika, Paula, Mariam, Bettina, Sudiptada, Dileep and Kabi who always stood by me through thick and thin during my stay in Szeged.

Finally, I would like to dedicate and thank the Almighty for showering me with His blessings, that helped me to endure the hard challenges and circumstances. I sincerely acknowledge my parents who always believed on my abilities and supported me throughout my career, yet last but not the least my husband Miltu with whom there is no meaning towards my achievements, the driving force towards my career goals.

8. Bibliography

Acharya G, Sonesson SE, Flo K, Räsänen J, Odibo A. Hemodynamic aspects of normal human fetoplacental (umbilical) circulation. Acta Obstetricia et Gynecologica Scandinavica 2016; 95(6):672-82.

Agarwal A, Aponte-Mellado A, Premkumar BJ, Shaman A, Gupta S. The effects of oxidative stress on female reproduction: A review. Reproductive Biology and Endocrinology [Internet] 2012; 10:49.

Al-Gubory KH, Fowler PA, Garrel C. The roles of cellular reactive oxygen species, oxidative stress, and antioxidants in pregnancy outcomes. International Journal of Biochemistry and Cell Biology 2010; 42(10):1634-50.

Alderton WK, Cooper CE, Knowles RG. Nitric oxide synthases: Structure, function, and inhibition. Biochemical Journal [Internet] 2001; 357:593–615.

American College of Obstetricians and Gynaecologists. Multifoetal gestations: twin, triplet, and higher-order multifoetal pregnancies. Practice Bulletin 169 2016; 128(4): e131-46.

Argyraki M, Damdimopoulou P, Chatzimeletiou K, Grimbizis GF, Tarlatzis BC, Syrrou M, Lambropoulos A. In-utero stress and mode of conception: Impact on the regulation of imprinted genes, foetal development, and future health. Human Reproduction Update 2019; 25(6):777-801.

Ávila JGO, Echeverri I, Plata CA de, Castillo A. Impact of oxidative stress during pregnancy on foetal epigenetic patterns and early origin of vascular diseases. Nutrition Reviews 2015; 73(1):12-21.

Bak A, Roszkowski K. Oxidative stress in pregnant women. Archives of Perinatal Medicine 2013; 19(3), 150-155.

Balogh G, Chakraborty P, Dugmonits KN, Péter M, Végh AG, Vígh L, Hermesz E. Sustained maternal smoking-associated changes in the physico-chemical properties of foetal RBC membranes might serve as early markers for vascular comorbidities. Biochimica et Biophysica Acta - Molecular and Cell Biology of Lipids 2020; 1865(4):158615.

Barker DJP, Godfrey KM, Gluckman PD, Harding JE, Owens JA, Robinson JS. Foetal nutrition and cardiovascular disease in adult life. The Lancet 1993; 341(8850):938-41.

Barthelmes J, Nägele MP, Ludovici V, Ruschitzka F, Sudano I, Flammer AJ. Endothelial dysfunction in cardiovascular disease and Flammer syndrome-similarities and differences. EPMA Journal 2017; 8(2):99-109.

Benedetti A, Comporti M, Esterbauer H. Identification of 4-hydroxynonenal as a cytotoxic product originating from the peroxidation of liver microsomal lipids. Biochimica et Biophysica Acta - Lipids and Lipid Metabolism [Internet] 1980; 620:281–296.

Benirschke K, Burton GJ, Baergen RN. Book chapter - Anatomy and Pathology of the Umbilical Cord. Pathology of the Human Placenta 5th edition 2012.

Berk BC, Haendeler J, Sottile J. Angiotensin II, atherosclerosis, and aortic aneurysms. Journal of Clinical Investigation 2000; 105(11):1525-6.

Blanchette H. The rising cesarean delivery rate in America: What are the consequences? Obstetrics and Gynecology 2011; 118(3):687-690.

Blondel B, Kaminski M. Trends in the occurrence, determinants, and consequences of multiple births. Seminars in Perinatology 2002; 26(4):239-49.

Bortolus R, Parazzini F, Chatenoud L, Benzi G, Bianchi MM, Marini A. The epidemiology of multiple births. Human Reproduction Update 1999; 5(2):179-87.

Bosman GJCGM. Disturbed red blood cell structure and function: An exploration of the role of red blood cells in neurodegeneration. Frontiers in Medicine 2018; 5:1–6.

Breathnach FM, McAuliffe FM, Geary M, Daly S, Higgins JR, Dornan J, Morrison JJ, Burke G, Higgins S, Dicker P, et al. Definition of intertwin birth weight discordance. Obstetrics and Gynecology 2011; 118(1):94-103.

Buhling KJ, Henrich W, Starr E, Lubke M, Bertram S, Siebert G, Dudenhausen JW. Risk for gestational diabetes and hypertension for women with twin pregnancy compared to a singleton pregnancy. Archives of Gynecology and Obstetrics 2003; 269(1):33-6.

Buonocore G, Perrone S. Biomarkers of oxidative stress in the foetus and new-born. Hematology Meeting Reports (formerly Haematologica Reports) 2009; 2(10).

Burton GJ, Jauniaux E. Oxidative stress. Best Practice and Research: Clinical Obstetrics and Gynaecology [Internet] 2011; 25:287–299.

Bydlowski SP, Debes AA, Maselli LMF, Janz FL. Características biológicas das células-tronco mesenquimais. Revista Brasileira de Hematologia e Hemoterapia 2009; 31, 25-35.

Capettini LSA, Cortes SF, Silva JF, Alvarez-Leite JI, Lemos VS. Decreased production of neuronal NOS-derived hydrogen peroxide contributes to endothelial dysfunction in atherosclerosis. British Journal of Pharmacology [Internet] 2011; 164:1738–1748.

Carpenter AE, Jones TR, Lamprecht MR, Clarke C, Kang IH, Friman O, Guertin DA, Chang JH, Lindquist RA, Moffat J, et al. CellProfiler: Image analysis software for identifying and quantifying cell phenotypes. Genome Biology 2006; 7(10): R100.

Casas AI, Dao VTV, Daiber A, Maghzal GJ, Lisa F Di, Kaludercic N, Leach S, Cuadrado A, Jaquet V, Seredenina T, et al. Reactive Oxygen-Related Diseases: Therapeutic Targets and Emerging Clinical Indications. Antioxidants and Redox Signaling 2015; 23(14):1171-85.

Cau SBA, Carneiro FS, Tostes RC. Differential modulation of nitric oxide synthases in aging: Therapeutic opportunities. Frontiers in Physiology [Internet] 2012; 3:218.

Chakraborty P, Dugmonits KN, Orvos H, Hermesz E. Mature twin neonates exhibit oxidative stress via nitric oxide synthase dysfunctionality: A prognostic stress marker in the red blood cells and umbilical cord vessels. Antioxidants 2020; 9(9), 845.

Chakraborty P, Dugmonits KN, Végh AG, Hollandi R, Horváth P, Maléth J, Hegyi P, Németh G, Hermesz E. Failure in the compensatory mechanism in red blood cells due to sustained smoking during pregnancy. Chemico-Biological Interactions 2019; 313:108821.

Choi SH, Park YS, Shim KS, Choi YS, Chang JY, Hahn WH, Bae CW. Recent trends in the incidence of multiple births and its consequences on perinatal problems in Korea. Journal of Korean Medical Science 2010; 25(8):1191-6.

Chung FL, Nath RG, Ocando J, Nishikawa A, Zhang L. Deoxyguanosine adducts of t-4-Hydroxy-2-nonenal are endogenous DNA lesions in rodents and humans: Detection and potential sources. Cancer Research [Internet] 2000; 60(6):1507-11.

Cleary-Goldman J, D'Alton ME. Growth Abnormalities and Multiple Gestations. Seminars in Perinatology 2008; 32(3):206-12.

Collins J. Global epidemiology of multiple births. Reproductive biomedicine online 2007; 15 Suppl 3:45-52.

Colton CA, Vitek MP, Wink DA, Xu Q, Cantillana V, Previti ML, Nostrand WE Van, Weinberg B, Dawson H. No synthase 2 (NOS2) deletion promotes multiple pathologies in a mouse model of Alzheimer's disease. Proceedings of the National Academy of Sciences of the United States of America 2006; 103(41):15273.

Cortese-krott MM, Kelm M. Redox Biology Endothelial nitric oxide synthase in red blood cells: Key to a new erythrocrine function? Redox Biology [Internet] 2014; 2:251–258.

Cortese-Krott MM, Rodriguez-Mateos A, Sansone R, Kuhnle GGC, Thasian-Sivarajah S, Krenz T, Horn P, Krisp C, Wolters D, Heiß C, et al. Human red blood cells at work: Identification and visualization of erythrocytic eNOS activity in health and disease. Blood 2012; 120(20):4229-37.

Courtney JA, Cnota JF, Jones HN. The role of abnormal placentation in congenital heart disease; Cause, correlate, or consequence? Frontiers in Physiology 2018; 9:1045.

Davis JM, Auten RL. Maturation of the antioxidant system and the effects on preterm birth. Seminars in Foetal and Neonatal Medicine 2010; 15(4):191-5.

Diederich L, Suvorava T, Sansone R, Keller TCS, Barbarino F, Sutton TR, Kramer CM, Lückstädt W, Isakson BE, Gohlke H, et al. On the effects of reactive oxygen species and nitric oxide on red blood cell deformability. Frontiers in Physiology 2018; 9:332.

Dimmeler S, Fleming I, Fisslthaler B, Hermann C, Busse R, Zeiher AM. Activation of nitric oxide synthase in endothelial cells by Akt- dependent phosphorylation. Nature 1999; 399(6736):601-5.

Ding H, Triggle CR. Endothelial cell dysfunction and the vascular complications associated with type 2 diabetes: assessing the health of the endothelium. Vascular health and risk management 2005; 1(1):55–71.

Doorn JA, Petersen DR. Covalent adduction of nucleophilic amino acids by 4-hydroxynonenal and 4-oxononenal. Chemico-Biological Interactions 2003; 143-144:93-100.

Dugmonits KN, Chakraborty P, Hollandi R, Zahorán S, Pankotai-Bodó G, Horváth P, Orvos H, Hermesz E. Maternal Smoking Highly Affects the Function, Membrane Integrity, and Rheological Properties in Foetal Red Blood Cells. Oxidative Medicine and Cellular Longevity 2019; 2019: 1509798.

Dugmonits KN, Ferencz A, Zahoran S, Lazar R, Talapka P, Orvos H, Hermesz E. Elevated levels of macromolecular damage are correlated with increased nitric oxide synthase expression in erythrocytes isolated from twin neonates. British journal of haematology 2016; 174:932–941.

Durante W, Johnson FK, Johnson RA. Arginase: A critical regulator of nitric oxide synthesis and vascular function. Clinical and Experimental Pharmacology and Physiology [Internet] 2007; 34:906–911.

Elms S, Chen F, Wang Y, Qian J, Askari B, Yu Y, Pandey D, Iddings J, Caldwell RB, Fulton DJ. Insights into the arginine paradox: evidence against the importance of the subcellular location of arginase and eNOS. American journal of physiology Heart and circulatory physiology [Internet] 2013; 305(5): H651-66.

Espinosa-Diez C, Miguel V, Mennerich D, Kietzmann T, Sánchez-Pérez P, Cadenas S, Lamas S. Antioxidant responses and cellular adjustments to oxidative stress. Redox Biology 2015; 6:183–197.

Esterbauer H, Schaur RJ, Zollner H. Chemistry and biochemistry of 4-hydroxynonenal, malonaldehyde and related aldehydes. Free Radical Biology and Medicine [Internet] 1991; 11(1):81-128.

Fahmy M. Umbilicus and Umbilical Cord 2018; Book chapter 1st edition: DOI:10.1007/978-3-319-62383-2.

Fan F, Sun L, Zhang D, Zhu L, Wang S, Wang D. Original Article Effects of red blood cell supernatants on hypoxia/reoxygenation injury in H9C2 cells. Int J Clin Exp Med [Internet] 2018; 11(4):3612-3619.

Feron O, Saldana F, Michel JB, Michel T. The endothelial nitric-oxide synthase-caveolin regulatory cycle. Journal of Biological Chemistry [Internet] 1998; 273(6):3125-8.

Foley MR. Maternal adaptations to pregnancy: Cardiovascular and hemodynamic changes. UpToDate 2018.

Ford J. Red blood cell morphology. International Journal of Laboratory Hematology 2013; 35(3):351-357.

Förstermann U. Janus-faced role of endothelial NO synthase in vascular disease: Uncoupling of oxygen reduction from NO synthesis and its pharmacological reversal. Biological Chemistry [Internet] 2006; 387(12):1521-33.

Förstermann U, Münzel T. Endothelial nitric oxide synthase in vascular disease: From marvel to menace. Circulation [Internet] 2006; 113(13):1708-14.

Fulton D, Gratton JP, McCabe TJ, Fontana J, Fujio Y, Walsh K, Franke TF, Papapetropoulos A, Sessa WC. Regulation of endothelium-derived nitric oxide production by the protein kinase Akt. Nature 1999; 399(6736):597-601.

Gallagher PG. Red cell membrane disorders. Hematology Am Soc Hematol Educ Program. 2005; 13-8.

Geng YJ, Wu Q, Muszynski M, Hansson GK, Libby P. Apoptosis of vascular smooth muscle cells induced by in vitro stimulation with interferon-γ, tumor necrosis factor-α, and interleukin-1β. Arteriosclerosis, Thrombosis, and Vascular Biology 1996; 16(1):19-27.

Georgeson GD, Szony BJ, Streitman K, Varga IS, Kovács A, Kovács L, László A. Antioxidant enzyme activities are decreased in preterm infants and neonates born via caesarean section. European Journal of Obstetrics and Gynecology and Reproductive Biology 2002; 103(2):136-139.

Giles W, O'Callaghan S, Read M, Gude N, King R, Brennecke S. Placental nitric oxide synthase activity and abnormal umbilical artery flow velocity waveforms. Obstetrics and Gynecology 1997; 89(1):49-52.

Gilliland SE, Speck ML. Biological Response of Lactic Streptococci and Lactobacilli to Catalase1. Applied Microbiology [Internet] 1969; 17(6):797-800.

Godfrey KM, Barker DJ. Foetal programming and adult health. Public Health Nutrition 2001; 4(2B):611-24.

Gongora MC, Qin Z, Laude K, Kim HW, McCann L, Folz JR, Dikalov S, Fukai T, Harrison DG. Role of extracellular superoxide dismutase in hypertension. Hypertension 2006; 48(3):473-81.

Granger JP, Alexander BT, Llinas MT, Bennett WA, Khalil RA. Pathophysiology of hypertension during preeclampsia linking placental ischemia with endothelial dysfunction. Hypertension 2001; 38(3 Pt 2):718-22.

Gremeau AS, Brugnon F, Bouraoui Z, Pekrishvili R, Janny L, Pouly JL. Outcome and feasibility of elective single embryo transfer (eSET) policy for the first and second

IVF/ICSI attempts. European Journal of Obstetrics and Gynecology and Reproductive Biology [Internet] 2012; 160(1):45-50.

Haas S de, Ghossein-Doha C, Kuijk SMJ van, Drongelen J van, Spaanderman MEA. Physiological adaptation of maternal plasma volume during pregnancy: a systematic review and meta-analysis. Ultrasound in Obstetrics & Gynecology 2017; 49(2):177-187.

Hackshaw A, Rodeck C, Boniface S. Maternal smoking in pregnancy and birth defects: A systematic review based on 173 687 malformed cases and 11.7 million controls. Human Reproduction Update 2011; 17(5):589-604.

Halliwell B. Reactive oxygen species in living systems: Source, biochemistry, and role in human disease. The American Journal of Medicine 1991; 91(3C):14S-22S.

Hayes E. Review of "Multiple Pregnancy: Epidemiology, Gestation & Perinatal Outcome. Second Edition." Journal of Experimental & Clinical Assisted Reproduction 2005; 2:12.

Heitzer T, Schlinzig T, Krohn K, Meinertz T, Münzel T. Endothelial dysfunction, oxidative stress, and risk of cardiovascular events in patients with coronary artery disease. Circulation [Internet] 2001; 104(22):2673-8.

Hileman EA, Achanta G, Huang P. Superoxide dismutase: An emerging target for cancer therapeutics. Expert Opinion on Therapeutic Targets 2001; 5(6):697-710.

Hollier LM, McIntire DD, Leveno KJ. The outcome of twin pregnancies according to intra-pair birth weight differences. Obstetrics and Gynecology 1999; 94(6):1006-10.

Horvath P, Wild T, Kutay U, Csucs G. Machine Learning Improves the Precision and Robustness of High-Content Screens. Journal of Biomolecular Screening 2011; 16(9):1059-67.

Huie RE, Padmaja S. The reaction of no with superoxide. Free Radical Research 1993; 18(4):195-9.

Hutter D, Kingdom J, Jaeggi E. Causes and Mechanisms of Intrauterine Hypoxia and Its Impact on the Foetal Cardiovascular System: A Review. International Journal of Pediatrics 2010; 2010:401323.

Jacobsson B, Ladfors L, Milsom I. Advanced maternal age and adverse perinatal outcome. Obstetrics and Gynecology 2004; 104(4):727-33.

Ježek P, Hlavatá L. Mitochondria in the homeostasis of reactive oxygen species in cell, tissues, and organism. International Journal of Biochemistry and Cell Biology [Internet] 2005; 37(12):2478-503.

Jones CA, Christensen AL, Salihu H, Carpenter W, Petrozzino J, Abrams E, Sills ES, Keith LG. Prediction of individual probabilities of livebirth and multiple birth events following in vitro fertilization (IVF): a new outcomes counselling tool for IVF providers and patients using HFEA metrics. Journal of experimental & clinical assisted reproduction [Internet] 2011; 8:3.

Kalyanaraman B. Teaching the basics of redox biology to medical and graduate students: Oxidants, antioxidants, and disease mechanisms. Redox Biology [Internet] 2013; 1(1):244-57.

Karbowski B, Bauch HJ, Schneider HPG. Functional differentiation of the vascular endothelium in high-risk pregnancies. Zeitschrift fur Geburtshilfe und Perinatologie 1989; 193(1):8-12.

Kehrer JP. The Haber-Weiss reaction and mechanisms of toxicity. Toxicology 2000; 149(1):43-50.

Kingdom JCP, Kaufmann P. Oxygen and placental villous development: origins of foetal hypoxia. Placenta 1997; 18(8):613-21.

Kingdom JCP, Kaufmann P. Oxygen and placental vascular development. Advances in Experimental Medicine and Biology 1999; 474:259-75.

Kirkinezos IG, Moraes CT. Reactive oxygen species and mitochondrial diseases. Seminars in Cell and Developmental Biology 2001; 12(6):449-57.

Kleinbongard P, Schulz R, Rassaf T, Lauer T, Dejam A, Jax T, Kumara I, Gharini P, Kabanova S, Özüyaman B, et al. Red blood cells express a functional endothelial nitric oxide synthase. Blood 2006; 107(7):2943-51.

Kleinert H, Art J, Pautz A. Regulation of the Expression of Inducible Nitric Oxide Synthase. Nitric Oxide 2010; 23(2):75-93.

Koppenol WH, Moreno JJ, Pryor WA, Ischiropoulos H, Beckman JS. Peroxynitrite, a Cloaked Oxidant Formed by Nitric Oxide and Superoxide. Chemical Research in Toxicology 1992; 5(6):834-42.

Krause BJ, Hanson MA, Casanello P. Role of nitric oxide in placental vascular development and function. Placenta [Internet] 2011; 32(11): 797–805.

Krotz S, Fajardo J, Ghandi S, Patel A, Keith LG. Hypertensive Disease in Twin Pregnancies: A Review. Twin Research 2002; 5(1):8-14.

Krüger-Genge A, Blocki A, Franke RP, Jung F. Vascular endothelial cell biology: An update. International Journal of Molecular Sciences [Internet] 2019; 20(18):4411.

Kuhn V, Diederich L, Keller TCS, Kramer CM, Lückstädt W, Panknin C, Suvorava T, Isakson BE, Kelm M, Cortese-Krott MM. Red Blood Cell Function and Dysfunction: Redox Regulation, Nitric Oxide Metabolism, Anaemia. Antioxidants & Redox Signaling 2017; 26(13):718-742.

Kültz D. Molecular and evolutionary basis of the cellular stress response. Annual Review of Physiology [Internet] 2005; 67:225–257.

Li H, Förstermann U. Uncoupling of endothelial NO synthase in atherosclerosis and vascular disease. Current Opinion in Pharmacology [Internet] 2013; 13(2):161-7.

Li H, Horke S, Förstermann U. Oxidative stress in vascular disease and its pharmacological prevention. Trends in Pharmacological Sciences [Internet] 2013; 34(6):313-9.

Linderkamp O, Ozanne P, Wu PYK, Meiselman HJ. Red blood cell aggregation in preterm and term neonates and adults. Pediatric Research 1984; 18(12):1356-60.

Liu J, García-Cardeña G, Sessa WC. Palmitoylation of endothelial nitric oxide synthase is necessary for the optimal stimulated release of nitric oxide: Implications for caveolae localization. Biochemistry [Internet] 1996; 35(41):13277-81.

Liu XM, Chapman GB, Peyton KJ, Schafer AI, Durante W. Carbon monoxide inhibits apoptosis in vascular smooth muscle cells. Cardiovascular Research 2002; 55(2):396-405.

Lowry OH, Rosebrough NJ, Farr AL, Randall RJ. Protein measurement with the Folin phenol reagent. The Journal of biological chemistry 1951; 193(1):265-75.

Lucas R, Fulton D, Caldwell RW, Romero MJ. Arginase in the vascular endothelium: Friend or foe? Frontiers in Immunology 2014; 5: 589.

Machin G. Non-identical monozygotic twins, intermediate twin types, zygosity testing, and the non-random nature of monozygotic twinning: A review. American Journal of Medical Genetics, Part C: Seminars in Medical Genetics 2009; 151C (2):110-27.

Manuel Barrios Arpi L. Histology of Umbilical Cord in Mammals. 2019; Open access peer-reviewed chapter: DOI:10.5772/intechopen.80766.

Marla SS, Lee J, Groves JT. Peroxynitrite rapidly permeates phospholipid membranes. Proceedings of the National Academy of Sciences of the United States of America 1997; 94(26):14243-8.

Martin JA, Hamilton BE, Osterman MJK. Three decades of twin births in the United States, 1980-2009. NCHS data brief 2012; (80):1-8.

Masilamani V, Alzahrani K, Devanesan S, Alqahtani H, AlSalhi MS. Smoking induced haemolysis: Spectral and microscopic investigations. Scientific Reports 2016; 6:21095.

Mattson MP. Hormesis and disease resistance: Activation of cellular stress response pathways. Human and Experimental Toxicology [Internet] 2008; 27(2):155-62.

Mauro A, Buscemi M, Provenzano S, Gerbino A. Human umbilical cord expresses several vasoactive peptides involved in the local regulation of vascular tone: Protein and gene expression of Orphanin, Oxytocin, ANP, eNOS, and iNOS. Folia Histochemica et Cytobiologica 2011; 49(2):211-8.

Mccord JM, Fridovich I. Superoxide dismutases: You've come a long way, baby. Antioxidants and Redox Signaling 2014; 20(10):1548-9.

Meekins JW, Luckas MJM, Pijnenborg R, McFadyen IR. Histological study of decidual spiral arteries and the presence of maternal erythrocytes in the intervillous space during the first trimester of normal human pregnancy. Placenta 1997; 18(5–6):459-464.

Messner B, Bernhard D. Smoking and Cardiovascular Disease. Arterioscler Thromb Vasc Biol 2014; 34(3):509-15.

Michel T, Feron O. Nitric oxide synthases: Which, where, how, and why? Journal of Clinical Investigation [Internet] 1997; 100(9):2146–2152.

Miller J, Chauhan SP, Abuhamad AZ. Discordant twins: Diagnosis, evaluation, and management. American Journal of Obstetrics and Gynecology 2012; 206(1):10-20.

Minami T, Muramatsu M, Kume T. Organ/tissue-specific vascular endothelial cell heterogeneity in health and disease. Biological and Pharmaceutical Bulletin [Internet] 2019; 42(10):1609-1619.

Minetti M, Agati L, Malorni W. The microenvironment can shift erythrocytes from a friendly to a harmful behavior: Pathogenetic implications for vascular diseases. Cardiovascular Research [Internet] 2007; 75(1):21-8.

Mizrahi O, Ish Shalom E, Baniyash M, Klieger Y. Quantitative Flow Cytometry: Concerns and Recommendations in Clinic and Research. Cytometry Part B - Clinical Cytometry 2018; 94(2):211-218.

Mohandas N, Gallagher PG. Red cell membrane: past, present, and future. Blood 2009; 112(10):3939-48.

Montorfano I, Becerra A, Cerro R, Echeverría C, Sáez E, Morales MG, Fernández R, Cabello-Verrugio C, Simon F. Oxidative stress mediates the conversion of endothelial cells into myofibroblasts via a TGF-b1 and TGF-b2-dependent pathway. Laboratory Investigation [Internet] 2014; 94(10):1068-82.

Nair J, Flora S De, Izzotti A, Bartsch H. Lipid peroxidation-derived etheno-DNA adducts in human atherosclerotic lesions. Mutation Research - Fundamental and Molecular Mechanisms of Mutagenesis [Internet] 2007; 621(1-2):95-105.

Naro E Di, Ghezzi F, Raio L, Franchi M, D'Addario V. Umbilical cord morphology and pregnancy outcome. European Journal of Obstetrics and Gynecology and Reproductive Biology 2001; 96(2):150-7.

Nedeljkovic ZS, Gokce N, Loscalzo J. Mechanisms of oxidative stress and vascular dysfunction. Postgraduate Medical Journal [Internet] 2003; 79(930):195–200.

Nishikawa E, Matsumoto T, Isige M, Tsuji T, Mugisima H, Takahashi S. Comparison of capacities to maintain hematopoietic stem cells among different types of stem cells derived from the placenta and umbilical cord. Regenerative Therapy 2016; 4:48–61.

Njaa BL.Book-Kirkbride's Diagnosis of Abortion and Neonatal Loss in Animals, 4th Edition.2011.

Nordberg J, Arnér ESJ. Reactive oxygen species, antioxidants, and the mammalian thioredoxin system. Free Radical Biology and Medicine [Internet] 2001; 31(11):1287-312.

Norwitz ER, Edusa V, Park JS. Maternal physiology and complications of multiple pregnancies. Seminars in Perinatology 2005; 29(5):338-48.

Obiechina NJ, Okolie VE, Eleje GU, Okechukwu ZC, Anemeje OA. Twin versus singleton pregnancies: the incidence, pregnancy complications, and obstetric outcomes in a Nigerian tertiary hospital. International Journal of Women's Health 2011; 3:227-30.

Özüyaman B, Grau M, Kelm M, Merx MW, Kleinbongard P. RBC NOS: regulatory mechanisms and therapeutic aspects. Trends in Molecular Medicine 2008; 14(7):314-22.

Packer MA, Porteous CM, Murphy MP. Superoxide production by mitochondria in the presence of nitric oxide forms peroxynitrite. Biochemistry and Molecular Biology International 1996; 40(3):527-34.

Pautz A, Art J, Hahn S, Nowag S, Voss C, Kleinert H. Regulation of the expression of inducible nitric oxide synthase. Nitric Oxide - Biology and Chemistry [Internet] 2010; 23(2):75-93.

Pernow J, Jung C. Arginase as a potential target in the treatment of cardiovascular disease: Reversal of arginine steal? Cardiovascular Research [Internet] 2013; 98(3):334-43.

Pernow J, Mahdi A, Yang J, Zhou Z. Red blood cell dysfunction: A new player in cardiovascular disease. Cardiovascular Research 2019; 115(11):1596-1605.

Perrone S, Laschi E, Buonocore G. Biomarkers of oxidative stress in the foetus and the new-born. Free Radical Biology and Medicine 2019; 142:23-31.

Perrone S, Negro S, Tataranno ML, Buonocore G. Oxidative stress and antioxidant strategies in newborns. Journal of Maternal-Foetal and Neonatal Medicine 2010; 23 Suppl 3:63-5.

Perrone S, Tataranno ML, Stazzoni G, Buonocore G. Biomarkers of oxidative stress in foetal and neonatal diseases. Journal of Maternal-Foetal and Neonatal Medicine 2012; 25(12):2575-8.

Phaniendra A, Jestadi DB, Periyasamy L. Free Radicals: Properties, Sources, Targets, and Their Implication in Various Diseases. Indian Journal of Clinical Biochemistry 2015; 30(1):11-26.

Pharoah POD, Glinianaia S V., Rankin J. Congenital anomalies in multiple births after the early loss of a conceptus. Human Reproduction 2009; 24(3):726–731.

Pison G, D'Addato A V. Frequency of twin births in developed countries. Twin Research and Human Genetics 2006; 9(2):250-9.

Pretorius E, Plooy JN Du, Soma P, Keyser I, Buys A V. Smoking and fluidity of erythrocyte membranes: A high-resolution scanning electron and atomic force microscopy investigation. Nitric Oxide - Biology and Chemistry 2013; 35:42-6.

Prieto CP, Krause BJ, Quezada C, Martin RS, Sobrevia L, Casanello P. Hypoxia-reduced nitric oxide synthase activity is partially explained by higher arginase-2 activity and

cellular redistribution in human umbilical vein endothelium. Placenta [Internet] 2011; 32(12):932-40.

Ratovitski EA, Bao C, Quick RA, McMillan A, Kozlovsky C, Lowenstein CJ. An inducible nitric-oxide synthase (NOS)-associated protein inhibits NOS dimerization and activity. Journal of Biological Chemistry 1999; 274(42):30250-7.

Rodríguez-Rodríguez P, Ramiro-Cortijo D, Reyes-Hernández CG, López de Pablo AL, Carmen González M, Arribas SM. Implication of oxidative stress in foetal programming of cardiovascular disease. Frontiers in Physiology 2018; 9: 602.

Schächinger V, Britten MB, Zeiher AM. Prognostic impact of coronary vasodilator dysfunction on adverse long-term outcome of coronary heart disease. Circulation [Internet] 2000; 101(16):1899-906.

Schödel J, Padmapriya P, Marx A, Huang PL, Ertl G, Kuhlencordt PJ. Expression of neuronal nitric oxide synthase splice variants in atherosclerotic plaques of apoE knockout mice. Atherosclerosis [Internet] 2009; 206(2):383–389.

Schwarz PM, Kleinert H, Förstermann U. Potential Functional Significance of Brain-Type and Muscle-Type Nitric Oxide Synthase I Expressed in Adventitia and Media of Rat Aorta. Arteriosclerosis, Thrombosis, and Vascular Biology [Internet] 1999; 19(11):2584-90.

Selye H. Stress and disease. Science [Internet] 1955; 122(3171):625-31.

Sharma AK, Taneja G, Khanna D, Rajput SK. Reactive oxygen species: Friend or foe? RSC Advances 2015; 5:57267–57276.

Shu X, Keller TCS, Begandt D, Butcher JT, Biwer L, Keller AS, Columbus L, Isakson BE. Endothelial nitric oxide synthase in the microcirculation. Cellular and Molecular Life Sciences 2015; 72(23):4561-4575.

Sibai BM, Hauth J, Caritis S, Lindheimer MD, MacPherson C, Klebanoff M, VanDorsten JP, Landon M, Miodovnik M, Paul R, et al. Hypertensive disorders in twin versus singleton gestations. American Journal of Obstetrics and Gynecology 2000; 182(4):938-42.

Sies H. Oxidative stress: A concept in redox biology and medicine. Redox Biology 2015; 4:180-3.

Silva BR, Pernomian L, Bendhack LM. Contribution of oxidative stress to endothelial dysfunction in hypertension. Frontiers in Physiology 2012; 3:441.

Singla PN, Tyagi M, Kumar A, Dash D, Shankar R. Foetal growth in maternal anaemia. Journal of Tropical Pediatrics 1997; 43(2):89-92.

Siu SC, Colman JM, Sorensen S, Smallhorn JF, Farine D, Amankwah KS, Spears JC, Sermer M. Adverse neonatal and cardiac outcomes are more common in pregnant women with cardiac disease. Circulation 2002; 105(18):2179-84.

Smith K, Li Y, Piccinini F, Csucs G, Balazs C, Bevilacqua A, Horvath P. CIDRE: An illumination-correction method for optical microscopy. Nature Methods 2015; 12(5):404-6.

Soma P, Pretorius E. Interplay between ultrastructural findings and atherothrombotic complications in type 2 diabetes mellitus. Cardiovascular Diabetology 2015; 14:96.

Spurway J, Logan P, Pak S. The development, structure, and blood flow within the umbilical cord with particular reference to the venous system. Australasian Journal of Ultrasound in Medicine 2012; 15(3): 97–102.

Stanek J. Hypoxic patterns of placental injury: A review. Archives of Pathology and Laboratory Medicine 2013; 137(5):706-20.

Stock S, Norman J. Preterm and term labor in multiple pregnancies. Seminars in Foetal and Neonatal Medicine 2010; 15(6):336-41.

Su R-N, Zhu W-W, Wei Y-M, Wang C, Feng H, Lin L, Yang H-X. Maternal and neonatal outcomes in multiple pregnancies: A multicentre study in the Beijing population. Chronic Diseases and Translational Medicine 2015; 1(4):197-202.

Tan BL, Norhaizan ME, Liew WPP, Rahman HS. Antioxidant and oxidative stress: A mutual interplay in age-related diseases. Frontiers in Pharmacology [Internet] 2018; 9:1162.

Thaete LG, Dewey ER, Neerhof MG. Endothelin and the regulation of uterine and placental perfusion in hypoxia-induced foetal growth restriction. Journal of the Society for Gynecologic Investigation 2004; 11(1):16-21.

Tomasian D, Keaney JF, Vita JA. Antioxidants and the bioactivity of endothelium-derived nitric oxide. Cardiovascular Research [Internet] 2000; 47(3):426–435.

Tsutsui M. Neuronal nitric oxide synthase as a novel anti-atherogenic factor. Journal of atherosclerosis and thrombosis [Internet] 2004; 11(2):41-8.

Uchida K, Stadtman ER. Covalent attachment of 4-hydroxynonenal to glyceraldehyde-3-phosphate dehydrogenase. Possible involvement of intra- and intermolecular cross-linking reaction. Journal of Biological Chemistry 1993; 268(9):6388-6393.

Vanhoutte PM, Shimokawa H, Feletou M, Tang EHC. Endothelial dysfunction and vascular disease – a 30th anniversary update. Acta Physiologica [Internet] 2017; 219(1):22-96.

Villegas E, Gilliland SE. Hydrogen Peroxide Production by Lactobacillus delbrueckii Subsp. Lactis I at 5°C. Journal of Food Science 1998; 63(6):1070–1074.

Vogel JP, Torloni MR, Seuc A, Betrán AP, Widmer M, Souza JP, Merialdi M. Maternal and Perinatal Outcomes of Twin Pregnancy in 23 Low- and Middle-Income Countries. PLoS ONE 2013; 8(8): e70549.

Watson JD. Type 2 diabetes **is** a redox disease. The Lancet 2014; 383(9919):841-3.

Weber MA, Sebire NJ. Genetics and developmental pathology of twinning. Seminars in Foetal and Neonatal Medicine 2010; 15(6):313-318.

Weissman A, Jakobi P, Bronshtein M, Goldstein I. Sonographic measurements of the umbilical cord and vessels during normal pregnancies. Journal of Ultrasound in Medicine 1994; 13(1):11-4.

Williams LA, Evans SF, Newnham JP. A prospective cohort study of factors influencing the relative weights of the placenta and the newborn infant. British Medical Journal 1997; 314(7098):1864-8.

Yang J, Gonon AT, Sjöquist PO, Lundberg JO, Pernow J. Arginase regulates red blood cell nitric oxide synthase and export of cardioprotective nitric oxide bioactivity. Proceedings of the National Academy of Sciences of the United States of America [Internet] 2013; 110(37):15049-54.

Yang Z, Ming XF. Arginase: The emerging therapeutic target for vascular oxidative stress and inflammation. Frontiers in Immunology 2013; 4:149.

Yoshida A, Watanabe K, Iwasaki A, Kimura C, Matsushita H, Wakatsuki A. Placental oxidative stress and maternal endothelial function in pregnant women with normotensive foetal growth restriction. Journal of Maternal-Foetal and Neonatal Medicine 2018; 31(8):1051-1057.

Young BC, Wylie BJ. Effects of Twin Gestation on Maternal Morbidity. Seminars in Perinatology 2012; 36(3):162-8.

Young IS, Woodside J V. Antioxidants in health and disease. Journal of Clinical Pathology [Internet] 2001; 54(3):176-86.

Yu X, Ge L, Niu L, Lian X, Ma H, Pang L. The dual role of inducible nitric oxide synthase in myocardial ischemia/reperfusion injury: Friend or foe? Oxidative Medicine and Cellular Longevity 2018; 2018:8364848.

Zahorán S, Szántó PR, Bódi N, Bagyánszki M, Maléth J, Hegyi P, Sári T, Hermesz E. Sustained maternal smoking triggers endothelial-mediated oxidative stress in the umbilical cord vessels, resulting in vascular dysfunction. Antioxidants 2021; 10(4):583.

Zhou C, Zou QY, Jiang YZ, Zheng J. Role of oxygen in fetoplacental endothelial responses: hypoxia, physiological normoxia, or hyperoxia? American journal of physiology Cell physiology 2020; 318(5): C943-C953.

Zhou Z, Mahdi A, Tratsiakovich Y, Zahorán S, Kövamees O, Nordin F, Uribe Gonzalez AE, Alvarsson M, Östenson CG, Hermesz E, Andersson DC, et al. Erythrocytes from Patients with Type 2 Diabetes Induce Endothelial Dysfunction Via Arginase I. Journal of the American College of Cardiology 2018; 72(7):769–780.

9. List of Publications

Number of scientific publications: 6

Total impact factor: 31.695

MTMT identification number: 10053026

1. **Payal Chakraborty**, Krisztina N. Dugmonits, Hajnalka Orvos, Edit Hermesz. Mature Twin Neonates Exhibit Oxidative Stress via Nitric Oxide Synthase Dysfunctionality: A Prognostic Stress Marker in the Red Blood Cells and Umbilical Cord Vessels. Antioxidants (2020); 9(9):845. doi: 10.3390/antiox9090845. IF: 6.312

2**. Payal Chakraborty**, Ali Khamit, Edit Hermesz. Foetal oxygen supply can be improved by an effective cross-talk between foetal red blood cells and the vascular endothelial layer. Biochim Biophys Acta Mol Basis Dis (2021); 1867(11), 166243. doi: 10.1016/j.bbadis.2021.166243. IF: 5.187

3. Balogh Gábor*, **Chakraborty Payal***, Dugmonits Krisztina*, Péter Mária*, Végh Attila G., Vígh László, Hermesz Edit. Sustained maternal smoking-associated changes in the **Physico-chemical** properties of foetal RBC membranes might serve as early markers for vascular comorbidities. Biochim Biophys Acta Mol Cell Biol Lipids (2020);1865(4):158615. doi: 10.1016/j.bbalip.2020.158615. IF: 4.698

4. **Chakraborty P***, Dugmonits KN*, Végh AG, Hollandi R, Horváth P, Maléth J, Hegyi P, Németh G, Hermesz E. Failure in the compensatory mechanism in red blood cells due to sustained smoking during pregnancy. Chem Biol Interact (2019); 313:108821. doi: 10.1016/j.cbi.2019.108821. IF: 5.192

5. Dugmonits KN, **Chakraborty P**, Hollandi R, Zahorán S, Pankotai-Bodó G, Horváth P, Orvos H, Hermesz E. Maternal Smoking Highly Affects the Function, Membrane Integrity, and Rheological Properties in Foetal Red Blood Cells. Oxid Med Cell Longev. (2019); 1509798. doi: 10.1155/2019/1509798. IF: 6.543

6. Nikolett Bódi, Diána Mezei, **Payal Chakraborty**, Zita Szalai, Bence Pál Barta, János Balázs, Zsolt Rázga, Edit Hermesz, Mária Bagyánszki. Correlation between the region-specific thickening of ganglionic basement membrane and regionally decreased matrix metalloproteinase 9 expression in myenteric ganglia and its environment in type 1 diabetes. World Journal of Diabetes. (2021). 12(5): 658–672. doi: 10.4239/wjd. v12.i5.658. IF: 3.763

*** Co-first authorship**

10. Summary

In the last 30 years, by modern *in-vitro* fertilization therapies, the proportion of twin/ multiple pregnancies have markedly increased and developed a new significant clinical database. There showed an elevation in the foetal, neonatal, and perinatal mortality rate of 3-6 times in twins and 5-15 times in other multiple pregnancies in comparison to singletons. The state of pregnancy with enhanced metabolism and demand for oxygen definitely causes a significant burden on both the mother and the developing foetus, which further gets increased during twin pregnancy. In comparison to singletons, twin siblings' experience an additional stress condition with the excessive oxygen demand, and sustains a long-lasting adverse intrauterine environment. Increased oxygen demand in the twin neonates develops an intrauterine hypoxic condition that can lead to loss of redox balance and follow with its harmful consequences such as delayed development commonly characterized by low birth weight, respiratory disorders, preterm birth, and morphological disorders.

During pregnancy, the placenta and umbilical cord are the vital temporary organs to maintain the *in-utero* foetal development. The umbilical cord is entirely embryonic in origin, and the cord blood vessels are considered as a direct extension of the foetal circulation. The umbilical cord vein transports oxygen-rich blood and nutrients from the placenta to the foetus, and the two arteries carry the deoxygenated blood and waste products back to the placenta. The proper functioning of UC blood vessels is crucial in the fetoplacental circulation, to maintain the adequate supply of nutrients and oxygen to the developing foetus.

The UC vascular system, including the endothelial cell layer together with the circulating red blood cell (RBC) population, are the primary targets that get affected due

to an increased oxidative stress condition. Thereby necessarily carrying the environmental-induced morphological and functional changes indicate towards the effects experienced during the *in-utero* foetal development. Moreover, analysing the complications related to RBCs and the endothelial layer of the umbilical cord might serve as an important diagnostic tool for understanding the basic pathological processes leading to neonatal vascular diseases. In our study, we hypothesized that any kind of underlying molecular changes that determines the redox status of the cord vein might indicate the quality of the "nutrition" transferred from the mother to foetus, while the condition of the arteries provides more information concerning the "actual state" of the foetus.

As the UC vessels lack innervations, it releases vasoactive entities like nitric oxide (NO) acting as the key in regulating the vascular tone and fetoplacental blood flow which gets derived by the endothelial nitric oxide synthase (NOS3) activity. The activation process of NOS3 is necessary to liberate the bioavailable NO, which depends on several factors. The active NOS3 dimeric conformational state is highly regulated by the L-arginine substrate concentration, subcellular localization, presence of co-factors (e.g. tetrahydrobiopterin), diverse interacting proteins, and the post-translational modification by phosphorylation at Ser1177 residue via PI3-kinase/Akt kinase pathway.

Impairment in the endothelial NO synthesis causes endothelial dysfunction. Recent studies draw attention to the possibility of an intimate communication between the vascular endothelium and the RBC population, which suggests RBCs can perform the vital sensory function in response to a wide range of vascular/endothelial dysfunctions/diseases. Most importantly current discoveries also presented that RBCs independently contain the functional NOS3 enzyme, which actively participates to synthesize, liberate, and export NO in the regulation of vascular tone.

In our work, we followed significant changes involved in the activation process of NOS3 that might affect the redox status and functionality of both the UC vessel's endothelial layer and red blood cells - with a direct correlation on the birth weight and maturity level of the new-born twins. Our study selected the parameters that influence the dimerization step of the NOS3 enzyme, in presence of the enzyme Arginase1. Secondly, an alternative upregulation of inducible NOS (NOS2) enzyme might be a possible approach towards a compensatory/rescue mechanism. Hence we collected and examined the umbilical cord and red blood cell samples from both mature and preterm twins and neonates born from singleton pregnancies with different percentile values (25-95%).

Our main findings can be summarized as follows:

(1) During twin pregnancy, the activation of the NOS3 pathway in the umbilical cord vessels depends on the maturity level of the developing foetus - mature: > 37 weeks and preterm: 33-35 weeks' birth –that follows a vascular-specific regulation:

(a) Expression and phosphorylation of NOS3 at position Ser1177 in the umbilical vein endothelial cells of premature (33-35 weeks) twin siblings is comparable to age-matched neonates, regardless of the neonatal birth weight.

(b) Contrastingly, in matured twins (>37 weeks), NOS3 expression and its activation by phosphorylation at Ser1177 residue is significantly lower than the level measured to their age-matched singletons irrespective of their birth weight.

(c) In the umbilical cord arteries, except the mature and premature normal-birthweight neonates, there are no significant changes detected in the NOS3 expression/activation when compared to their age-matched singletons.

(2) Except the mature twins with normal birthweight, in all the other examined populations showed, that the RBC-NOS3-NO pathway under hypoxic conditions may significantly contribute to the improvement of vascular tone and thus able to maintain the foetal blood flow due to an elevation in the NOS3 expression and/or activation.

(3) Apart from the preterm neonates having a gestational age of 95^{th} ~~%~~ percentile, most likely the levels of bioavailable NOS3-NO and RBC-NOS3-NO are unsatisfactory in all the other investigated groups, and thus an alternative NO-producing pathway NOS2 is highly induced to improve the foetal blood flow.

(4) The expression level of Arginase1 in the RBCs of twin neonates is increased, which is partly due to the excessive presence of superoxide anions in the vascular system.

(5) In the case of twin pregnancies, the level of pro-oxidant peroxynitrite anion in foetal RBCs is increased, which can also be associated with the higher availability of the superoxide anions.

(6) Increased macromolecular damages were observed in connection to the elevated levels of the peroxynitrite anion, which was detected and determined by measuring the accumulation of 4-hydroxynonenal (4-HNE) level. Irrespective of maturity, arteries, and circulating RBCs were primarily affected. It is also shown that at the matured stages of twin pregnancy, the 4-HNE levels get significantly increased in the arteries.

(7) Irrespective of the maturity level in the twin neonates, there occurs an increased frequency of morphological variants in the foetal RBCs. These phenotypic differences may be a useful indicator for any disturbances in the functional and/or physicochemical properties of the RBCs.

11. Összefoglaló

A modern *in vitro* megtermékenyítési terápiák alkalmazásának köszönhetően az utóbbi 30 évben megnőtt az iker/többes terhességek aránya, mely lehetőséget nyújtott új, klinikai szempontból jelentős adatbázis kiépítésére. Ikerterhesség esetén a magzati/újszülött kori halálozás 3-6 szorosa, míg többszörös terhesség esetén 5-15-szerese az egyszeres terhességek során tapasztalt értékeknek. A várandóság jelentős terhet jelent úgy az anya, mint a fejlődő magzat szervezetére. Az ikerterhesség fokozott oxigén igénye intrauterin hipoxiás állapot kialakulását eredményezi, mely a redox egyensúly elvesztéséhez vezethet, ennek összes következményével együtt, mint például fejlődései visszamaradottság, melyet leggyakrabban alacsony születési súly jellemez, légzési rendellenességek, koraszülöttség és morfológiai rendellenességek.

A terhesség alatt a placenta és a köldökzsinór létfontosságú ideiglenes szervet képeznek a magzat fejlődésének fenntartása érdekében. A köldökzsinór teljes mértékben embrionális eredetű, a benne futó erek a magzati keringés közvetlen kiterjesztésének tekinthetőek. A köldökzsinór véna szállítja az oxigén dús vért és táplálékot a méhlepénytől a magzatig, a két artéria pedig a „fáradt" vért és a salakanyagot vissza a placentába. Az erek megfelelő működése meghatározó a fetoplacentális keringésben, a fejlődő magzat megfelelő tápanyag és oxigénellátásában.

A köldökzsinór vaszkuláris rendszere, ezen belül is az endotél sejtréteg, együtt a keringő vörösvértes populációval a fokozott oxidatív stressz elsődleges elszenvedői, ezáltal szükségszerűen hordozzák a környezet indukálta morfológiai és funkcionális változásokat, melyek jelzés értékűek lehetnek a magzatra gyakorolt hatást illetően is. Ezért a vörösvértestek és a köldökzsinór endotél rétegével kapcsolatos komplikációk elemzése fontos eszköze lehet az újszülött kori érrendszeri betegségekhez vezető patológiás

folyamatok megértésének. Munkánk során feltételeztük, hogy a vénában bekövetkező változások jelzik az anya felől érkező, a magzati keringésbe jutó „káros anyagok" megjelenését, mintegy lenyomatai a magzatot ért káros hatásoknak. Az artériák állapota pedig a magzati válaszreakciókat tükrözi, így információt nyújtva az újszülöttek tényleges állapot tekintve.

A köldökzsinór erek nem rendelkeznek beidegzéssel, ezért az endotél sejtek nitrogén monoxid szintáz (NOS3) aktivitása kulcsfontosságú az értónus és a fetoplacentális véráramlás szabályozásában. A NOS3 függő NO termelést több tényező befolyásolja. A NOS3 enzim dimer formában aktív. Ennek képződésben és a megfelelő elektron transzfer fenttartásában olyan tényezők játszanak szerepet, mint az L-arginin szubsztrát koncentrációja, az enzim szubcelluláris lokalizációja, ko-faktorok (pl. a tetrahidrobiopterin) és kölcsönható fehérjepartnerek jelenléte, posztranszlációs módosítások, mint például a Ser1177 oldallánc foszforilációja a PI3- / Akt-kináz útvonalon keresztül.

Az endoteliális NO szintézis károsodása endoteliális diszfunkciót eredményezhet. A közelmúltban megjelent tanulmányok felhívják a figyelmet egy intim kommunikáció lehetőségére az ér-endotél és a vörösvértest populáció között, mely alapján feltételezhető hogy a vörösvértestek létfontosságú szenzor funkciót látnak el a vaszkuláris / endoteliális diszfunkciók / betegségek széles skálájára reagálva. Ugyancsak a közelmúlt jelentős felfedezései közt kell megemlítenünk, hogy a vörösvértestek önálló, funkcionális NOS3 enzimmel rendelkeznek mely lehetővé teszi számukra, hogy nem csupán az endotél eredetű NO „sülyesztőjeként" működjenek, hanem maguk is aktív szereplőivé váljanak az értónus szabályozásának, a NO szintetizáló és exportáló funkciójuk révén.

Munkánk során a NOS3 aktivációs folyamatának változásaira fókuszáltunk, amelyek befolyásolhatják mind a köldökzsinór erek endoteliális rétegének, mind az vörös vértesteknek a redox állapotát, funkcionalitását - jelentős hatást gyakorolva az újszülött ikrek születési súlyára és érettségi szintjére. Vizsgálataink kiterjedtek a NOS3 enzim dimerizációját befolyásoló paraméterekre, mint például az Argináz-1 enzim jelenlétére, illetve az indukálható NOS (NOS2) enzim, mint egy lehetséges, „*built in*" kompenzációs mechanizmus aktiválódására. A vizsgált köldökzsinór és vörösvértest (VVT) minták érett és koraszülött iker és egyes terhességből született újszülöttektől származnak, különböző percentilis értékkel (25-95%).

Főbb megállapításaink a következőkben foglalhatók össze:

(1) Ikerterhesség alatt a köldökzsinór erekben a NOS3 útvonal a fejlődő magzat érettségi szintjétől - érett: > 37. hét, koraszülött: 33-35. hét - függően, valamint ér-specifikus módon szabályozott:

(a) a terhesség 33-35. hetében a NOS3 expressziója és foszforilációja a Ser_{1177} pozícióban az ikerterhességből származó köldökzsinór véna endoteliális sejtekben összevethető a korban megegyező egyes terhesség során mért adatokkal, függetlenül az újszülöttek súlyától

(b) ezzel szemben a terhesség előrehaladtával (> 37. hét), a NOS3 expresszió jelentősen elmarad az egyes terhesség során mért szinttől, függetlenül az újszülöttek súlyától

(c) a köldökzsinór artériákban, az érett, normál súlyú újszülöttektől eltekintve, nincs jelentős változás a NOS3 expressziójában / aktivációjában az egyes terhesség során mért adatokhoz képest

(2) Az érett, normál súlyú újszülöttek kivételével, a VVT-NOS3-NO útvonal jelentősen hozzájárulhat az értónus és ezzel a magzati véráramlás javításához, a magas NOS3 expresszió és / vagy aktiváció következtében.

(3) Valószínűsíthető, hogy a koraszülött ~ 95% percentilis újszülöttek kivételével, a biológiailag hozzáférhető NOS3-NO és VVT-NOS3-NO szint nem kielégítő, a magzat véráramlásának javítása érdekében alternatív NO-termelő útvonal, a NOS2 expresszió indukálódik.

(4) Az iker újszülöttek vörösvértestjeiben az Arginase1 expressziójának emelkedett a szintje, mely részben a rendszerben nagymennyiségben termelődő szuperoxid anion jelenlétére vezethető vissza.

(5) Ikerterhesség esetén a magzati vörösvértestekben megemelkedett a pro-oxidáns peroxi-nitrit anion szint, mely szintén összefüggésbe hozható magas szuperoxid anion elérhetőséggel.

(6) A peroxi-nitrit anion szinttel összefüggésben emelkedett membránkárosodás figyelhető meg, melynek meghatározására a hidroxi nonenal (HNE) akkumuláció mérését alkalmaztuk. Az érettségi szinttől függetlenül, elsősorban az artériák és a keringő VVT-k érintettek. A terhesség előrehaladtával az artériákban jelentősen nő a HNE szint.

(7) Az újszülöttek érettségi szintjétől függetlenül a magzati vörösvértestekben megemelkedett a morfológiai variánsok száma iker terhesség során. Ezen fenotípusos eltérések hasznos indikátorként szolgálhatnak a funkcionális és / vagy fizikai-kémiai tulajdonságaikban bekövetkező bármilyen zavar esetén.

12. Appendix

Figure S1. Representative epifluorescent images of the arterial endothelium in relation to NOS3 expression and its phosphorylation level.

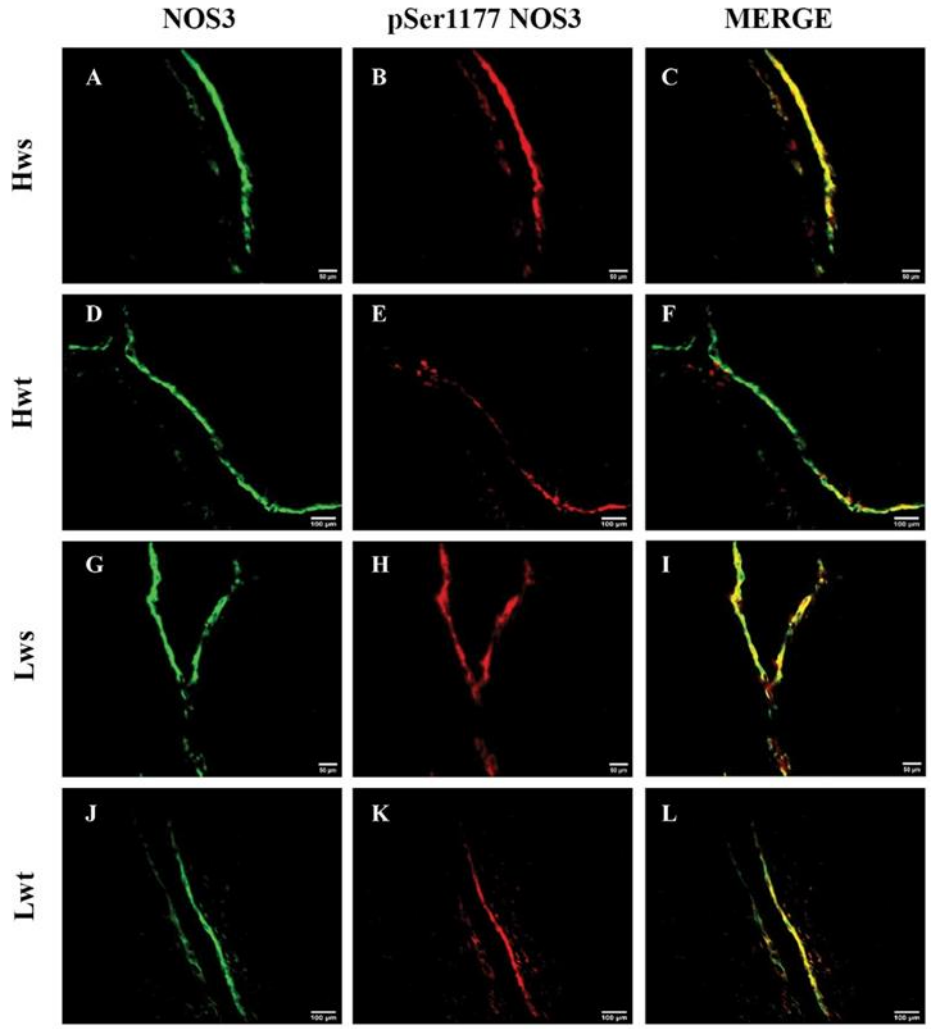

Representative epifluorescent images of immunolabelled arterial endothelium originated from Hws, Hwt, Lws, and Lwt samples. Panels (A, D, G, and J) show immunolabelling with mouse primary anti-NOS3 antibody followed by an Alexa Fluor® 488 secondary antibody. Panels (B, E, H, and K) show immunolabelling with a rabbit anti-pSer1177 NOS3 primary antibody followed by an Alexa Fluor® 647 secondary antibody. Panels (C, F, I, and L) present the merged images. Slides were mounted and examined under an epifluorescence microscope (Nikon Eclipse 80i, 100x and 50x immersion objective; Nikon Zeiss Microscopy GmbH, Jena, Germany).

Figure S2. Representative epifluorescent images of the venous endothelium in relation to the NOS3 expression and its phosphorylation level.

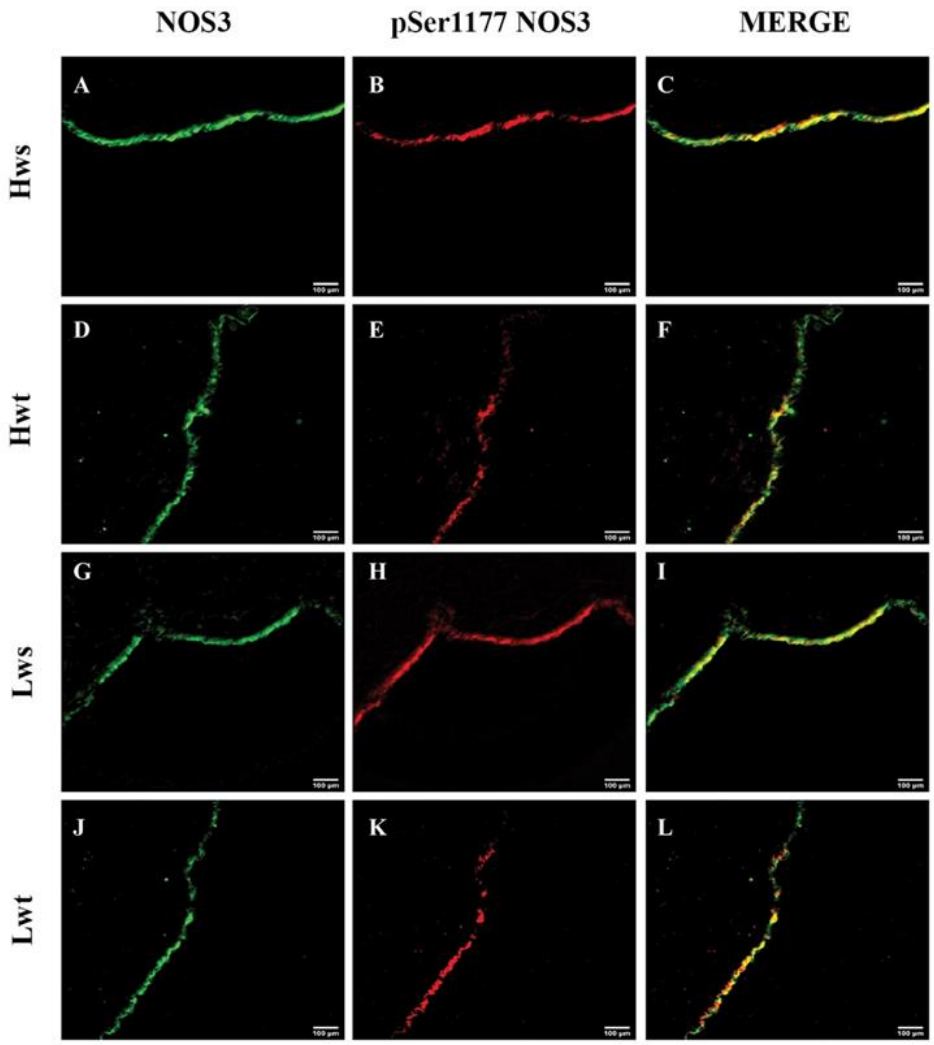

Representative epifluorescent images of immunolabelled venous endothelium originated from Hws, Hwt, Lws, and Lwt samples. Panels (A, D, G, and J) show immunolabelling with mouse primary anti-NOS3 antibody followed by an Alexa Fluor® 488 secondary antibody. Panels (B, E, H, and K) show immunolabelling with a rabbit anti-pSer1177 NOS3 primary antibody followed by an Alexa Fluor® 647 secondary antibody. Panels (C, F, I, and L) present the merged images. Slides were mounted and examined under an epifluorescence microscope (Nikon Eclipse 80i, 100x and 50x immersion objective; Nikon Zeiss Microscopy GmbH, Jena, Germany). (Nikon Eclipse 80i, 100x and 50x immersion objective; Nikon Zeiss Microscopy GmbH, Jena, Germany).

Figure S3. Represents epifluorescent images of the arterial cord endothelium sections immunolabelled with the Arginase1, NOS2, and 4-HNE.

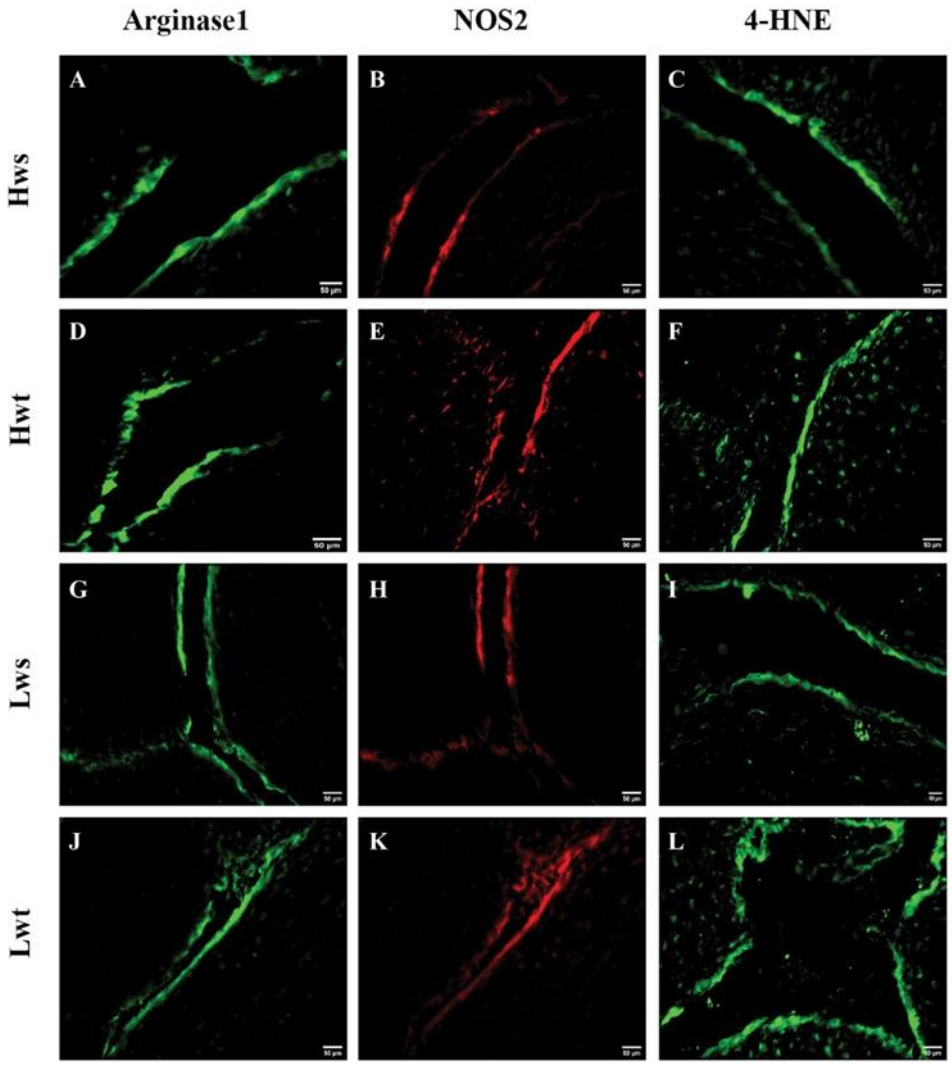

Representative epifluorescent images of immunolabelled arterial endothelium originated from Hws, Hwt, Lws, and Lwt samples. The panels (A, D, G, and J) show immunolabelling with a mouse primary anti-Arginase1 antibody followed by an Alexa Fluor® 488 secondary antibody. In a similar manner, panels (B, E, H, and K) present samples immunolabelling with a rabbit primary anti-NOS2 antibody followed by an Alexa Fluor® 647 secondary antibody, and the panels (C, F, I and L) exhibit immunolabelling with a mouse primary anti-4-HNE antibody followed by an Alexa Fluor® 488 secondary antibody. The slides were mounted and examined under an epifluorescence microscope (Nikon Eclipse 80i, 100x and 50x immersion objective; Nikon Zeiss Microscopy GmbH, Jena, Germany).

Figure S4. Visualization of the vein endothelium sections epifluorescent images immunolabelled with the Arginase1, NOS2, and 4-HNE.

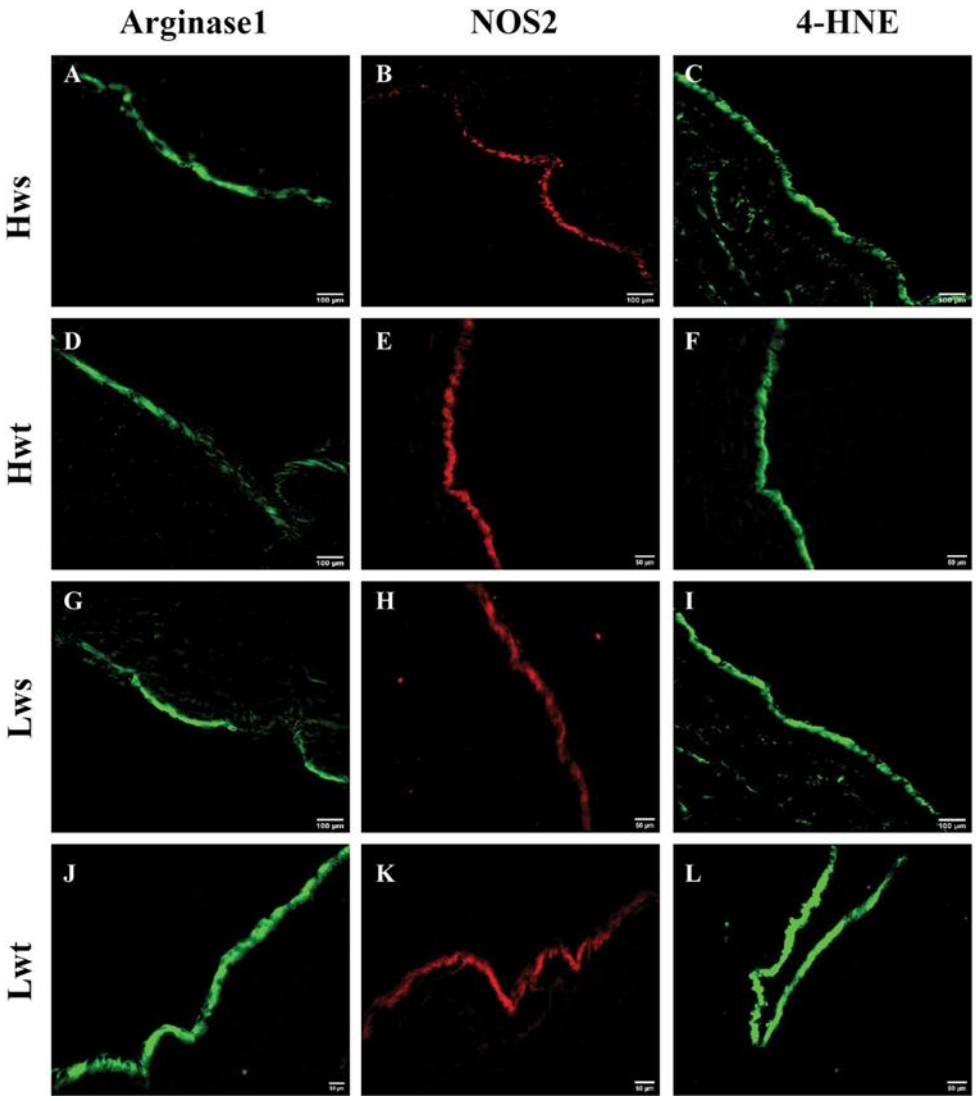

Representative epifluorescent images of immunolabelled venous endothelium originated from Hws, Hwt, Lws, and Lwt samples. The panels (A, D, G, and J) show immunolabelling with a mouse primary anti-Arginase1 antibody followed by an Alexa Fluor® 488 secondary antibody. In **a** similar manner, panels (B, E, H, and K) present samples immunolabelling with a rabbit primary anti-NOS2 antibody followed by an Alexa Fluor® 647 secondary antibody, and the panels (C, F, I and L) exhibit immunolabelling with a mouse primary anti-4-HNE antibody followed by an Alexa Fluor® 488 secondary antibody. The slides were mounted and examined under an epifluorescence microscope (Nikon Eclipse 80i, 100x and 50x immersion objective; Nikon Zeiss Microscopy GmbH, Jena, Germany).

Figure S5. Representative epifluorescent images showing NOS3 and pNOS3 levels in the umbilical cord arterial endothelium

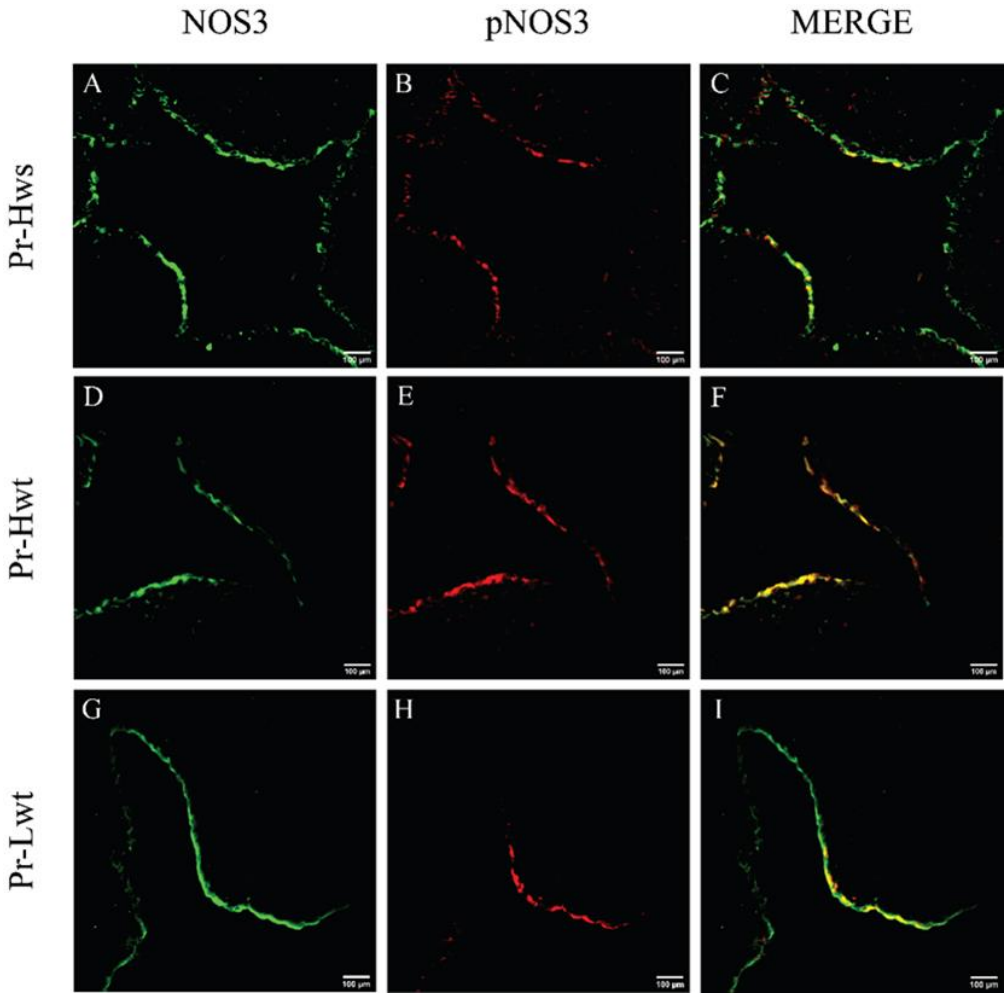

Representative epifluorescent images on immunolabelled arterial endothelium originated from premature, non-discordant, high (Pr-Hwt), and low (Pr-Lwt) weight twins and age-matched high weight singleton (Pr-Hws). Panels (A, D, and G) show immunolabelling with mouse primary anti-NOS3 antibody followed by Alexa Fluor® 488 secondary antibody staining. Panels (B, E, and H) show immunolabelling with a rabbit anti-pNOS3 primary antibody followed by Alexa Fluor® 647 secondary antibody staining. Panels (C, F, and I) present the merged images. Slides were mounted and examined under an epifluorescence microscope (Nikon Eclipse 80i, 100x immersion objective; Nikon Zeiss Microscopy GmbH, Jena, Germany).

Figure S6. Representative epifluorescent images showing NOS3 and pNOS3 levels in the umbilical cord vein endothelium

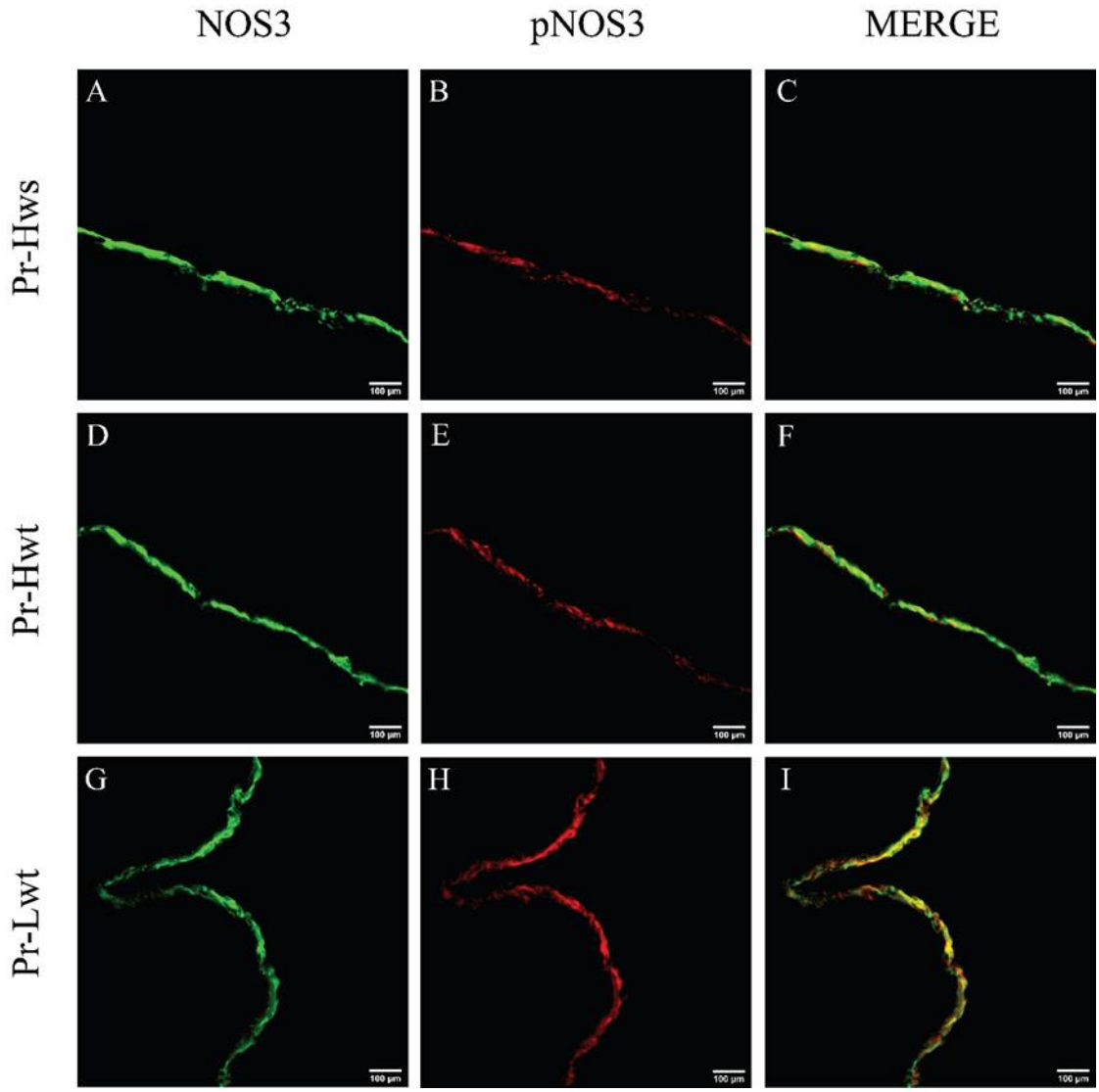

Representative epifluorescent images on immunolabelled venous endothelium originated from premature, non-discordant, high (Pr-Hwt), and low (Pr-Lwt) weight twins and age-matched high weight singleton (Pr-Hws) samples. Panels (A, D, and G) show immunolabelling with mouse primary anti-NOS3 antibody followed by Alexa Fluor® 488 secondary antibody staining. Panels (B, E, and H) show immunolabelling with a rabbit anti-pNOS3 primary antibody followed by Alexa Fluor® 647 secondary antibody staining. Panels (C, F, and I) present the merged images. Slides were mounted and examined under an epifluorescence microscope (Nikon Eclipse 80i, 100x immersion objective; Nikon Zeiss Microscopy GmbH, Jena, Germany).

Figure S7. Epifluorescent images represent arterial cord endothelium immunolabelled with Arginase1, NOS2, and 4-HNE

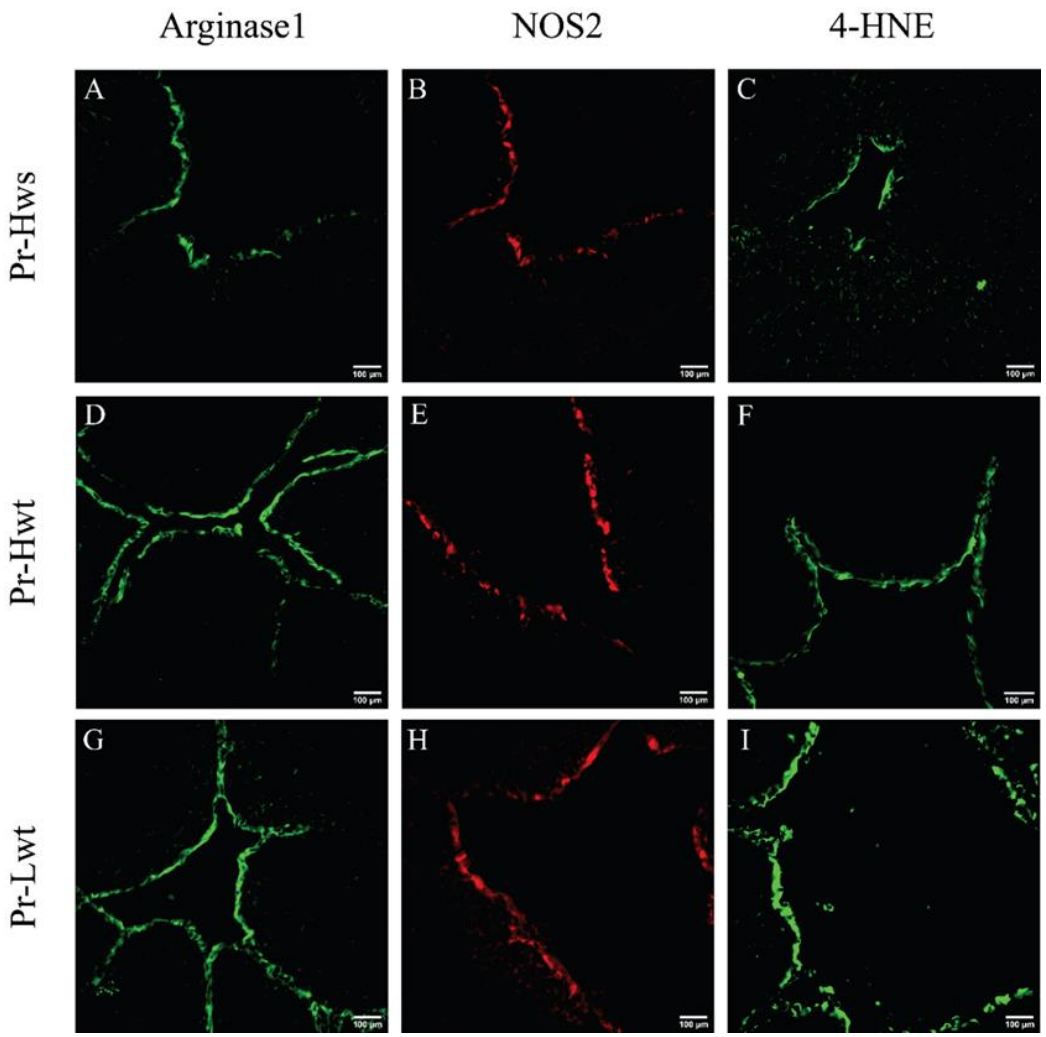

Representative epifluorescent images on immunolabelled arterial endothelium originated from premature, non-discordant, high (Pr-Hwt), and low (Pr-Lwt) weight twins and age-matched high weight singleton (Pr-Hws). Panels (A, D, and G) show immunolabelling with a mouse primary anti-Arginase1 antibody followed by Alexa Fluor® 488 secondary antibody staining. In a similar manner, panels (B, E, and H) present samples that were immunolabelled with a rabbit primary anti-NOS2 antibody followed by an Alexa Fluor® 647 secondary antibody. Panels (C, F, and I) exhibit immunolabelling with a mouse primary anti-4-HNE antibody followed by an Alexa Fluor® 488 secondary antibody. The slides were mounted and examined under an epifluorescence microscope (Nikon Eclipse 80i, 100x immersion objective; Nikon Zeiss Microscopy GmbH, Jena, Germany).

Figure S8. Epifluorescent images represent venous endothelium immunolabelled with Arginase1, NOS2, and 4-HNE

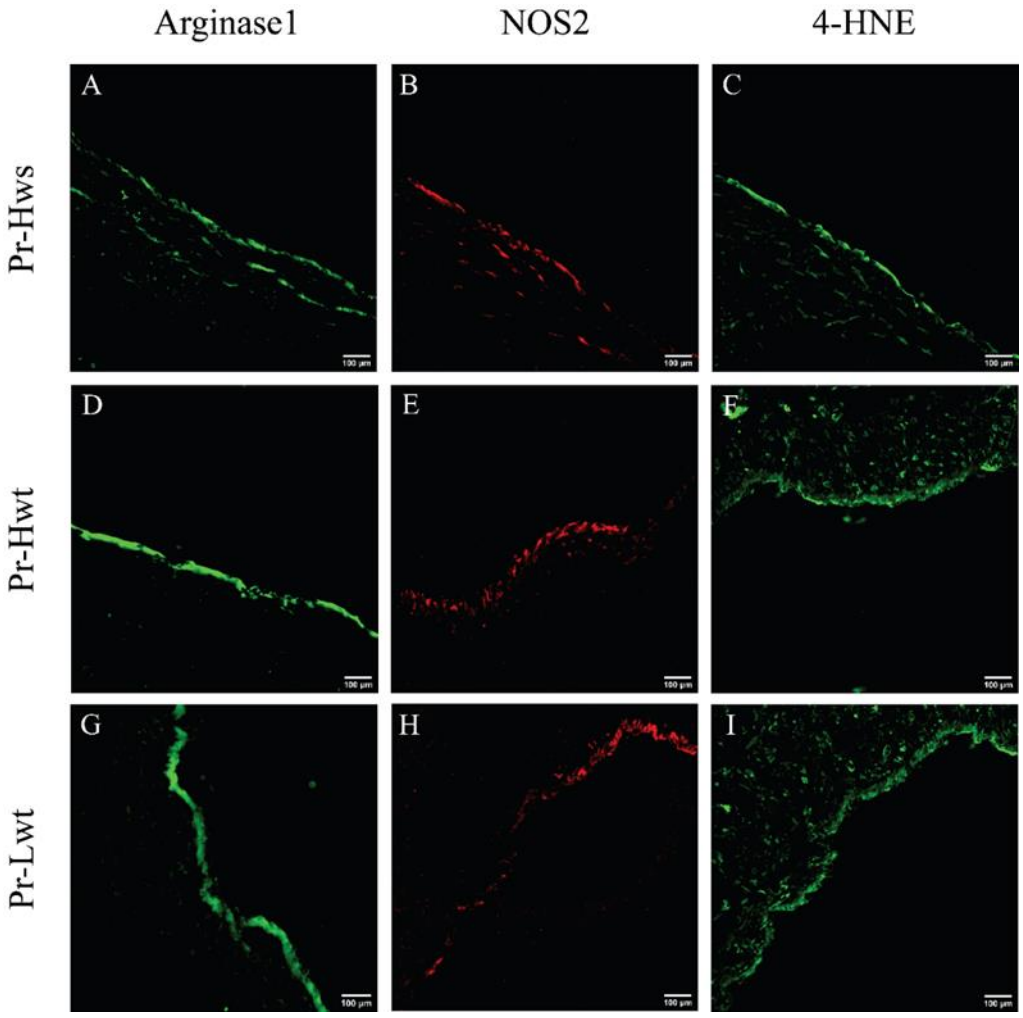

Representative epifluorescent images on immunolabelled venous endothelium originated from premature, non-discordant, high (Pr-Hwt), and low (Pr-Lwt) weight twins and age-matched high weight singleton (Pr-Hws) samples. Panels (A, D, and G) show immunolabelling with a mouse primary anti-Arginase1 antibody followed by an Alexa Fluor® 488 secondary antibody. In a similar manner, panels (B, E, and H) present samples that were immunolabelled with a rabbit primary anti-NOS2 antibody followed by an Alexa Fluor® 647 secondary antibody. Panels (C, F, and I) exhibit immunolabelling with a mouse primary anti-4-HNE antibody followed by an Alexa Fluor® 488 secondary antibody. The slides were mounted and examined under an epifluorescence microscope (Nikon Eclipse 80i, 100x immersion objective; Nikon Zeiss Microscopy GmbH, Jena, Germany).

Figure S9. Representative epifluorescent images on umbilical cord arterial endothelium showing NOS3 expression and its phosphorylation level

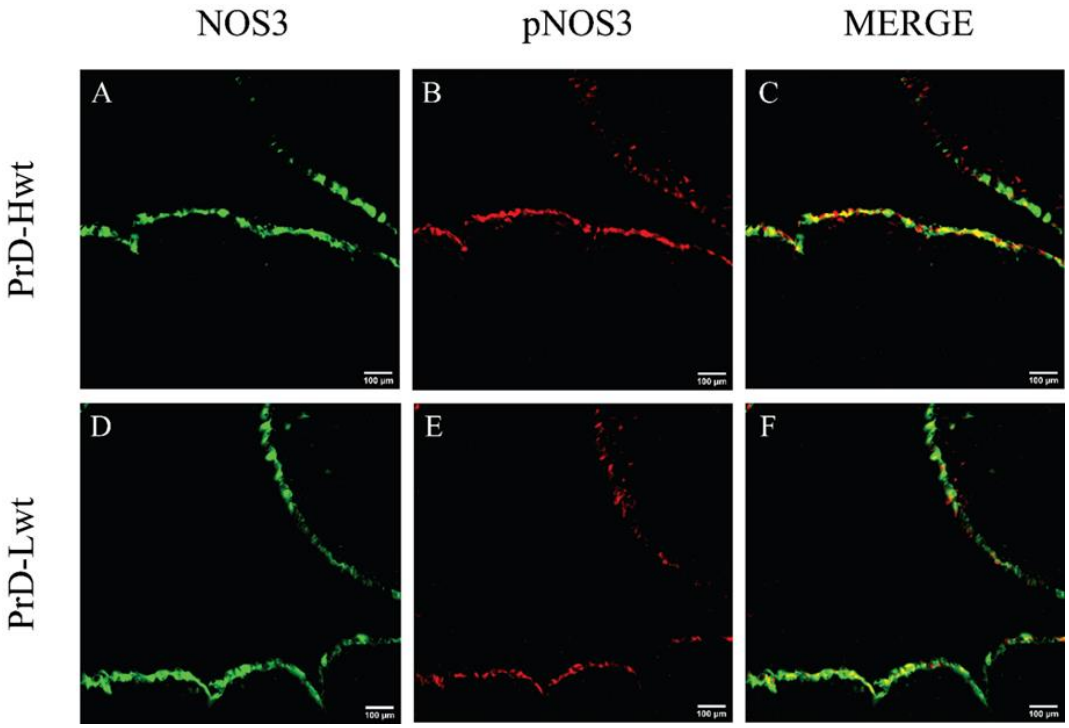

Representative epifluorescent images on immunolabelled arterial endothelium originated from premature, discordant, high and low-weight siblings (PrD-Hwt and PrD-Lwt). Panels (A, D) show immunolabelling with mouse primary anti-NOS3 antibody followed by an Alexa Fluor® 488 secondary antibody. Panels (B, E) show immunolabelling with a rabbit anti-pNOS3 primary antibody followed by Alexa Fluor® 647 secondary antibody staining. Panels (C, F) present the merged images. Slides were mounted and examined under an epifluorescence microscope (Nikon Eclipse 80i, 100x immersion objective; Nikon Zeiss Microscopy GmbH, Jena, Germany).

Figure S10. Representative epifluorescent images on umbilical cord vein endothelium showing NOS3 expression and its phosphorylation level

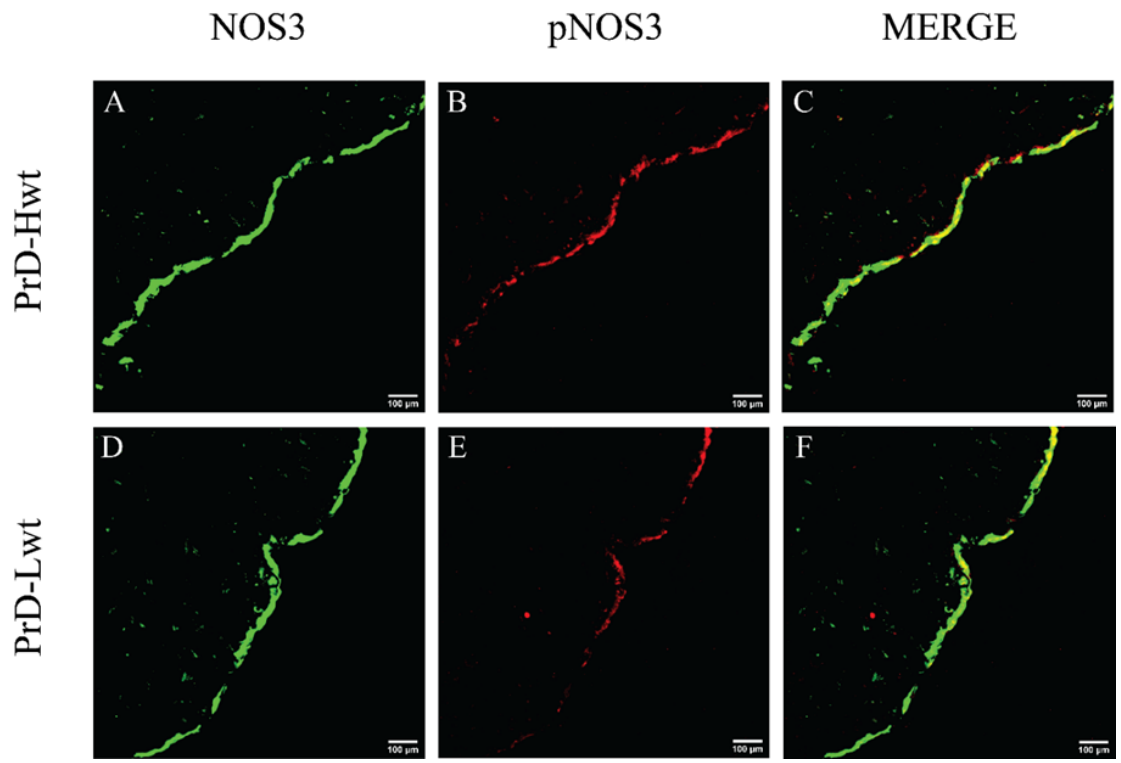

Representative epifluorescent images on immunolabelled venous endothelium originated from premature, discordant, high and low-weight twin pairs (PrD-Hwt and PrD-Lwt). Panels (A, D) show immunolabelling with mouse primary anti-NOS3 antibody followed by Alexa Fluor® 488 secondary antibody staining. Panels (B, E) show immunolabelling with a rabbit anti-pNOS3 primary antibody followed by an Alexa Fluor® 647 secondary antibody. Panels (C, F) present the merged images. Slides were mounted and examined under an epifluorescence microscope (Nikon Eclipse 80i, 100x immersion objective; Nikon Zeiss Microscopy GmbH, Jena, Germany).

Figure S11. Epifluorescent images represent arterial endothelium immunolabelled with Arginase1, NOS2, and 4-HNE

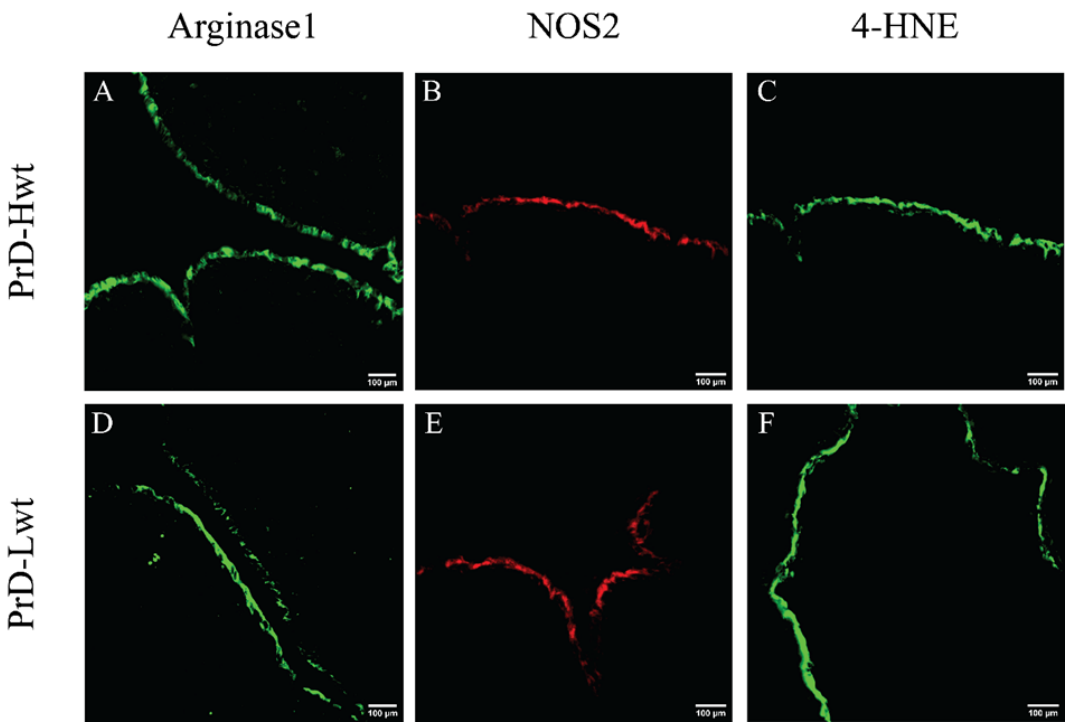

Representative epifluorescent images on immunolabelled arterial endothelium originated from premature, discordant, high and low-weight twin pair samples (PrD-Hwt and PrD-Lwt). Panels (A, D) show immunolabelling with a mouse primary anti-Arginase1 antibody followed by Alexa Fluor® 488 secondary antibody staining. In a similar manner, panels (B, E) present samples that were immunolabelled with a rabbit primary anti-NOS2 antibody followed by Alexa Fluor® 647 secondary antibody. Panels (C, F) exhibit immunolabelling with a mouse primary anti-4-HNE antibody followed by an Alexa Fluor® 488 secondary antibody. Slides were mounted and examined under an epifluorescence microscope (Nikon Eclipse 80i, 100x immersion objective; Nikon Zeiss Microscopy GmbH, Jena, Germany).

Figure S12. Epifluorescent images represent venous endothelium immunolabelled with Arginase1, NOS2, and 4-HNE

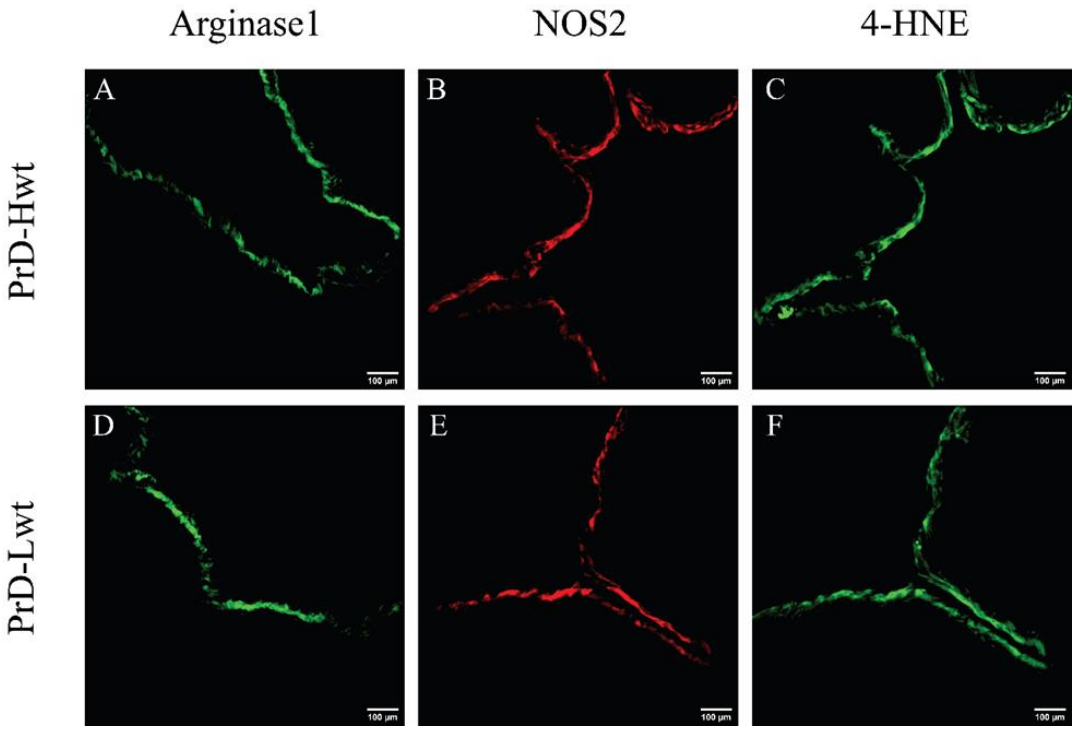

Representative epifluorescent images on immunolabelled venous endothelium originated from premature, discordant, high and low-weight twin pairs (PrD-Hwt and PrD-Lwt). Panels (A, D) show immunolabelling with a mouse primary anti-Arginase1 antibody followed by Alexa Fluor® 488 secondary antibody staining. In a similar manner, panels (B, E) present samples that were immunolabelled with a rabbit primary anti-NOS2 antibody followed by Alexa Fluor® 647 secondary antibody staining. Panels (C, F) exhibit immunolabelling with a mouse primary anti-4-HNE antibody followed by an Alexa Fluor® 488 secondary antibody. Slides were mounted and examined under an epifluorescence microscope (Nikon Eclipse 80i, 100x immersion objective; Nikon Zeiss Microscopy GmbH, Jena Germany)